

2011

## Encoding of Temporal Sound Features in the Rodent Superior Paraolivary Nucleus

Richard A. Felix II  
*West Virginia University*

Follow this and additional works at: <https://researchrepository.wvu.edu/etd>

---

### Recommended Citation

Felix, Richard A. II, "Encoding of Temporal Sound Features in the Rodent Superior Paraolivary Nucleus" (2011). *Graduate Theses, Dissertations, and Problem Reports*. 3396.  
<https://researchrepository.wvu.edu/etd/3396>

This Dissertation is protected by copyright and/or related rights. It has been brought to you by the The Research Repository @ WVU with permission from the rights-holder(s). You are free to use this Dissertation in any way that is permitted by the copyright and related rights legislation that applies to your use. For other uses you must obtain permission from the rights-holder(s) directly, unless additional rights are indicated by a Creative Commons license in the record and/ or on the work itself. This Dissertation has been accepted for inclusion in WVU Graduate Theses, Dissertations, and Problem Reports collection by an authorized administrator of The Research Repository @ WVU. For more information, please contact [researchrepository@mail.wvu.edu](mailto:researchrepository@mail.wvu.edu).

**Encoding of Temporal Sound Features in the  
Rodent Superior Paraolivary Nucleus**

Richard A. Felix II

Dissertation submitted to the  
School of Medicine  
at West Virginia University  
in partial fulfillment of the requirements  
for the degree of

Doctor of Philosophy  
in  
Neuroscience

Albert S. Berrebi, Ph.D., Chair

Ariel Agmon, Ph.D.

R. Michael Burger, Ph.D.

James W. Lewis, Ph.D.

George A. Spirou, Ph.D.

Department of Neurobiology and Anatomy

Morgantown, West Virginia

2011

Keywords: auditory, inhibition, amplitude modulation, gap detection, inferior colliculus

## **Abstract**

### **Encoding of Temporal Sound Features in the Rodent Superior Paraolivary Nucleus**

**Richard A. Felix II**

The superior paraolivary nucleus (SPON) is a prominent cell group in the mammalian brainstem. SPON neurons are part of a monaural circuit that encodes temporal sound features in the ascending auditory pathway. Such attributes of acoustic signals are critical for speech perception in humans and likely equally as important in animal communication. While basic properties of SPON neurons have been characterized in some detail, a comprehensive examination of mechanisms that underlie their ability to precisely represent temporal information is lacking. Furthermore, little is known of how the SPON impacts its primary target, the inferior colliculus. Combinations of electrophysiological, pharmacological and histological techniques were used to investigate SPON neuronal responses to stimuli whose temporal parameters were systematically varied. In addition, properties of neurons in the inferior colliculus were examined before and after reversible inactivation of the SPON in order to explore its functional role in hearing. An after-hyperpolarization rebound mechanism was shown to generate the hallmark offset response of SPON neurons *in vitro*. Single-cell labeling techniques provided a detailed morphological description of cell bodies and dendrites and revealed a homogeneous population of neurons. Moreover, subthreshold ionic currents and synaptic neurotransmitter receptor systems were shown to mediate the precision of responses to temporal features of sound *in vivo*. It was also demonstrated that input from the SPON shapes response properties of inferior colliculus neurons to both periodic and singular temporal stimulus features. Taken together, these results suggest the SPON likely has a substantial role in temporal processing that has not been taken into account in the current understanding of the central auditory system. Demonstrating a functional role for the SPON in hearing will expand our knowledge of neuronal circuits responsible for representing biologically important sounds in both normal hearing and hearing impaired states.

## Acknowledgements

I thank my mentor Dr. Berrebi for guidance and support throughout my time as a graduate student. I also thank Dr. Anna Magnusson for training and support for *in vitro* experiments and for providing a nurturing lab environment for my time in Stockholm. To my committee members Drs. Spirou, Agmon, Burger and Lewis, thank you for providing guidance for my various research projects and for being generous with your time.

## Table of Contents

	page
<b>Acknowledgements</b> .....	iii
<b>Table of contents</b> .....	iv
<b>Index of figures</b> .....	vi
<b>Index of tables</b> .....	viii
<b>List of abbreviations</b> .....	ix
<b>Chapter 1: Introduction</b>	
Literature review .....	02
Rationale .....	09
Objectives .....	10
<b>Chapter 2: Morphological characterization of physiologically identified neurons of the mouse superior paraolivary nucleus</b>	
Abstract .....	16
Introduction .....	17
Methods .....	19
Results	
Distinct types of SPON neurons based on physiological properties .....	23
Morphological characterization of SPON neurons .....	26
Discussion .....	29
<b>Chapter 3: Effects of ketamine on response properties of neurons in the superior paraolivary nucleus of the mouse</b>	
Abstract .....	48
Introduction .....	49
Methods .....	51
Results	
Effects of acepromazine sedation .....	58
Responses to pure tones .....	58
Aurality and responses to broadband noise .....	59
Frequency response maps .....	61
Responses to sinusoidally amplitude modulated tones .....	61
Effects of ketamine during paired recordings .....	62
Ketamine anesthesia effects in independent and paired recordings .....	63
Discussion .....	65
<b>Chapter 4: Ion channels and transmitter receptors shape responses to sinusoidally amplitude-modulated tones in the rodent superior paraolivary nucleus</b>	
Abstract .....	88

Introduction .....	89
Methods .....	91
Results	
SPON neurons in the mouse are tuned to low-rate modulated stimuli .....	96
Ih and LVA Ca <sup>2+</sup> currents shape mouse responses to tone and SAM stimuli .....	97
Inhibitory transmitter systems shape phase-locking properties in the rat .....	100
Effects of excitatory transmitters on responses to SAM tones in the rat .....	102
Discussion .....	104
<b>Chapter 5: The superior paraolivary nucleus shapes temporal response properties of neurons in the inferior colliculus</b>	
Abstract .....	123
Introduction .....	124
Methods .....	126
Results	
Control experiments .....	132
SPON inactivation increased post-stimulus spiking of IC neurons .....	133
IC responses to SAM stimuli were altered after SPON inactivation .....	134
Gap detection thresholds in the IC increased following SPON inactivation .....	136
Discussion .....	138
<b>Chapter 6: General Discussion</b>	
Summary .....	158
Discussion .....	161
Conclusions .....	164
<b>References</b> .....	166
<b>Curriculum Vitae</b> .....	184

## Index of Figures

	page
<b>Chapter 1</b>	
1.1. Coronal view of a circuit for processing monaural information in the central auditory system .....	12
1.2 Overview of inputs and projections of SPON neurons in the coronal plane.....	13
<b>Chapter 2</b>	
2.1 Localization of filled neurons recorded within the SPON .....	35
2.2 Correlated physiological and morphological properties of SPON neurons .....	36
2.3 The mouse SPON has two physiologically distinct cell types .....	37
2.4 Properties of type 1 and type 2 SPON neurons .....	38
2.5 Analysis of electrophysiological variables .....	39
2.6 An example of a reconstructed SPON neuron .....	40
2.7 Reconstructions of representative SPON neurons .....	41
2.8 Some SPON neurons had highly oriented dendritic fields .....	42
2.9 Examples of possible dendro-dendritic contacts between SPON neurons .....	43
<b>Chapter 3</b>	
3.1 SPON recording sites were marked by injecting biocytin from recording pipettes during each experiment .....	74
3.2 Distribution of thresholds and characteristic frequencies of independent single units recorded either with ketamine (Ket+) or without ketamine (Ket-) anesthetic in the mouse SPON .....	75
3.3 Classification of the main response types observed in the mouse SPON .....	76
3.4 Aurality of independent mouse responses .....	77
3.5 Comparison of SPON responses to pure tones and broadband noise .....	78
3.6 Typical frequency response maps of unanesthetized mouse units .....	79
3.7 SPON responses to sinusoidally amplitude-modulated (SAM) tones .....	80
3.8 Responses to SAM tones for independent groups of unanesthetized (Ket-) and ketamine-anesthetized (Ket+) units .....	82
3.9 Examples of responses of paired SPON units directly before and after ketamine administration .....	83
3.10 Responses to SAM tones for paired units recorded before and after ketamine was administered .....	84
3.11 Population data for response properties of SPON units before and after ketamine administration .....	85
<b>Chapter 4</b>	
4.1 Schematic representation of synaptic inputs to the rodent SPON .....	112
4.2 Neuronal responses in the SPON are not affected by the application of	

current or vehicle solutions .....	113
4.3 Mouse SPON neurons exhibited two types of modulation transfer functions in response to SAM stimuli .....	114
4.4 ZD7288 and Mibefradil alter the spiking of SPON neurons in the mouse .....	115
4.5 Ih currents contribute to SAM tuning in the mouse SPON .....	116
4.6 LVA Ca <sup>2+</sup> currents contribute to SAM tuning in the mouse SPON .....	117
4.7 Blockade of glycine and GABA <sub>A</sub> receptors alters the spiking patterns of rat SPON neurons.....	118
4.8 Inhibitory neurotransmitter systems shape phase-locking properties of rat SPON neurons .....	119
4.9 Glycine receptor blockade decreases phase-locking to low modulation frequency (MF) SAM stimuli and increases spiking for rat SPON neurons .....	120
4.10 Excitatory neurotransmitter systems affect response magnitude and phase-locking abilities of rat SPON neurons .....	121

## Chapter 5

5.1 Localization of recording sites in the superior paraolivary nucleus (SPON) and central nucleus of the inferior colliculus (ICC) .....	145
5.2 Definitions of analysis windows for IC recordings .....	146
5.3 Effective SPON inactivation was achieved using extracellular iontophoresis .....	148
5.4 Time course of drug action depends on the distance from the point of drug ejection to the SPON target neuron .....	149
5.5 SPON inactivation alters spiking patterns of IC neurons to pure tones .....	150
5.6 Spiking of sustained IC neurons was altered following SPON inactivation .....	151
5.7 SPON inactivation impacts phase-locking of representative IC neurons to SAM stimuli .....	152
5.8 Phase-locking to SAM stimuli was reduced for IC neurons following SPON inactivation .....	153
5.9 SPON inactivation diminished the ability of a representative onset IC neuron to respond to short gaps between tones .....	154
5.10 SPON inactivation diminished the ability of a representative sustained IC neurons to respond to short gaps between tones .....	155
5.11 IC neurons exhibit elevated gap detection thresholds following SPON inactivation .....	156



## Index of Tables

	page
<b>Chapter 2</b>	
2.1 Electrophysiological and morphological variables used for characterizing SPON cells. ....	44
2.2 Correlations between values for physiological and morphological variables .....	45
2.3 Average values and standard errors for physiological and morphological variables.....	46
<b>Chapter 3</b>	
3.1 Summary of comparisons between independent SPON unit responses recorded with and without ketamine anesthesia.....	86

## List of Abbreviations

AMPA	2-amino-3-(5-methyl-3-oxo-1,2-oxazol-4-yl)propanoic acid
AP	action potential
BBN	broad band noise
CF	characteristic frequency
CN	cochlear nuclei
CPP	(±)3-(2-carboxypiperazin-4-yl)-propyl-1-phosphonic acid
DMPO	dorsomedial paraolivary nucleus
DNLL	dorsal nucleus of the lateral lemniscus
FM	frequency modulated
FSL	first-spike latency
GABA	gamma-amino butyric acid
GAD	glutamic acid decarboxylase
GZ	gabazine (SR95531)
Hz	hertz
IC	inferior colliculus
ICC	central nucleus of the inferior colliculus
Ih	hyperpolarization-activated inward cation current
KET	ketamine
kHz	kilohertz
LSO	lateral superior olive
LVA	low-voltage activated
MF	modulation frequency
MGB	medial geniculate body
MNTB	medial nucleus of the trapezoid body
ms	milliseconds
MSO	medial superior olive
NBQX	1,2,3,4-tetrahydro-6-nitro-2,3-dioxobenzo[f]quinoxaline-7-sulfonamide
NMDA	<i>N</i> -methyl-D-aspartate
PCA	principal component analysis
PSTH	peri-stimulus time histogram
SAM	sinusoidally amplitude-modulated
SOC	superior olivary complex
SPON	superior paraolivary nucleus
STRYCH	strychnine
Th	threshold
TLC	tectal-longitudinal column
VCN	ventral cochlear nucleus
VGAT	vesicular GABA transporter
VNLL	ventral nucleus of the lateral lemniscus
VNTB	ventral nucleus of the trapezoid body
VS	vector strength

# **Chapter One**

## **Introduction**

## **Literature Review**

### *Introduction*

The ability to discriminate communication sounds in order to generate appropriate behaviors is critical for the survival of all mammals. Sounds emitted as pressure waves are collected by the pinna, amplified by the middle ear and converted into electrical signals by sensory receptor cells in the cochlea. Acoustic information is then carried by nerve fibers into the brain, where various sound features are extracted and encoded by specialized groups of neurons throughout the auditory pathway. The result of this neuronal processing is the perception of a sound stimulus that has meaning to the organism (Fay, 1988; Gentner and Margoliash, 1994; Malmierca and Hackett, 2010).

Features of biologically relevant sounds can be separated into spectral and temporal components, both of which are important for auditory processing of animal vocalizations and human speech (Phillips, 1999; Walton, 2010). Although the auditory system is often characterized by frequency tuning properties, many neurons are more sensitive to temporal properties of stimuli than to spectral content (Nagarajan et al., 2002; Theunissen and Doupe, 1998). Temporal characteristics of sound can be further divided into recurring features, such as periodically driven rhythm and pitch (Joris et al., 2004; Langner, 1992), or singular features, including starts and stops or gaps in stimuli (Phillips, 1999; Walton, 2010). In order for accurate sound encoding to occur, neurons must represent temporal features on a sub-millisecond scale which requires both morphological and physiological adaptations (Trussell, 2002). Brainstem neurons that are highly sensitive to changes in temporal stimulus attributes target the auditory midbrain, a major site of convergence of ascending sound processing circuits (Winer and Schreiner, 2005). Integration of excitatory and inhibitory inputs at the level of the midbrain gives rise to novel neuronal response properties that are better able to discriminate complex sounds, including vocalizations, compared to brainstem nuclei (Holmstrom et al., 2007; Portfors and Felix II, 2005).

### *Monaural circuits in the auditory brainstem*

The complexity of low level processing in the central auditory system exceeds that of other sensory systems (Winer and Schreiner, 2005). The superior olivary complex (SOC) is a constellation of nuclei located in the brainstem that are typically only one synapse removed from the auditory nerve (Willott, 1983). Yet even at this early stage in the auditory pathway, more than a dozen distinct cell groups take part in multiple parallel processing streams that converge on the inferior colliculus (IC) in the midbrain (Irvine, 1992). Historically, the functions of SOC circuits have been framed in terms of binaural sound localization. Specifically, sound location is extracted by the medial and lateral superior olives, which compare timing and level differences of acoustic signals arriving at each ear, respectively (Grothe et al., 2010; Tollin, 2003). Neurons in the IC then integrate sound localization information provided by the SOC with bilateral inhibitory inputs from the dorsal nucleus of the lateral lemniscus. This convergence of excitatory and inhibitory inputs enhances the ability of the auditory system to track moving objects in the environment (Pollak et al., 2002). While binaural sound processing is critical for normal behavior and worthy of the attention it has received from researchers, monaural processing is also important, yet our knowledge of the functional role of monaural systems in hearing is lacking.

One example of the importance of monaural processing comes from psychoacoustic studies that demonstrated human speech perception under reverberant conditions relied primarily on monaural cues (Plomp, 1976; Culling et al., 2003). In studies of non-human mammals, a monaural brainstem to midbrain circuit was implicated in encoding neuronal selectivity for frequency modulated (FM) sweeps, a sound feature important for conspecific communication (Holmstrom et al., 2010). Two monaural brainstem nuclei, the ventral nucleus of the lateral lemniscus (VNLL) and the superior paraolivary nucleus (SPON) provide well-timed inhibitory input at the onset and offset of stimuli to their target neurons in the IC (Pollak et al., 2011; Fig. 1.1). The temporal precision of these inputs is created by the primary afferents to both the VNLL and SPON, octopus cells of the ventral cochlear nucleus (VCN) and principal cells of the medial nucleus of the trapezoid body (MNTB) (Irvine, 1992). These sources of inhibition shape excitatory inputs to IC neurons, which originate in the VCN, by creating a novel “on-off”

response type that is selective for FM sweep direction (Pollak et al., 2011). A multitude of rodent vocalizations contain FM sweep components (Nyby and Whitney, 1983; Portfors, 2007), and thus the importance of monaural systems can be extrapolated to a broader inclusion for processing communication sounds in general. Therefore, this dissertation aims to investigate the properties that govern sensitivity to temporal sound features of neurons in the monaural SPON and to explore a functional role for the SPON in shaping properties of IC neurons. By systematically studying how monaural inputs are integrated at the level of the IC, we will gain insight into how these pathways may underlie the encoding of vocalizations in the mammalian brain. The next section of this general introduction provides background of the anatomy and physiology of the SPON, followed by further rationale and objectives for the experiments included in this dissertation.

### *Inputs to the SPON*

The bulk of knowledge regarding synaptic inputs to the SPON has been revealed with tract tracing studies, primarily in the rat, mouse and gerbil. Although some differences in the connectivity of SPON neurons have been reported, several sources of inputs are consistent across species (Fig. 1.2). Tract tracing experiments demonstrated that retrograde tracer deposits made in the main target of SPON projections in the midbrain labeled both cell bodies and fibers in the SPON (Saldaña and Berrebi, 2000). The interpretation of this finding was that labeled fibers could belong to SPON neurons, and represent axon collaterals that branch within the nucleus to innervate other SPON cells. This potential source of SPON input has yet to be characterized fully.

*Cochlear Nucleus:* Excitatory inputs to SPON neurons originate primarily from the contralateral ventral cochlear nucleus (Grothe et al., 1994; Kuwabara and Zook, 1991; Morest 1968; Smith et al., 1991; Warr 1972). Octopus and multipolar cell types have been identified as sources of SPON inputs, which are presumably glutamatergic and likely tonotopically organized (Friauf and Ostwald, 1988; Schofield, 1995; Thompson and Thompson, 1991).

*Medial Nucleus of the Trapezoid Body:* Inputs from the ipsilateral medial nucleus of the trapezoid body (MNTB) represent a major source of glycinergic inhibition (Bledsoe et al., 1990; Helfert et al., 1989; Kuwabara and Zook, 1991; Moore and Caspary, 1983; Schofield, 1994; Smith et al., 1998). Although the MNTB has traditionally been characterized by its role in sound localization (Park et al., 1997; Pollak et al., 2003), it provides a substantial input to the SPON through axon collaterals (Banks and Smith, 1992; Saldaña et al., 2009; Sommer et al., 1993; Spangler et al., 1985).

*Tectal Longitudinal Column:* A novel auditory nucleus located in the midbrain tectum was recently characterized and termed the tectal-longitudinal column (TLC) (Aparicio et al., 2010, Marshall et al., 2008; Saldaña et al., 2007). The TLC has reciprocal connections with the SPON which are primarily ipsilateral (Viñuela et al., 2011). While the SPON projection is known to be GABAergic (Kulesza Jr. and Berrebi, 2000), it is likely that the descending projection from the TLC is also GABAergic (Mugnaini and Oertel, 1985).

#### *Targets of the SPON*

*Inferior Colliculus:* SPON projections represent a major inhibitory input to the inferior colliculus (IC), the primary auditory midbrain nucleus (Beyerl, 1978; Saldaña et al., 2009; Saldaña and Berrebi, 2000; Schofield, 1991). The anatomy and physiology of the IC has been studied extensively, particularly the central nucleus, as it occupies a prominent position in the ascending auditory pathway (Caspary et al., 2008; Davis, 2005; Winer and Schreiner, 2005). Although excitatory inputs to the IC primarily drive neuronal spiking, inhibition has been shown to play a critical role in shaping response properties (Faingold, 1991; Pollak et al., 2003; 2011). In the rat, SPON axons densely innervate the IC with fibers that ramify within the central nucleus and possess both terminal and *en passant* boutons (Saldaña et al., 2009). In addition, axons of SPON neurons form a laminar plexus that is oriented parallel to the known fibrodendritic laminae of the IC (Malmierca et al., 1993; Saldaña et al., 2009). Furthermore, based on

retrograde tracing of IC deposits, SPON to IC projections are topographic and presumably tonotopic in nature (Saldaña and Berrebi, 2000).

The role of IC neurons in encoding temporal features of sound has been well documented (Frisina, 2001; Joris et al., 2004) In response to SAM stimuli, IC neurons exhibit precise entrainment to a lower range of modulation frequencies compared to cells in most brainstem nuclei from which they receive inputs (Frisina, 2001). Also, gap encoding by IC neurons in rodents is comparable with gap detection thresholds found in human psychophysics studies (Phillips, 1999; Snell et al., 1994; Walton, 2010; Walton et al., 1997).

*Medial Geniculate Body:* Although their main target is the IC, SPON neurons also directly project ipsilaterally to the medial division of the medial geniculate body (MGB) in the thalamus (Jin and Berrebi, 2006). Due to its recent discovery, little is known about this SPON projection. One potential role for the SPON to MGB circuit is in processing the emotional salience of auditory stimuli, as the medial MGB constitutes part of the thalamo-amygdala projection (LeDoux et al., 1984; 1990).

### *SPON Organization*

In the rat, the species in which the SPON has been studied most extensively, the size of the nucleus either rivals or exceeds that of other prominent SOC nuclei (Kulesza Jr. et al., 2002). Other species that have a relatively large SPON include mice, bats and rabbits (Kuwabara and Zook, 1999; Felix II and Berrebi, 2007). Although the SPON is reduced in size in mammals with good low frequency hearing, an SPON-like structure is easily identifiable in the SOC of all mammals studies thus far (listed in Saldaña and Berrebi, 2000), including humans (Kulesza Jr., 2008), suggesting it may play a fundamental role in sound processing over a wide range of species specialized for different hearing requirements.

In a detailed study of rat SPON morphology, cell bodies were described as a homogeneous population of multipolar neurons (Saldaña and Berrebi, 2000). In addition, cell bodies and dendritic arbors were flattened and oriented in the parasagittal plane, with



some dendritic trees extending beyond the ventral border of the nucleus into the ventral nucleus of the trapezoid body (Saldaña and Berrebi, 2000). In the mouse, the morphology of SPON neurons was described as multipolar, with long dendrites that had no particular orientation (Ollo and Schwartz, 1979).

Neurons in the rat SPON are immunoreactive to glutamic acid decarboxylase, the synthetic enzyme for GABA (Gonzalez-Hernandez et al., 1996; Kulesza Jr. and Berrebi, 2000; Mugnaini and Oertel, 1985); thus, the SPON is a GABAergic nucleus. Based on immunocytochemistry and *in situ* hybridization studies, SPON neurons are known to possess NMDA and AMPA glutamate receptors (Petralia et al., 1994; Sato et al., 1999), whose activation is presumably mediated by inputs from the cochlear nucleus. The SPON also expresses receptors for glycine and GABA (Friauf et al., 1997; 1998). While glycine receptors are activated by MNTB inputs (Banks and Smith, 1992), the sources of GABA in the SPON remain unknown, but potentially arise within the SPON (see above).

### *SPON Physiology*

*Responses to pure tones:* Over the past decade or so, several studies have focused on physiological responses of SPON neurons to sound stimuli (Behrend et al., 2002; Dehmel et al., 2002; Kadner and Berrebi, 2008; Kadner et al., 2006; Kulesza Jr. et al., 2003; 2007; Kuwada and Batra, 1999). Although differences in neuronal behavior exist between studies, there is general agreement that the SPON contains populations of cells that have spiking triggered by the offset of tone stimuli and with very little spontaneous activity (Dehmel et al., 2002; Kadner and Berrebi, 2008; Kadner et al., 2006; Kulesza Jr. et al., 2003; 2007; Kuwada and Batra, 1999). The offset spiking response of SPON neurons is generated primarily by release from inhibition from the MNTB that occurs during sound stimulation (Grothe, 1994; Kopp-Scheinflug et al., 2010; Kulesza Jr. et al., 2007; Kuwada and Batra, 1999; Magnusson et al., 2010). Another feature commonly reported in SPON studies is the predominance of contralaterally driven responses (Dehmel et al., 2002; Kulesza Jr. et al., 2003; Kuwada and Batra, 1999). In addition, SPON neurons have broad frequency tuning, particularly at the low frequency region of tuning curves, and elevated response thresholds compared to neurons that provide their main inputs (Dehmel

et al., 2002; Kadner and Berrebi, 2008; Kopp-Scheinpfug et al., 2008; Kulesza Jr. et al., 2003). Neurons within the SPON also appear to be tonotopically organized, with cells most sensitive to low frequencies positioned laterally and progressively higher frequencies represented medially (Kulesza Jr. et al., 2003).

*Responses to amplitude modulation:* A hallmark of the SPON neuronal response is the ability to synchronously spike to fluctuations in the amplitude of acoustic signals (Behrend et al., 2002; Kadner and Berrebi, 2008; Kulesza Jr. et al., 2003; Kuwada and Batra, 1999). The ability to represent periodic changes in the sound envelope is thought to be important in processing of both animal vocalizations and human speech (Drullman, 1995; Langner, 1997). Entrainment of SPON responses to cycles of amplitude modulation is extremely precise, especially for low modulation frequencies (Kadner and Berrebi, 2008; Kuwada and Batra, 1999). At very low modulation frequencies ( $< 20$  Hz), SPON neurons respond to each cycle of modulation; at higher modulation rates (20-400 Hz), spiking is only entrained to a subset individual cycles, albeit with a high degree of precision, and at high modulation frequencies ( $> 400$  Hz), amplitude modulation is no longer resolved and the stimulus is recognized as a tone, eliciting only offset spiking (Kadner and Berrebi, 2008). In general, SPON neurons exhibit synchronous spiking to all rates of modulation to which a consistent response is evoked.

*Responses to stimulus gaps:* The ability to detect silent periods, or gaps, within ongoing sound stimuli is used as a measure of temporal acuity in humans and is of clinical relevance (Phillips, 1999). Correlates of gap detection have been found in several animal models, including rats and mice (Syka et al., 2002; Walton, 2010). A recent study by Kadner and Berrebi (2008) found that rat SPON neurons are able to signal very short gaps on the order of 1 millisecond. This range of gap sensitivity is comparable to corresponding thresholds in both rat and human behavioral studies (Green and Forrest, 1989; Leitner et al., 1993; Rybalko and Syka, 2005; Snell et al., 1994).

While basic properties of SPON neurons have been characterized in some detail across several species, a systematic study of mechanisms that underlie their sensitivity to

temporal stimulus features has not been attempted. Although reports of various basic SPON response properties have yielded conflicting results, there is general agreement that the SPON is well-suited to play a substantial role in temporal processing; however this idea needs to be explored in more detail. The absence of a defined role for the SPON in the central auditory system has led to the rationale for the present dissertation, which is addressed below.

## **Rationale**

The accurate encoding of temporal sound information is vitally important for normal behavior in mammals. In fact, speech can be recognized when spectral content is severely degraded and the auditory system must rely primarily on temporal cues (Shannon et al., 1995). In addition, deficits in temporal discrimination tasks, such as gap detection, have been associated with central auditory processing disorders (Ison et al., 2005; Moore, 2006). Furthermore, the ability to discriminate temporal stimulus features is likely also important for normal rodent function, as behavioral gap detection thresholds are similar in rodents and humans (Ohl et al., 1999). The SPON is well suited to play a role in processing temporal auditory information. In addition to exhibiting precise responses to temporal stimulus cues, SPON neurons provide a major source of inhibitory input to the IC, which is known to be critical for encoding temporal information (Frisina, 2001; Joris et al., 2004). Thus, the SPON is in a position to substantially shape IC response properties. Until recently, monaural SOC nuclei, like the SPON, have received less attention compared to binaural cell groups involved in sound localization. However, psychoacoustic evidence suggests that speech perception relies primarily on monaural processing (Plomp, 1976; Culling et al., 2003). Therefore, the monaural circuit consisting of the ventral cochlear nucleus, MNTB, SPON and IC are worthy of further investigation, as each of these areas contains cells that are highly responsive to temporal cues of acoustic signals.

The purpose of this dissertation is to use physiological, pharmacological and histological techniques to characterize SPON neurons and their responses to temporal stimulus features. The contributions of SPON inputs to temporal processing will be

examined in mouse and rat and the functional role of the SPON will be explored by reversibly silencing its input to the IC and observing changes in IC response properties. The knowledge garnered from experiments that comprise this dissertation will give rise to a more complete understanding of how temporal information is represented in the auditory system, and the contribution of the SPON in those pathways.

## **Objectives**

*Study 1: Are there morphologically distinct cell types in the SPON?*

To determine whether separate classes of cells are present in the mouse SPON, physiologically characterized neurons were filled with a dye and three-dimensional reconstructions were made. Analyses of the reconstructions were used to show whether cells represent a homogeneous or heterogeneous population based on the morphological characteristics of the soma and dendritic arbors. In addition, labeled axons were examined to determine if connections exist between SPON neurons. Potential correlations between morphological and physiological attributes were also explored.

*Study 2: Does anesthesia alter the behavior of SPON neurons?*

Differences in the response properties of SPON neurons have been reported by several groups, the majority of which used anesthetic agents in order to make data collection more practical for *in vivo* experiments. While some of the variations in SPON response properties were likely due to species differences, another possibility is the variance artificially introduced by anesthetic regimens used during experimentation. Given the known effects of anesthesia on neuronal transmitter systems, it is plausible that previous reports may not accurately represent the activity of SPON neurons in the normal waking state. Therefore, a mouse model was used to examine SPON responses in both the anesthetized state and in a newly developed unanesthetized experimental preparation. A second goal of this study was to provide a first characterization of neuronal responses to sound in the SPON of the mouse.

*Study 3: How do ion currents and transmitter systems shape SPON neuronal responses?*

SPON neurons have a proposed role in encoding temporal features of sound stimuli. To dissect the mechanisms that underlie responses to amplitude modulated stimuli, ion channels and transmitter receptors responsible for generating SPON offset spiking were systematically blocked. The comparison of responses before and after blockade provided insight into the relative contributions of each system and how the integration of ion currents and synaptic inputs create precise spiking to periodic stimuli.

*Study 4: What is the functional role of the SPON in forming properties of IC neurons?*

The SPON provides substantial transient offset GABAergic inhibition to the inferior colliculus. Despite this prominent input, little is known of the role of the SPON in shaping IC response properties. Therefore, responses of IC neurons to SAM and gap stimuli were recorded before and after SPON input was blocked. The results helped clarify a functional role for the SPON in hearing.

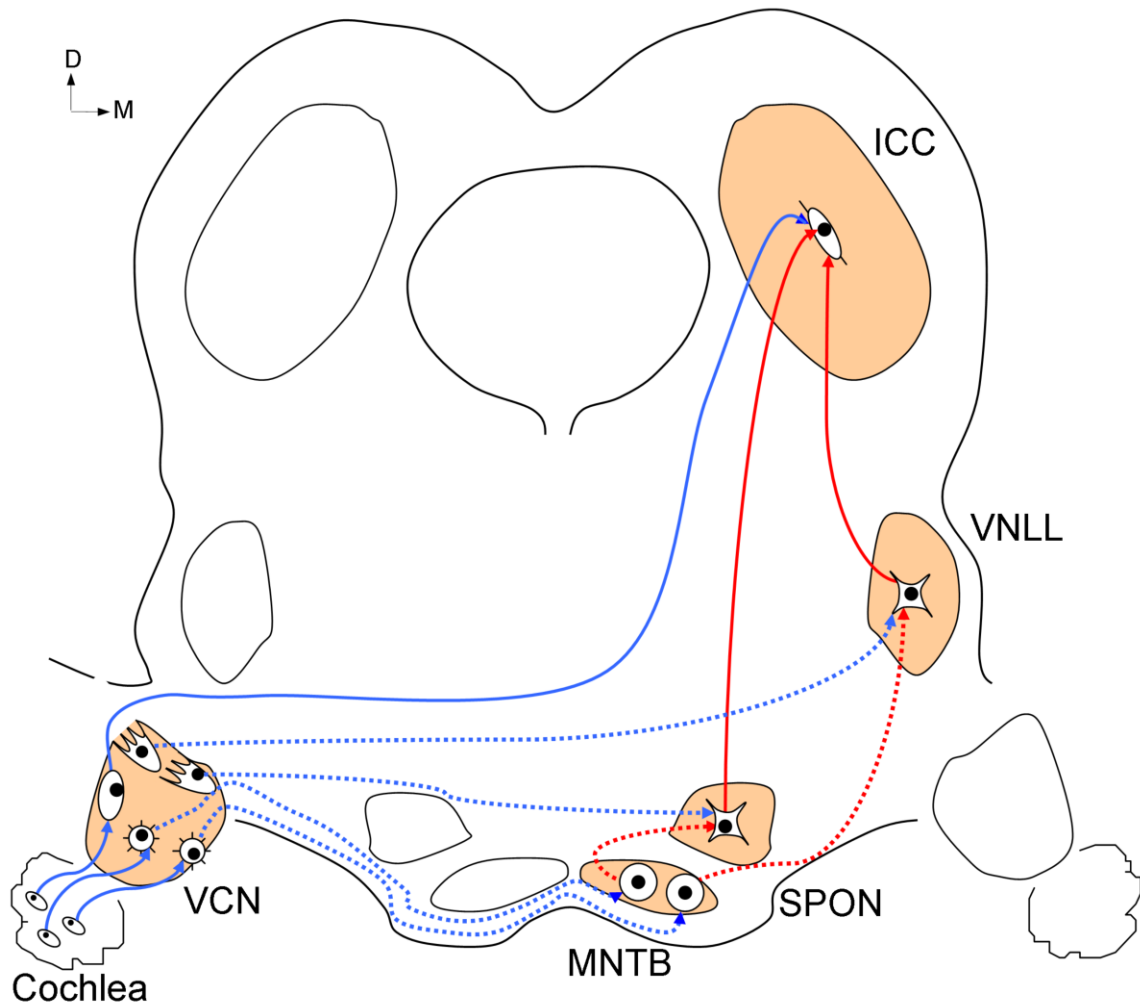


*Figure 1.1.* Coronal view of a circuit for processing monaural information in the central auditory system. The central nucleus of the inferior colliculus receives direct excitatory input from the contralateral ventral cochlear nucleus. Temporally precise inhibitory inputs from the superior paraolivary nucleus and ventral nucleus of the lateral lemniscus also project ipsilaterally to the inferior colliculus and shape response properties in the midbrain. The primary inputs to both inhibitory nuclei include the contralateral ventral cochlear nucleus and ipsilateral medial nucleus of the trapezoid body. D: dorsal; M: medial; ICC: central nucleus of the inferior colliculus; VCN: ventral cochlear nucleus; SPON: superior paraolivary nucleus; VNLL: ventral nucleus of the lateral lemniscus; MNTB: medial nucleus of the trapezoid body.

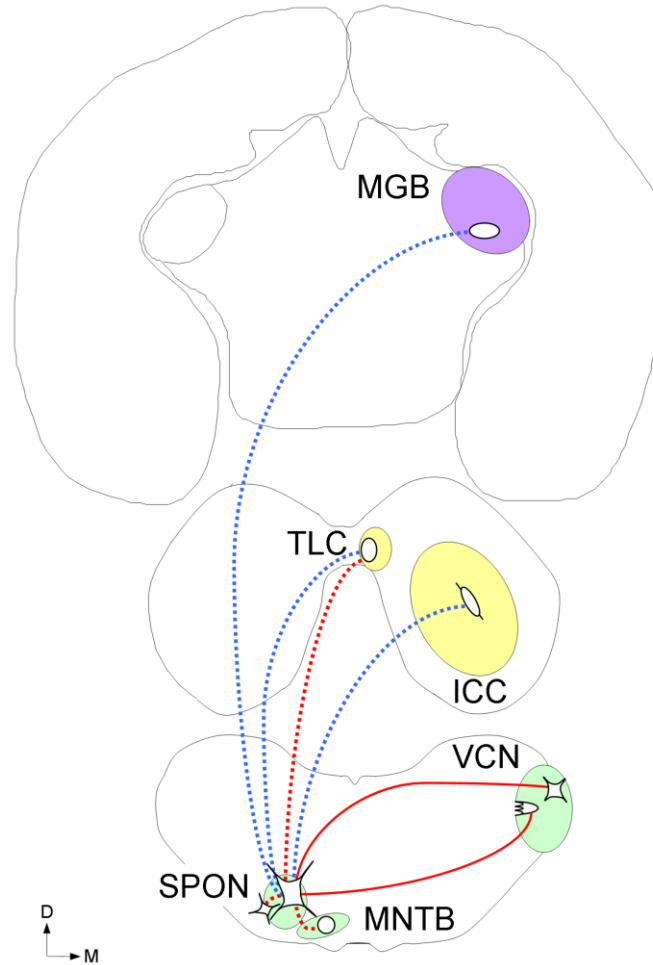


*Figure 1.2.* Overview of inputs and projections of SPON neurons in the coronal plane. At the level of the brainstem (green), SPON neurons receive excitatory synaptic inputs from octopus and multipolar cells of the contralateral VCN and inhibitory inputs from ipsilateral MNTB principal cells and from neighboring neurons within the SPON. The main targets of SPON projections include principal cells of the ICC in the midbrain (yellow), and the MGB in the auditory thalamus (purple). In addition, SPON neurons have reciprocal connections with the TLC, located in the midbrain tectum (yellow). Lines denoting inputs to SPON neurons are labeled red and projections are labeled blue. Excitatory and inhibitory connections are shown as solid and dashed lines, respectively. D: dorsal; M: medial; SPON: superior paraolivary nucleus; ICC: central nucleus of the inferior colliculus; MNTB: medial nucleus of the trapezoid body; VCN: ventral cochlear nucleus; MGB: medial geniculate body; TLC: tectal longitudinal column.

## **Chapter Two**

### **Morphological characterization of physiologically identified neurons of the mouse superior paraolivary nucleus**



## **Abstract**

The superior paraolivary nucleus (SPON) is a prominent cell group in the mammalian brainstem that provides a major GABAergic input to the auditory midbrain. While the physiology and morphology of SPON neurons have been described in several species, a detailed characterization of these attributes has not been attempted in the same study. Using a combination of *in vitro* recordings and three-dimensional cell reconstructions, the structure and function of the SPON were investigated in detail for the first time in the mouse. The results demonstrate that SPON neurons exhibit two types of rebound spiking to the offset of stimuli; one type exhibiting short duration, high amplitude action potentials and a second type marked by longer duration, complex spiking. In addition, cells were morphologically homogeneous, although slight variations in the size and shape of cell bodies and dendrites were present.

## **Introduction**

The superior paraolivary nucleus (SPON) is a prominent GABAergic cell group in the brainstem that has been implicated in the encoding of temporal features of sound (Kadner and Berrebi, 2008; Kulesza Jr. and Berrebi, 2000). The SPON receives its main synaptic inputs from octopus and multipolar cells of the ventral cochlear nucleus (Friauf and Ostwald, 1988; Kuwabara et al., 1991; Thompson and Thompson, 1991; Saldaña et al., 2009; Schofield, 1995) and from principal cells of the medial nucleus of the trapezoid body (Banks and Smith, 1992; Kuwabara and Zook, 1991; 1992; Saldaña et al., 2009; Sommer et al., 1993). Like most auditory brainstem nuclei, the main projections of SPON neurons target the inferior colliculus in the midbrain (Beyerl, 1978; Nordeen et al., 1983; Saint Marie and Baker, 1990; Saldaña et al., 2009; Saldaña and Berrebi, 2000; Schofield, 1991). In addition to a major projection to the midbrain, recent tract tracing studies have revealed that SPON neurons also have direct projections to the medial geniculate body in the thalamus (Jin and Berrebi, 2006), and to a newly characterized auditory nucleus, the tectal-longitudinal column, located in midbrain tectum (Aparicio et al., 2010; Saldaña et al., 2007; Viñuela et al., 2011).

Morphological features of SPON neurons have been characterized most extensively in rodents. In the rat, cells are described as homogeneous, with dendritic arbors that are flattened in the sagittal plane (Saldaña and Berrebi, 2000). In the gerbil and guinea pig, multiple distinct cell types were reported based on soma size and shape and on the attributes of neuronal processes (Kuwabara and Zook, 1999; Schofield, 1991). Variations in the shape and size of SPON cell bodies and dendrites were also observed in the mouse; however, these differences did not warrant subdivision into distinct classes of neurons (Ollo and Schwartz, 1979).

The presence of distinct cell types in the gerbil and guinea pig SPON are thought to correspond to separate populations that provide afferent inputs to the inferior colliculus and cochlear nucleus, respectively (Kuwabara and Zook, 1999; Schofield, 1991). Although there is evidence that the SPON is part of the descending olivocochlear pathway in these rodent species (Aschoff and Ostwald 1987; 1988; Nordeen et al., 1983; Winter et al., 1989), this is not the case for the rat (Saldaña et al., 2009; Vetter and

Mugnaini, 1991; Vetter et al., 1992; 1993). It is not definitively known whether the mouse SPON contains distinct cell types that project to different targets; however, recent evidence suggests that a subpopulation of neurons may be present based on unique physiological properties (Magnusson et al., 2010).

To determine whether separate classes of cells are present in the mouse SPON, cells were physiologically characterized *in vitro* and filled with a neuronal dye. Three-dimensional reconstructions of filled cells were then generated, providing detailed information of morphological characteristics of cell bodies and dendrites.

## Methods

### *Slice preparation*

A total of 21 CBA/CaJ (n= 17) and C57/bl6 (n= 4) mice aged postnatal day 5-14 were used for this study. Animals were decapitated while deeply anesthetized with sodium pentobarbital (5 mg/ml) and the brainstem was removed and placed in cold low sodium, high sucrose artificial cerebrospinal fluid (aCSF; see below). Transverse brainstem slices containing the superior olivary complex were obtained at a thickness of 150 or 200  $\mu\text{m}$  using a vibratome (VT1200; Leica, Wetxlar, Germany), and incubated in 32° C normal aCSF (see below) for 20-30 minutes, after which they were allowed to cool to room temperature. Recordings were obtained within 4-5 hours from the start of the brain slice preparation.

### *Solutions*

The low sodium, high sucrose aCSF contained (mM): 85 NaCl, 2.5 KCl, 1.25 NaH<sub>2</sub>PO<sub>4</sub>, 25 NaHCO<sub>3</sub>, 75 sucrose, 25 glucose, 0.5 CaCl<sub>2</sub>, 4 MgCl<sub>2</sub>; whereas the normal aCSF contained (mM): 125 NaCl, 2.5 KCl, 1.25 NaH<sub>2</sub>PO<sub>4</sub>, 26 NaHCO<sub>3</sub>, 25 glucose, 2 CaCl<sub>2</sub>, 1 MgCl<sub>2</sub>. Solutions were bubbled continuously with carbogen gas (95% O<sub>2</sub>, 5% CO<sub>2</sub>), to maintain a pH of 7.4. For current clamp recordings the internal pipette solution contained (mM): 130 K-gluconate, 5 KCl, 10 HEPES, 1 EGTA, 2 Na<sub>2</sub>-ATP, 2 Mg-ATP, 0.3 Na<sub>3</sub>-GTP, 10 Na<sub>2</sub>-phosphocreatinine, adjusted to pH 7.3 with KOH.

### *Recording procedures*

Slices were transferred to a recording chamber perfused (~3 ml per minute) with oxygenated aCSF at room temperature (25  $\pm$  2° C). Cells were viewed with an upright microscope (Zeiss Axioscope, Oberkochen, Germany) equipped with a digital CCD camera (Orca 2, Hamamatsu, Tokyo, Japan) using a 40x water immersion objective (Achromplan, Zeiss) and infrared-differential interference optics. SPON cells were

visualized by their large somata in an area medial to the lateral superior olive. Whole-cell current clamp experiments were performed with a Multiclamp 700B amplifier (Axon Instruments, Foster City, CA, USA) using borosilicate glass microelectrodes with a tip resistance of 5-10 M $\Omega$ . Recorded signals were filtered with a low-pass 4-pole Bessel filter at 10 kHz, sampled at 20 kHz and digitized using a Digidata 1422A interface (Axon Instruments). Voltages reported in the following results section were not corrected for a liquid junction potential of 11.6 mV. Experiments were performed in current clamp mode by injecting 500 ms square wave current pulses ranging from -700 to 300 pA in 100 pA steps. For each cell, the resting membrane potential, input resistance, percent sag, as well as the spike number, amplitude, duration, and the first spike latency from the stimulus offset were measured for responses to a -300 pA current injection. In cases where a spiking response was not evoked by the -300 pA current, measurements were taken from the response to the lowest magnitude hyperpolarizing current that elicited action potentials. Descriptions of the physiological properties that were measured for each response are provided in Table 2.1 Stimulus generation and offline analysis of data were performed using pClamp software (version 10.2; Axon Instruments).

### *Immunocytochemistry*

SPON neurons were filled with 0.1% Neurobiotin contained in the patch pipette and visualized with Texas Red streptavidin (20  $\mu$ g/ml; Molecular Probes, Eugene, OR, USA). Following recordings, brain slices were placed in 4% paraformaldehyde overnight. Immunohistochemistry was applied to free floating brain slices by rinsing with phosphate buffered saline (PBS) and then exposing slices to a blocking solution (BS) containing 1% bovine serum albumin and 0.5% Triton X-100 in PBS. Next, sections were incubated with a primary antibody of rabbit anti-VGAT (1:400; Vector Labs, Burlingame, CA, USA). VGAT immunoreactivity was visualized with a secondary antibody raised in donkey conjugated to Alexa 488 (1:200; Molecular Probes) in BS for two hours at room temperature. Sections were then rinsed and cover-slipped with Vectashield medium (Vector Labs). Sections were examined with a fluorescence microscope (Observer Z1, Zeiss, Germany) equipped with a digital camera (AxioCam, MRm, Zeiss).

Immunolabeling was identified with red and green filters that permitted visualization of Texas Red and VGAT, respectively. Images from red and green channels were acquired digitally and overlaid (AxioVision version 4.8, Zeiss) to view filled neurons against background VGAT staining of the superior olivary complex.

### *Cell reconstructions*

Brain slices that contained successfully filled neurons were imaged on a laser scanning confocal microscope (LSM 510; Zeiss, Germany) using a 40x oil immersion lens (0.8 NA, Zeiss). Cell reconstructions were performed with Imaris (version 7.2.3; Bitplane, Zurich, Switzerland). A combination of automatic and manual tracing functions was used to map the cell bodies and processes of fluorescent cells. For cell bodies, three-dimensional volume and sphericity were measured. For dendrites, the following parameters were measured: convex hull volume, convex hull sphericity, total dendrite length, number of Sholl intersections (25  $\mu\text{m}$  increments), and number of dendrite endpoints. Descriptions of the measured soma and dendrite properties are described in Table 2.1. Axons were identified based on their small diameters compared to primary dendrites. For some neurons, axons appeared damaged, while axons for other neurons could not be clearly identified; thus, due to an inadequate sample of well-filled axons, quantitative analyses of properties of these processes were not attempted in this study.

### *Principal component analysis and cluster analysis*

Data matrices were constructed, with each row corresponding to a SPON neuron and each column corresponding to a physiological or morphological variable. To determine whether distinct groups of neurons existed based on the parameters described above, principal component analysis (PCA) was performed using data mining software (Unscrambler X, version 10.1, Oslo, Norway). The purpose of PCA was to identify the number of clusters that shared similar features. PCA decreases the dimensionality of the data set while preserving much of the variance by mapping the coordinate system defined by the original variables to a new, lower dimensional coordinate system. These new

coordinates defined by principal components are orthogonal, linear combinations of the original variables. If some of the original variables are correlated, the principal components act to reduce redundancy. Thus, a new space is created through PCA onto which data sets can be projected and classified by cluster analysis (Benavides-Piccione et al., 2005; McGarry et al., 2010).

Based on the results of PCA, specific numbers of clusters were chosen and cluster analysis was performed on the data sets in the principal component vector space. Hierarchical clustering was performed using Euclidian distance squared as the multi-dimensional distance metric and Ward's method as the linkage rule (Ward, 1963). Group means and standard errors were calculated for each variable and groups were compared for significant differences (Mann Whitney U test). Significant differences between groups signaled which variables were important.

## Results

A total of 28 neurons were recorded in mouse SPON. Of these, 17 cells were successfully filled with neurobiotin and used for three-dimensional reconstructions. An additional five SPON cells that neighbored recorded units were also extensively filled by an undetermined mechanism and included in morphological analyses. The locations of cells within the SPON that provided both physiological and morphological data and had brainstem overview images are shown in Figure 2.1. Neurons that yielded physiological data, but were not successfully filled, were presumed to be in the SPON based on their responses to hyperpolarizing current injections (Kopp-Scheinflug et al., 2010; Magnusson et al., 2010) and schematic drawings of the brain slice that were made before removal of the pipette from the tissue. To assess whether distinct classes of SPON neurons were present based on physiology and morphology, principal component analysis (PCA) was performed on the 17 units described above using a set of variables described in Table 2.1. Based on the PCA results, no distinct cell types were found when cell physiology and morphology were combined in the analysis. A likely factor in this negative result is the large number of variables relative to the small number of cells. Thus, to maximize the statistical power of the PCA, physiological and morphological properties were analyzed separately to increase the ratio of the number of cells to the number of variables used. Apart from PCA, scatterplots were constructed using physiological and morphological variables to determine whether any relationships were present. Measures of correlation strength for these plots are listed in Table 2.2. Of the 25 comparisons examined, two had statistically significant correlations. Specifically, mean spike duration was positively correlated with total dendritic length ( $p= 0.02$ , Spearman rank-order test) and mean spike amplitude was negatively correlated with dendritic hull sphericity ( $p= 0.02$ , Spearman; Fig. 2.2).

### *Distinct types of SPON neurons based on physiological properties*

The complete series of electrophysiological tests in the recording protocol was conducted for 28 neurons in the mouse SPON. Tests consisted of a series of current injections from -



500 to 300 pA in 100 pA increments. Responses to depolarizing current pulses were measured, but spiking was highly variable. Three main discharge patterns were observed in response to 100 pA depolarization: onset (n= 11; 1-3 spikes), sustained-adapting (n= 9; 3-30 spikes) and sustained-regular (n= 4; 5-25 spikes) (for definitions of discharge patterns see Peruzzi et al., 2000). Three additional units required currents greater than 100 pA to elicit spiking, and one unit did not spike to the highest magnitude of current injection (300 pA). Also, 9 of 11 onset patterns changed to sustained-adapting when the current level was increased from 100 to 300 pA. Due to the high variability of responses to depolarizing stimuli, the focus of this study was on rebound depolarization and spiking to hyperpolarizing stimuli, which was more consistent across cells and stimulus levels. In addition, offset spiking is more prominent and thought to exert greater influence on synaptic targets compared to spiking during the stimulus *in vivo* (Felix II et al., 2011; Kadner and Berrebi, 2008). To determine whether cells represented a homogeneous or heterogeneous population, PCA was performed on the data set. To limit the number of variables used in the PCA, only the following parameters were used: first spike latency from the stimulus offset, percent voltage sag, spike number, and mean action potential duration and amplitude. The first two principal components based on these values accounted for 98% of the variance in the data set. Unsupervised hierarchical clustering was then performed to determine whether two distinct types of neuronal responses were present. Inspection of the cluster analysis revealed that two basic types of neurons were present, hereafter termed Type 1 and Type 2 units (Fig. 2.3A). PCA confirmed that units belonging to the two groups were clearly separated along the first, but not the second, principal component (Fig. 2.3B). For PCA, the loadings of the data matrix provide information about how much each variable used in the analysis contributes to the explained variance for each principal component. Loadings can range from -1.0 to 1.0, and the closer a variable loading value is to these extremes, the more variance it accounts for. Conversely, values close to zero account for very little variance for a given principal component. For the current data set, the most variance for principal component 1 was accounted for by mean action potential amplitude, followed by mean first spike latency, with loading values of 0.95 and 0.28, respectively. In contrast, mean action potential duration, number of spikes and percent voltage sag accounted for little variance, with

values of -0.05, -0.03 and 0.0009, respectively. For principal component 2, mean action potential latency and amplitude again accounted for the majority of variance, however, in this case, the loading value for latency was much larger (0.96) compared to spike amplitude (-0.28). Loading values for mean action potential duration, number of action potentials and mean percent sag were 0.05, -0.01 and -0.002, respectively.

Values for physiological variables from all recorded units are shown in Table 2.3. Representative neuronal responses are shown for Type 1 and Type 2 units in Figure 2.4. The example of a Type 1 unit shows a characteristic sag in membrane voltage following the onset of the stimulus that increases in magnitude with increasing stimulus current level (Fig. 2.4A). Type 2 units also had prominent voltage sag that increased with the stimulus magnitude (Fig. 2.4B). When responses to the stimulus offset were examined, Type 1 units were marked by sharp, high amplitude spikes (Fig. 2.4C), compared to Type 2 units, which had broad action potentials (Fig. 2.4D). In addition, Type 2 cells often (39% of units) possessed one high amplitude spike, followed by a series of low amplitude spikelets (Fig. 2.4D); this type of response was not observed for any Type 1 units. Type 1 cells were recorded in locations throughout the SPON (Fig. 2.4E), whereas Type 2 cell recordings were restricted to the dorsolateral region (Fig. 2.4F) based on histologically verified cell reconstructions. Due to the low number of neurons in the data set, it is difficult to know whether Type 2 units are restricted to the dorsolateral SPON or if a sampling bias was responsible for the observed proximity of cell locations. Classification of a neuron into Types 1 or 2 did not depend on the age of the animal, as there was no significant difference between the age of the animals in each group ( $p= 0.31$ , Mann Whitney U test).

Figure 2.5 displays comparisons for each of the other five response variables used for segregation of Type 1 and Type 2 neurons. With respect to the average first spike latency from the stimulus offset, there was no difference in values for Type 1 ( $14.87 \pm 2.60$  ms) and Type 2 ( $12.20 \pm 0.40$  ms) units ( $p= 0.40$ , Mann Whitney U test; Fig. 2.5A). A significant difference was observed in average spike duration between cell types ( $1.68 \pm 0.21$  ms versus  $3.09 \pm 0.01$  ms for Type 1 and Type 2 units, respectively;  $p= 0.04$ , Mann Whitney U test; Fig. 2.5B). The most highly significant difference between groups was in the average spike amplitude, where Type 1 units possessed higher amplitudes

( $71.02 \pm 1.78$  mV) compared to Type 2 units ( $53.23 \pm 0.01$  mV;  $p < 0.001$ , Mann Whitney U test; Fig. 2.5C). No difference in the average number of spikes was found between Type 1 and Type 2 cells ( $p = 0.09$ , Mann Whitney U test; Fig. 2.5D), although there appeared to be a trend where Type 1 units tended to have fewer spikes ( $1.30 \pm 0.15$ ) compared to Type 2 units ( $1.94 \pm 0.22$ ). For the average percentage voltage sag at the beginning of responses, both cell types were statistically equivalent ( $28.46 \pm 3.73$  % versus  $23.31 \pm 2.19$  % for Type 1 and Type 2 units, respectively;  $p = 0.19$ , Mann Whitney U test; Fig. 2.5E).

Resting membrane potential and input resistance were not included in the PCA due to an attempt to limit the number of variables used. The entire population of SPON units had an average resting membrane potential of  $-51.31 \pm 0.75$  mV and an average input resistance of  $94.45 \pm 7.13$  M $\Omega$ . For the two SPON cell types determined by PCA and cluster analysis, there was no significant difference in either resting membrane potential ( $p = 0.10$ , Mann Whitney U test) or input resistance ( $p = 0.12$ , Mann Whitney U test).

### *Morphological characterization of SPON neurons*

A total of 22 SPON neurons were filled with neurobiotin. Of these, 17 were characterized physiologically. Five sections had a second labeled cell that had lower levels of fluorescence compared to neighboring filled cells, and thus were not considered to be recorded from. Following recordings, brain slices were processed to reveal filled SPON neurons, as well as background VGAT staining, which outlined brainstem auditory nuclei (Fig. 2.6A). These brainstem overview images were used to locate filled cells within the SPON (Fig. 2.1B). Three-dimensional reconstructions were then performed for each filled cell (Fig. 2.6B) and morphological measurements were obtained, as described in Table 2.1. Unfortunately, axons could not be reliably reconstructed for all neurons, and thus information regarding these processes was excluded from further analyses. Both PCA and cluster analysis returned no distinct groups among morphological variables of cell bodies and dendrites. Based on these results, mouse SPON neurons are considered to be a morphologically-homogeneous population, similar to findings from the rat SPON

(Kulesza Jr. and Berrebi, 2000; Saldaña and Berrebi, 2000). Although no distinct subtypes were present, some variability across morphological parameters was present. A list of average values for all morphological measurements is given in Table 2.3.

Neurons had an average cell body volume of  $5949.60 \pm 445.97 \mu\text{m}^3$ , with sizes ranging from  $3910.40$  to  $8134.06 \mu\text{m}^3$ . Cell body sphericity ranged from highly spherical (0.89) to elongated (0.49), with an average value of  $0.69 \pm 0.02$ . Dendritic fields were characterized by both size and shape. The total length of dendrites had a range of  $399.82$  to  $2005.74 \mu\text{m}$ , with an average of  $912.01 \pm 102.44 \mu\text{m}$ . The sizes of dendritic fields were also estimated by measuring the convex hull for each neuron, which averaged  $741481.43 \pm 87913.53 \mu\text{m}^3$ , and ranged from  $180848$  to  $1460630 \mu\text{m}^3$ . While some dendrites appeared to extend beyond the image field of view, the majority were clearly contained within the confocal image stack. The average orientation of dendrites was measured by convex hull sphericity. All dendritic sphericity values were greater than 0.65, with an average value of  $0.73 \pm 0.01$ , suggesting that the dendrites of SPON neurons may have a preferred orientation. However, a specific direction for such a preferred orientation could not be generalized based on the current data set.

The properties of dendritic fields were examined more closely by performing a Sholl analysis. This metric measured how many times dendrites crossed concentric spheres located at  $25 \mu\text{m}$  intervals, beginning at the cell body. As with neurons in other brain regions (Benavides-Piccione et al., 2005; McGarry et al., 2010), the number of intersections increased from  $7.20 \pm 1.24$  at  $25 \mu\text{m}$  to  $8.60 \pm 1.57$  and  $8.80 \pm 1.53$  at  $50 \mu\text{m}$  and  $75 \mu\text{m}$ , respectively, then decreased to  $4.00 \pm 1.00$  at  $100 \mu\text{m}$  from the cell body. To further characterize dendritic fields, the total number of branching points was measured and was highly variable, ranging from 8 to 31, with an average of  $20.29 \pm 3.23$ . In addition, the total number of terminal dendrite points was measured and averaged  $27.48 \pm 3.47$ , with a range of 7 to 39.

Examples of typical SPON neurons are shown in Figure 2.7. These cells were marked by large cell bodies ( $> 6000 \mu\text{m}^3$ ) and dendrites that projected in the dorsomedial and ventrolateral directions. Neurons that fit this description represented 13 of 22 filled cells. Another pattern observed in 4 neurons consisted of dendrites that extended ventrally over long distances ( $> 150 \mu\text{m}$ ) with little branching. Examples of 2 of these

cells are shown in Figure 2.8. The remaining neurons were highly variable in their dendritic orientation and branching patterns, but generally appeared to possess dendrites that extended in many directions and had high degrees of branching. An additional interesting feature from the cell morphology data set was the presence of a second filled cell. In each of the five cases where two cells in the same slice were reconstructed, dendrites of neighboring cells appeared to contact each other at multiple locations (Fig. 2.9). The majority of dendro-dendritic contacts appeared *en passant*; however, in a few instances, the dendrite of one cell appeared to terminate on the dendrite of a neighboring cell (Fig. 2.9 top left panel inset). Although, a potential cell to cell interaction has been proposed for neighboring SPON neurons, it was in the context of axo-dendritic, not dendro-dendritic connections (Saldaña et al., 2009; Saldaña and Berrebi, 2000).

## Discussion

The results presented here provide the first detailed characterization of physiologically and morphologically characterized neurons in the mouse SPON. Using principal component analysis (PCA) and hierarchical clustering methods, two distinct neuronal types were described based on responses to hyperpolarizing current injections. One type was marked by highly transient, large amplitude action potentials; while the second type had lower amplitude action potentials with larger spike widths. After using PCA to examine morphological features of SPON neurons, no distinct subtypes were found; although some variations in the size and shapes of cell bodies and dendritic arbors were observed. No distinct cell types were discovered based on a combination of physiological and morphological properties using PCA, however values for mean spike duration and total dendritic length, as well as mean spike amplitude and dendritic hull sphericity were correlated, respectively. It is unclear if these relationships are functionally important or an artifact of the limited sample size. In either case, these potential structure-function properties are worthy of additional studies that are more focused on these attributes.

### *Physiological response properties of SPON neurons in vitro*

Within the last decade, there has been a focus on characterizing the physiological properties of SPON cells *in vivo* (Behrend et al., 2002; Dehmel et al., 2002; Kulesza Jr. et al., 2003; 2007; Kadner and Berrebi, 2008; Kadner et al., 2006), however, little is known about the intrinsic properties of these cells. Recently, two studies characterizing SPON neuronal responses *in vitro* have been reported (Kopp-Scheinflug et al., 2010; Magnusson et al., 2010). Findings from these reports provide evidence that spiking is generated by a rebound from hyperpolarizing current injections, and that hyperpolarization-activated outward (I<sub>h</sub>) currents mediate spiking responses. The results from the current study are in agreement with these findings, as neuronal responses showed rebound spiking and a clear sag in the membrane voltage following the stimulus onset, typically attributed to I<sub>h</sub> currents (Aizenman and Linden, 1999; Sun and Wu, 2008). While spiking to the stimulus offset is an accepted feature of SPON responses,

there have been conflicting reports regarding the nature of spiking. For example, Kopp-Scheinflug and colleagues (2010) found that SPON spiking was sometimes “chopper-like” with bursts of spiking interrupted by regular periods of silence. In addition, rebound spiking was often delayed with respect to the stimulus offset. In contrast, Magnusson et al. (2010) observed spiking that was very transient (1-3 spikes) and occurred after only a short delay from the end of current pulses. SPON responses recorded in the present study had bursts of 1-4 spikes that generally occurred within 25 ms of the stimulus offset. However, in two cases, first spike latencies exceeded 40 ms, suggesting that delayed spiking occurs, but is rare. Another finding from previous SPON recordings was the presence of a subset of responses characterized by one large action potential followed by a burst of lower amplitude spikelets (Magnusson et al., 2010). Such responses were also observed in the present study (see Fig. 2.4D) and comprised 7 of 18 Type 2 units. Units that had complex spiking were found to represent a type of SPON neuron based on the amplitude and duration of action potential; however, Magnusson et al. (2010) found no differences between complex and simple spiking SPON neurons after statistically comparing cell properties. Thus, further characterization is needed for a more complete classification of complex spiking cells in the SPON. For instance, adding Mibefradil or  $\text{Ni}^{2+}$  to the bath during in vitro experiments could shed light on whether complex spiking observed for SPON neurons is mediated by calcium, and whether abolishing calcium currents could transform Type 2 responses into Type 1.

#### *Morphological characteristics of SPON neurons*

To determine whether distinct cell types were present in the SPON, values for seven morphological variables were analyzed with PCA. Variables included: soma volume and sphericity, dendritic length, branch points, terminal points and convex hull volume and sphericity. Based on PCA, multiple distinct neuronal morphologies were not present, although variations in cell size and shape were observed. One limitation of the PCA was the limited number of cells in the data set ( $n=22$ ). For an optimal outcome of PCA, the number of cells should be at least five times greater than the number of variables used (Morrison, 1967), which was not the case in this study. Thus, additional experiments are

ongoing in an attempt to verify the results presented here with increased statistical power. Based on the data from the current data set, SPON cells in the mouse appear to be a homogeneous population, similar to reports in the rat (Kulesza Jr. and Berrebi, 2000; Saldaña and Berrebi, 2000).

The only other report of SPON cell morphology in the mouse is from Ollo and Schwartz (1979). Using Golgi staining methods, neurons were described as large and either round or spindle shaped, with long dendrites that emerged from the cell body in all directions. In addition, cells were reported to have the same shape, regardless of the plane of sectioning. In the present study, neurons were found to be large with long dendrites in many cases. However, cell body sphericity measures indicated that the majority of cells were neither round nor spindle-shaped, but somewhere in between. While some dendrites emerged from the cell body in many directions, most (17 of 22) either had dendrites oriented in the dorsomedial and ventrolateral directions or ventrally; although, this directionality did not warrant separate classes of cells based on PCA. The general SPON cell body shape corresponds most closely with reports in the rat (Saldaña and Berrebi, 2000), where an intermediate shape between round and spindle was described. However, unlike the rat, dendrites of mouse neurons did not have a homogeneous orientation in the sagittal plane. One interesting finding from Saldaña and Berrebi (2000) was the presence of cells in the ventral SPON that had dendrites extending ventrally over long distances into the ventral nucleus of the trapezoid body. Some cells in the present study clearly possessed long ventrally-oriented dendrites; however, they were primarily located in dorsal areas of the SPON, and whether their dendrites extended beyond the borders of the SPON could not be determined based on brainstem overview images.

In general, it appears that the mouse and rat SPON share similar morphological features that may be different from those in other rodent species. There is evidence that both the gerbil and guinea pig may have separate classes of SPON neurons; one type characterized by a large, round cell body sends axonal projections to the inferior colliculus, and a second type that has a highly elongated cell body sends axons to the cochlear nucleus (Kuwabara and Zook, 1999; Schofield, 1991). Because the mouse SPON has a homogeneous cell population, similar to the rat whose SPON is not part of the descending auditory pathway (Saldaña et al., 2009; Vetter and Mugnaini, 1991;



Vetter et al., 1992; 1993), it is presumed that efferent projections to the mouse cochlear nucleus are not present; although a rigorous tract tracing study is needed to definitively map mouse SPON connections. Differences in SPON connectivity between species may be due to evolutionary pressures exerted in each animal model, as mice and rats have audiograms sensitive to relatively high frequencies (Ehret, 1976; Kelly and Masterton, 1977), whereas hearing in gerbils and guinea pigs extends to lower frequencies (Heffner et al., 1971; Rosowski et al., 1999; discussed in Kadner and Berrebi, 2008).

Direct projections of SPON axons go to the inferior colliculus (Saldaña et al., 2009; Saldaña and Berrebi, 2000), medial geniculate body (Jin and Berrebi, 2006) and the tectal-longitudinal column (Aparicio et al., 2010; Saldaña et al., 2007; Viñuela et al., 2011). Another potential target of SPON neurons are neighboring cells within the nucleus. Previous tract tracing studies revealed that SPON neurons give rise to extensive axon collaterals within the nucleus, although the targets of individual axons could not be resolved (Saldaña et al., 2009; Saldaña and Berrebi, 2000). In addition, there is evidence for delayed spiking to periodic sound envelope modulation thought to be mediated by GABA (Kadner and Berrebi, 2008). It has been proposed that the source of this GABAergic input could be from SPON autapses (Kadner and Berrebi, 2008; Kulesza Jr. et al., 2000). In the current study, axons were only identified for a subset of neurons. Many of the axons that were reconstructed appeared damaged. Thus, it was difficult to observe axonal branching, as many of these neurites appeared to have degenerated and did not extend far from the cell body. For the few axons that did extend over large distances, no branching was observed. However, extensive dendro-dendritic contacts between neighboring SPON cells were observed. While it is not known whether these contacts have functional significance, dendro-dendritic intercellular communication is important in other neural systems (Campbell et al., 2009; Cove et al., 2009; Harding, 1971; Sloper and Powell, 1978). Dye-coupling, i.e., neuronal connections via gap junctions that are permeable to dyes, is seen throughout the developing brain (Kandler and Katz, 1995; Peinado et al., 1993). In some cases, dye-coupling increases during development and peaks as late as postnatal day 14, after which, coupling steadily decreases into adulthood (Kandler and Katz, 1998). Labeling of neighboring neurons in the present study occurred in animals whose ages ranged from from postnatal day 5-7.

Thus, dye-coupling is a possible explanation for the observation of multicell labeling. Another explanation that may account for labeled cell pairs is the possibility that the neurobiotin-filled recording electrode impaled a SPON cell during the process of obtaining a whole-cell patch recording from a neighboring neuron. In this scenario, a brief puncture by the electrode may have been sufficient for moderate labeling of one cell, while the longer time period that the electrode remained on the second cell during the recording protocol yielded much stronger labeling. This pattern of disparate immunofluorescence intensity was seen in all labeled cell pairs.

### *Functional Implications*

Spiking to the offset of sound stimuli is a hallmark of SPON neurons common to all species that have been studied thus far (gerbil: Dehmel et al., 2002; rat: Kulesza Jr. et al., 2003; rabbit: Kuwada and Batra, 1999). The results presented herein provide evidence that offset spiking is mediated by a rebound from hyperpolarizing stimuli. The current study also demonstrates that the well-timed, transient nature of SPON spiking described *in vivo* is also present *in vitro*. To date, responses of mouse SPON neurons to sound have not been characterized *in vivo*. Chapters 3 and 4 of this dissertation explore this topic.

In addition to describing physiological properties, morphological features of mouse SPON neurons were characterized. The findings show that neurons are similar in structure to what has been described for the rat SPON, as opposed to other rodent species. The homology between the mouse and rat is explored further in Chapter 3 of this dissertation, as physiological response properties are characterized for the mouse *in vivo*. The demonstration of highly homologous structure and function relationships of the mouse and rat SPON will accelerate understanding of the role of this nucleus in the ascending auditory pathway, as knowledge gathered from past rat studies can guide future experiments that utilize genetic technologies better suited for the mouse model.

## **Acknowledgements**

I gratefully acknowledge Dr. Anna Magnusson training and guidance for slice recordings and immunohistochemistry. I also thank Dr. Magnusson for help with data analysis and interpretation. I thank Drs. Anders Fridberger and Stefan Jacob assistance with confocal imaging. I also thank Dr. Brian Hoffpauir and Mr. Joel Eisenhofer for their help with 3D cell reconstructions.

## A The Superior Olivary Complex

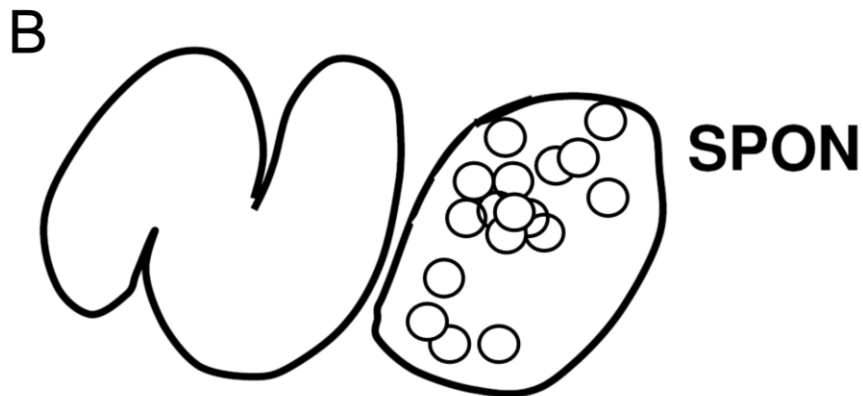
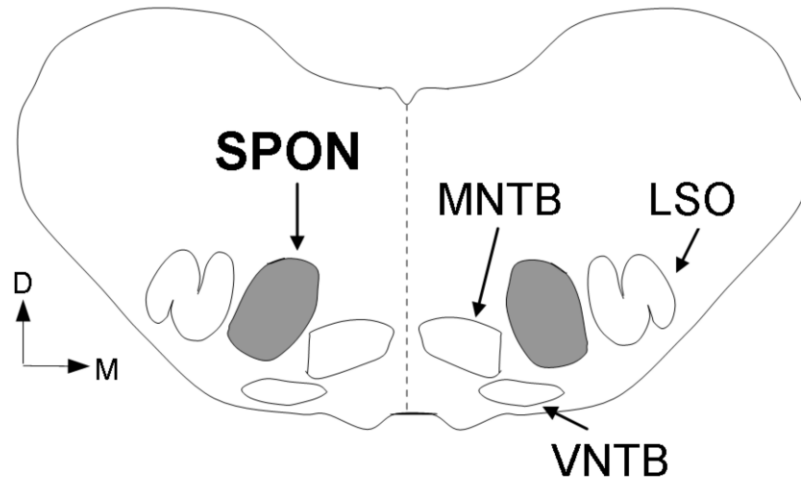


*Fig. 2.1.* Localization of filled neurons recorded within the SPON. (A) Schematic diagram of auditory nuclei in the mouse superior olivary complex. The SPON is bordered medially by the MNTB, laterally by the LSO and ventrally by the VNTB. (B) Schematic diagram of the SPON showing the location of each filled cell from which physiological recordings were obtained and brainstem overview images were collected. D: dorsal; M: medial; MNTB: medial nucleus of the trapezoid body; LSO: lateral superior olive; VNTB: ventral nucleus of the trapezoid body.

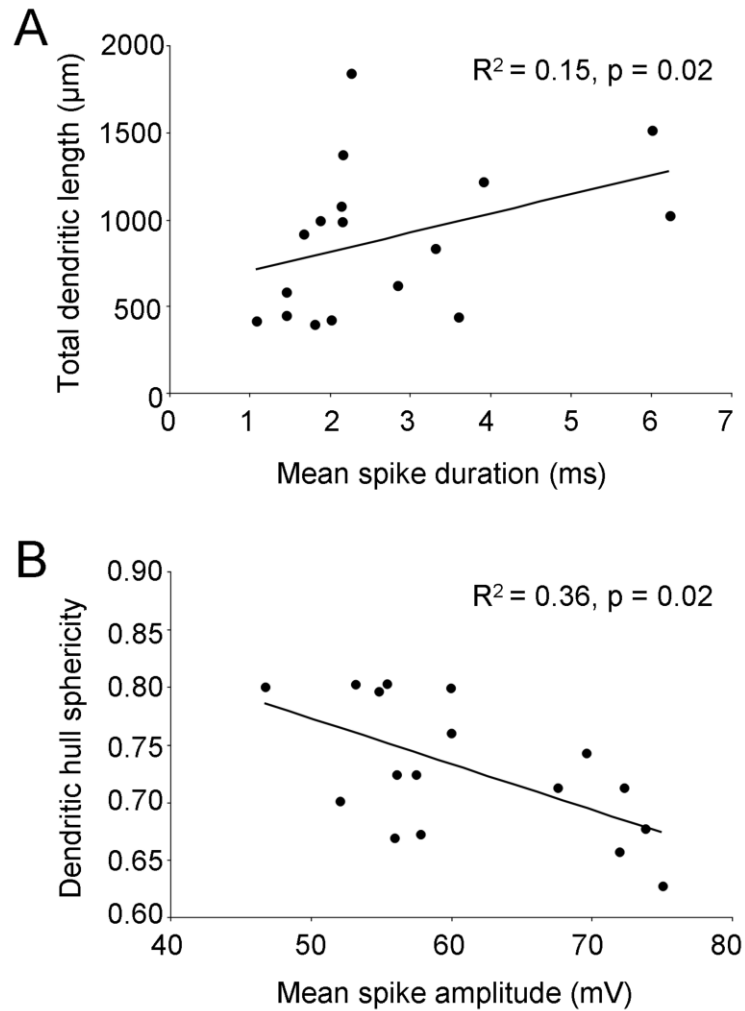


*Fig. 2.2.* Correlated physiological and morphological properties of SPON neurons. (A) The correlation between total dendritic length and mean spike duration were positively correlated. (B) Dendritic hull sphericity and mean spike amplitude exhibited a negative correlation. p values are based on the Spearman rank-order test.

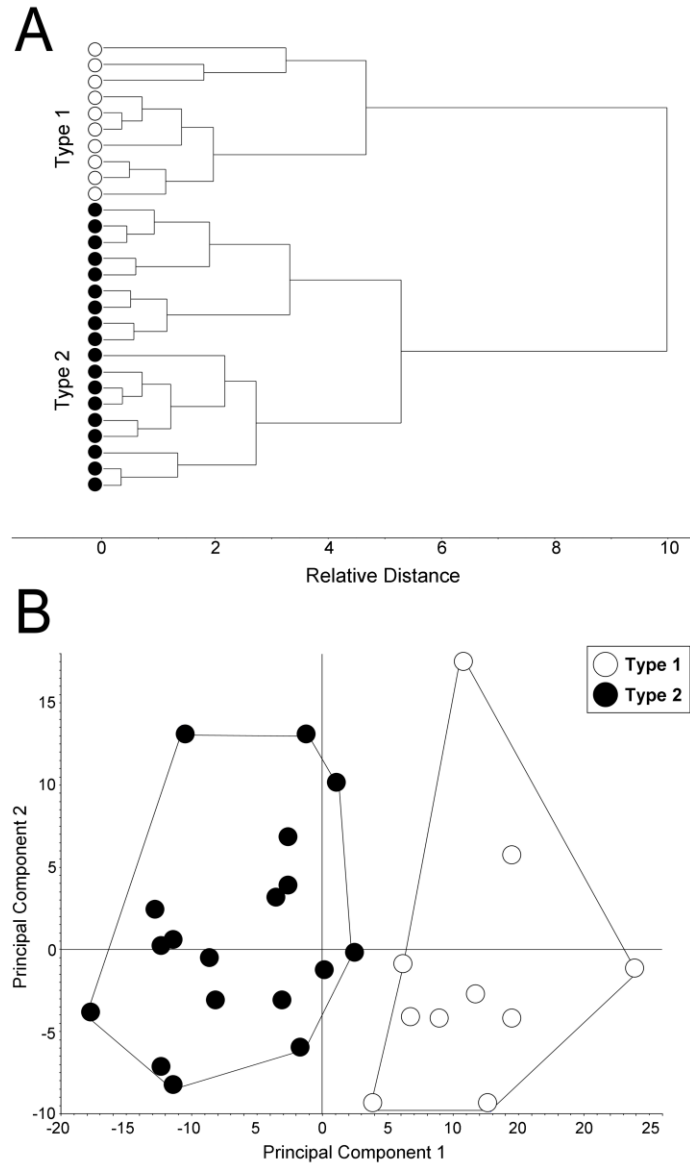


*Fig. 2.3.* The mouse SPON has two physiologically distinct cell types. (A) Ward's method of hierarchical unsupervised clustering based on 5 electrophysiological variables applied to 28 SPON neurons. The first 2 principal components were retained for cluster analysis. The x-axis of the dendrogram shows the relative distance between clusters based on the linkage distance by Euclidian distance squared. The y-axis of the dendrogram shows individual cells for Type 1 (open circles; n= 10) and Type 2 (filled circles; n= 18) SPON units. (B) Scatterplot of the data set in principal component space. The clusters for Type 1 and Type 2 neurons were well differentiated along the first principal component, as shown by non-overlapping convex hulls.

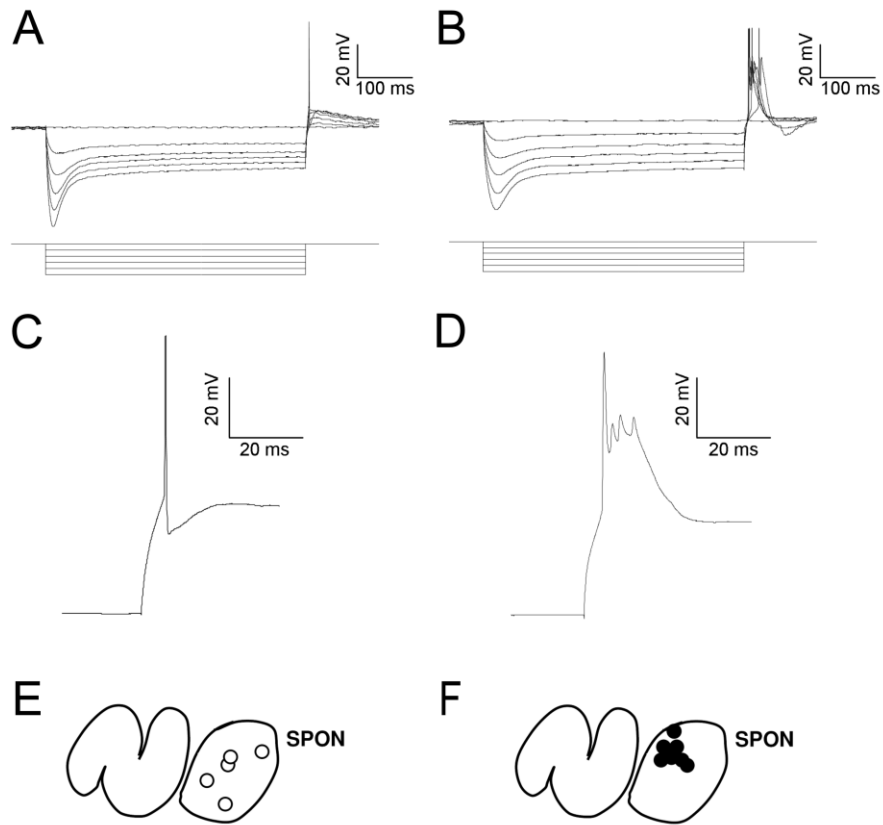


*Fig. 2.4.* Properties of Type 1 and Type 2 SPON neurons. Responses to a series of hyperpolarizing currents varying in amplitude between 0 and -500 pA are shown for representative Type 1 (A) and Type 2 (B) neurons. Type 1 units had responses marked by fewer spikes, shorter spike durations and higher spike amplitudes (C) compared to Type 2 units (D). Schematic diagrams of the locations cells in the SPON that were recorded and filled are shown for Type 1 (E) and Type 2 (F) units.

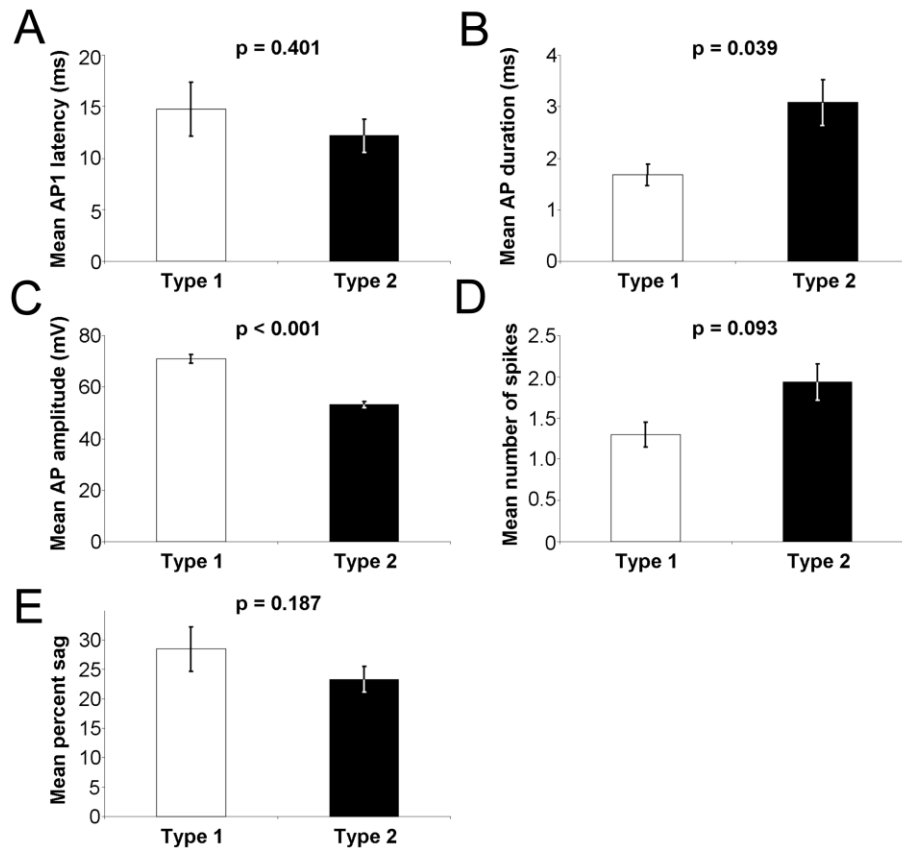


*Fig. 2.5.* Analysis of electrophysiological variables. Comparison of physiological variables distinguishing Type 1 and 2 units with respect to mean action potential latency (A), mean action potential duration (B), mean action potential amplitude (C), mean number of spikes (D), and mean percent voltage sag (see Methods for description). AP: action potential; AP1: first action potential. P values represent results of the Mann Whitney U test for unmatched pairs, with the significance level set to  $p < 0.05$ .



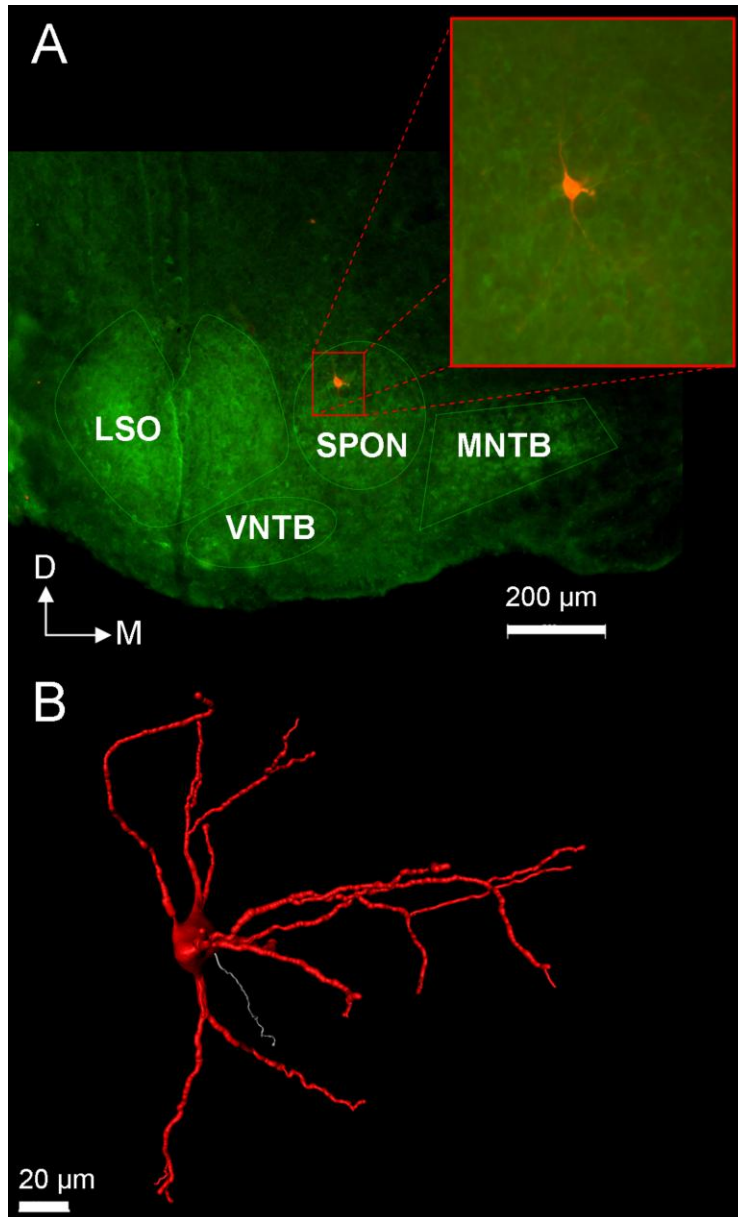


*Fig. 2.6.* An example of a reconstructed SPON neuron. (A) Overview of the left brainstem showing VGAT staining (green) to outline the nuclei of the superior olivary complex and neurobiotin labeling (red) of the filled cell. Inset: enlarged image of the filled SPON cell. (B) Snapshot of the 3D reconstructed neuron shown in part A in the coronal plane. The white filament represents the axon. D: dorsal; M: medial; SPON: superior paraolivary nucleus; MNTB: medial nucleus of the trapezoid body; VNTB: ventral nucleus of the trapezoid body; LSO: lateral superior olive.

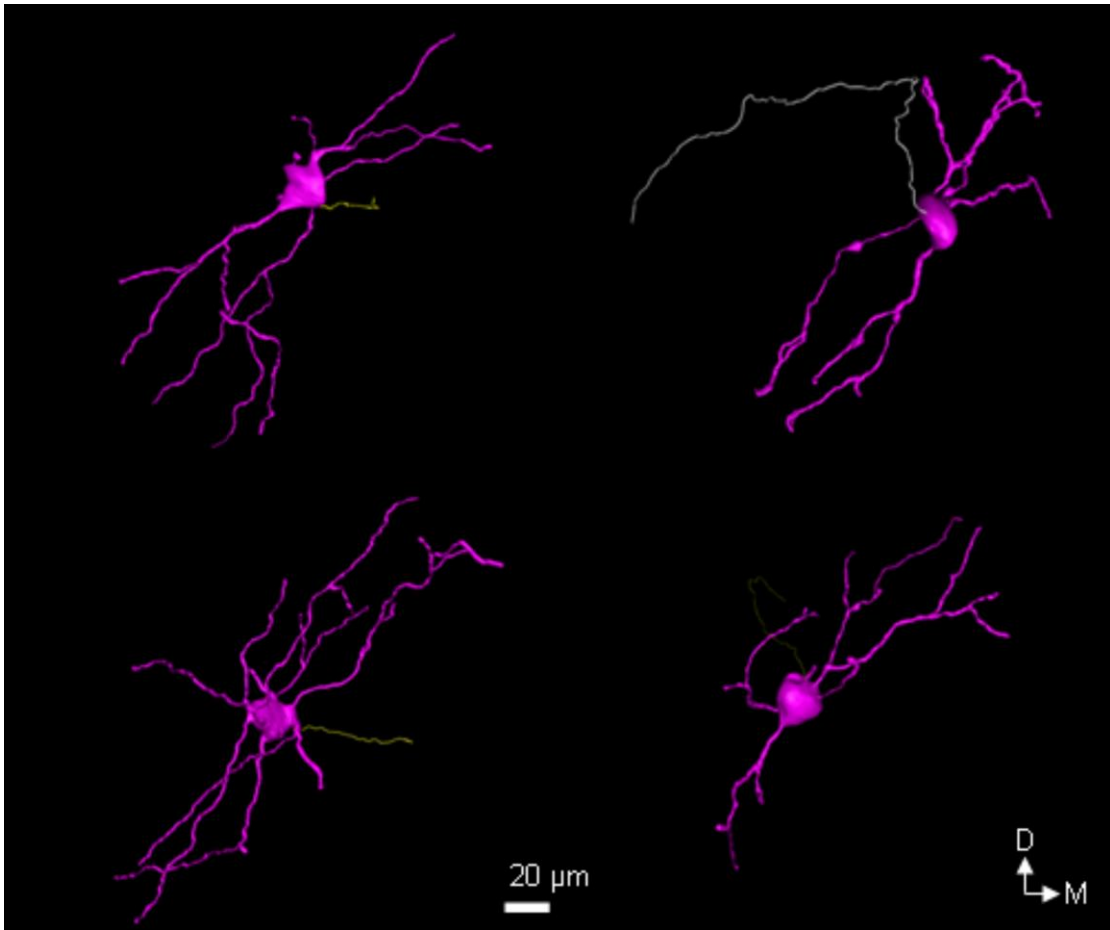


*Fig. 2.7.* Reconstructions of representative SPON neurons. Typical neurons had large cell bodies and dendritic arbors that extended in the dorsomedial and ventrolateral directions. Cells that fit this basic description comprised 13 of 22 filled neurons. D: dorsal; M: medial.

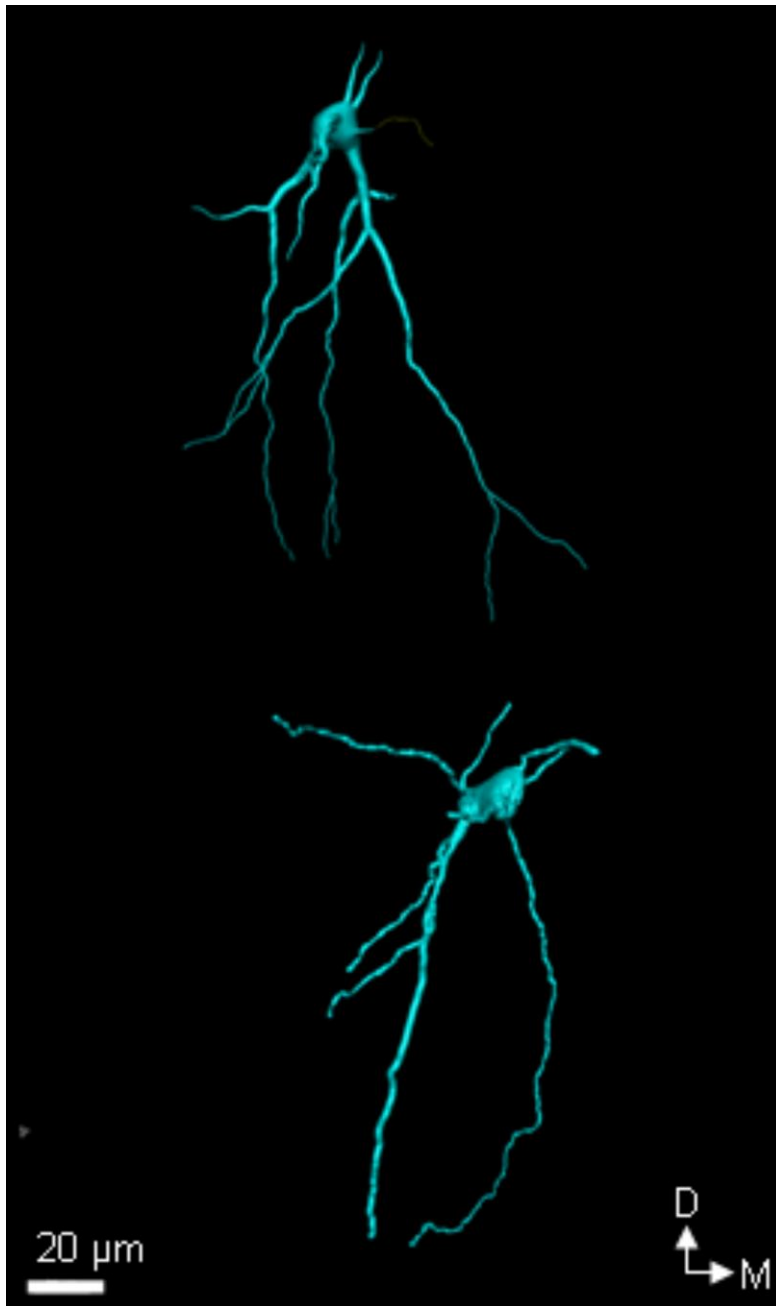


*Fig. 2.8.* Some SPON neurons had highly oriented dendritic fields. Examples of two of the five neurons that had long dendrites extending ventrally are shown. D: dorsal; M: medial.

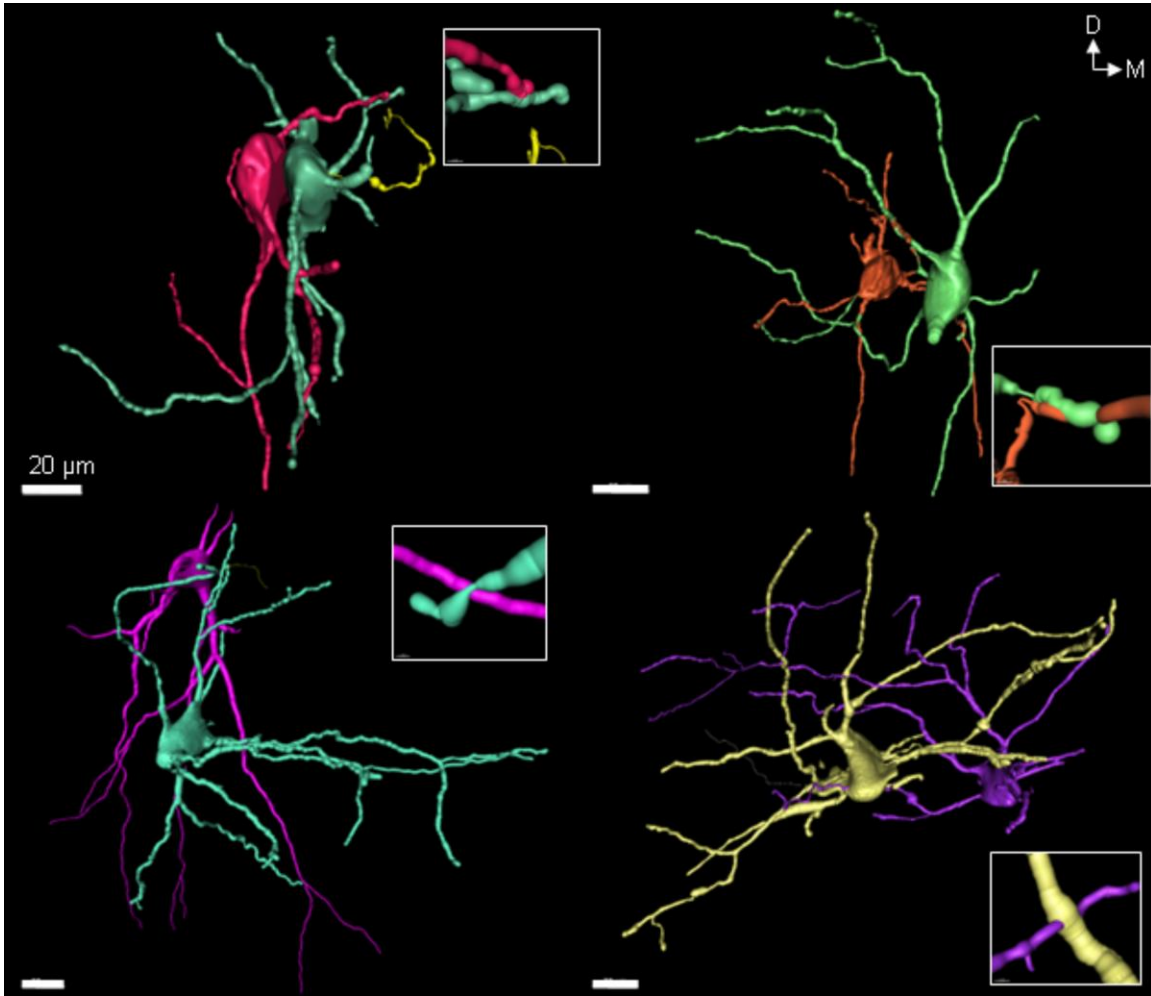


*Fig. 2.9.* Examples of possible dendro-dendritic contacts between SPON neurons. Examples are shown for four of the five cases in which whole cell recordings on one SPON cell resulted in two labeled cells. In each case, multiple instances of contacts between dendrites were observed. An example of dendro-dendritic contacts for each cell pair is shown enlarged in the insets. D: dorsal; M: medial.

Table 2.1. Electrophysiological and morphological variables used for characterizing SPON cells.

<b>Variable</b>	<b>Description</b>
<b>VARIABLES DESCRIBING PHYSIOLOGICAL RESPONSES</b>	
Resting membrane potential (mV)	Stable membrane potential with no current applied
Input resistance (M $\Omega$ )	Calculated from the smallest hyperpolarizing and depolarizing current steps
Spike number	Number of spikes following -300 pA current or lowest hyperpolarizing current magnitude to evoke a response
Spike amplitude (mV)	Mean spike amplitude of all action potentials (APs)
Spike duration (ms)	Mean time from the onsets of the APs, calculated at the inflection point, to the offsets, calculated as the return to the same voltage as before AP onsets
Spike latency (ms)	Time from the end of the stimulus to the inflection point of the first AP
Percent sag	Ratio of the evoked I <sub>h</sub> current-mediated voltage sag and the steady state membrane voltage
<b>VARIABLES DESCRIBING THE SOMA</b>	
Soma volume ( $\mu\text{m}^3$ )	Volume of the soma
Soma sphericity	Ratio of the surface area of a sphere (with the same volume as the soma) to the surface area of the soma
<b>VARIABLES DESCRIBING THE DENDRITES</b>	
Total dendrite length ( $\mu\text{m}$ )	Sum of lengths of all dendrite segments, measured along tracing (not straight line distance)
Dendritic node total	Total number of dendritic nodes (branching points)
Dendritic terminal points	Total number of dendritic terminal points (end points)
Convex hull volume ( $\mu\text{m}^3$ )	Volume of the 3-D convex polygon created by connecting the distal dendrite segment endpoints
Convex hull sphericity	Ratio of the surface area of a sphere (with the same volume as the dendritic convex hull) to the surface area of the convex hull
Dendritic Sholl crossings	The number of dendritic segments that cross Sholl sections at 25, 50, 75 and 100 $\mu\text{m}$ from the soma

Table 2.2. Correlations between values for physiological and morphological variables.

<b>Variable Combination</b>	<b>R<sup>2</sup></b>	<b>p value*</b>
First-spike latency - Dendritic hull volume	< 0.001	0.07
First-spike latency - Dendritic hull sphericity	< 0.001	0.73
First-spike latency - Dendritic length (total)	0.02	0.64
First-spike latency - Dendritic nodes	0.11	0.19
First-spike latency - Dendritic terminals	0.12	0.26
Mean spike duration - Dendritic hull volume	0.03	0.13
Mean spike duration - Dendritic hull sphericity	0.17	0.09
Mean spike duration - Dendritic length (total)	0.15	0.02
Mean spike duration - Dendritic nodes	0.16	0.28
Mean spike duration - Dendritic terminals	0.04	0.79
Mean spike amplitude - Dendritic hull volume	0.03	0.99
Mean spike amplitude - Dendritic hull sphericity	0.05	0.02
Mean spike amplitude - Dendritic length (total)	0.01	0.76
Mean spike amplitude - Dendritic nodes	0.04	0.78
Mean spike amplitude - Dendritic terminals	0.07	0.71
Number of spikes - Dendritic hull volume	0.16	0.27
Number of spikes - Dendritic hull sphericity	0.10	0.48
Number of spikes - Dendritic length (total)	0.02	0.19
Number of spikes - Dendritic nodes	0.04	0.20
Number of spikes - Dendritic terminals	0.07	0.44
Percent voltage sag - Dendritic hull volume	0.08	0.92
Percent voltage sag - Dendritic hull sphericity	0.12	0.10
Percent voltage sag - Dendritic length (total)	0.13	0.22
Percent voltage sag - Dendritic nodes	0.03	0.65
Percent voltage sag - Dendritic terminals	0.01	0.99

\* As determined by the Spearman rank-order correlation coefficient.

Table 2.3. Average values and standard errors for physiological and morphological variables.

<b>Variable</b>	<b>Mean Value</b>
<b>VARIABLES DESCRIBING PHYSIOLOGICAL RESPONSES</b>	
Resting membrane potential (mV)	-51.31 ± 0.75
Input resistance (MΩ)	94.45 ± 7.13
Spike number	1.71 ± 0.16
Spike amplitude (mV)	60.58 ± 1.93
Spike duration (ms)	2.59 ± 0.31
Spike latency (ms)	13.15 ± 1.39
Percent sag	25.15 ± 1.96
<b>VARIABLES DESCRIBING THE SOMA</b>	
Soma volume (μm <sup>3</sup> )	5949.60 ± 445.97
Soma sphericity	0.69 ± 0.02
<b>VARIABLES DESCRIBING THE DENDRITES</b>	
Total dendrite length (μm)	912.01 ± 102.44
Dendritic node total	20.29 ± 3.23
Dendritic terminal points	27.48 ± 3.47
Convex hull volume (μm <sup>3</sup> )	741481.43 ± 87913.53
Convex hull sphericity	0.73 ± 0.01
Sholl crossings – 25 μm	7.2 ± 1.24
Sholl crossings – 50 μm	8.6 ± 1.57
Sholl crossings – 75 μm	8.8 ± 1.53
Sholl crossings – 100 μm	4.0 ± 1.0

## **Chapter Three**

### **Effects of ketamine on response properties of neurons in the superior paraolivary nucleus of the mouse**

This work was submitted for publication to Neuroscience



## **Abstract**

The superior paraolivary nucleus (SPON) is a prominent brainstem structure that provides strong inhibitory input to the auditory midbrain. Previous studies established that SPON neurons encode temporal sound features with high precision. These earlier characterizations of SPON responses were recorded under the influence of ketamine, a dissociative anesthetic agent and known antagonist of NMDA receptors. Because excitatory neurotransmission via NMDA receptors contributes to their response properties, single unit extracellular recordings of SPON neurons were performed in the presence and absence of ketamine. In doing so, this study represents the first in vivo examination of the SPON of the mouse. Herein, independent groups of SPON neurons are characterized that did or did not receive ketamine, as well as neurons that were recorded both prior to and following ketamine administration. In all conditions, SPON neurons exhibited contralaterally-driven spikes triggered by the offset of pure tone stimuli. Ketamine lowered both evoked and spontaneous spiking, decreased the sharpness of frequency tuning and increased auditory thresholds and first-spike latencies. In addition, ketamine limited the range of modulation frequencies to which neurons phase-locked to sinusoidally amplitude-modulated tones, although vector strengths remained high in all conditions that evoked sufficient spiking. These results suggest that ketamine anesthesia lowers the general excitability of SPON neurons, but does not substantially affect the temporal precision of their offset responses.

## Introduction

The ability to precisely encode temporal sound features is a critical requirement of the central auditory system, and the superior paraolivary nucleus (SPON) appears well-suited to carry out temporal processing tasks. This nucleus has been most extensively studied in rats, where SPON neurons respond sensitively to gaps in pure tones and to modulations of sinusoidally amplitude-modulated (SAM) tones (Kadner and Berrebi, 2008). These properties are consistent with the known cell types from which the SPON receives its synaptic innervation (discussed in Behrend et al., 2002; Kulesza Jr. et al., 2007). Specifically, the SPON is the target of excitatory inputs from octopus and multipolar cells of the cochlear nucleus (Friauf and Ostwald, 1988; Thompson and Thompson, 1991; Schofield and Cant, 1995), which fire precisely-timed action potentials that exhibit a high degree of synchronicity in response to SAM stimuli (Rhode et al., 1983; Rhode and Greenberg, 1994; Golding et al., 1995; 1999; Ferragamo et al., 1998; Oertel, 1999; Trussell, 1999). Moreover, the medial nucleus of the trapezoid body (MNTB), whose glycinergic neurons produce primary-like responses to pure tones and also phase-lock with high accuracy to SAM tones, provides a strong input to the SPON (Morest, 1968; Bledsoe et al., 1990; Banks and Smith, 1992; Forsythe and Barnes-Davies, 1993; Schofield and Cant, 1995; Sommer et al., 1993; Smith et al., 1998; Kadner and Berrebi, 2008).

Previous *in-vivo* studies of SPON physiology were conducted under ketamine anesthesia (Behrend et al., 2002; Dehmel et al., 2002; Kulesza Jr. et al., 2003; 2007; Kadner et al., 2006; Kadner and Berrebi, 2008), which has the potential to alter the balance of excitatory and inhibitory inputs that contribute to neuronal response properties (Kulesza Jr. et al., 2007). Ketamine is known to alter brainstem auditory evoked potentials, resulting in higher peak latencies (Church and Gritzke, 1987; Smith and Mills, 1989; 1991) and elevated thresholds (van Looij et al., 2004); both of these effects are likely mediated by antagonism of the N-methyl-D-aspartate glutamate receptor (NMDAR; Anis et al., 1983; Harrison and Simmonds, 1985). NMDARs are widely distributed in auditory brainstem structures, including the SPON (Petrulia et al., 1994a, b; Sato et al., 1999), cochlear nucleus (Bilak et al., 1996; Sato et al., 1998; Petrulia et al.,

1994a, b; 2000), and MNTB (Petralia et al., 1994a, b; Sato et al., 1999; Nakagawa et al., 2000). Moreover, *in-vivo* and *in-vitro* physiological studies of the auditory brainstem and midbrain have shown that pharmacologic blockade of NMDARs reduces excitability in many cell types (*cochlear nucleus*: Martin, 1985; Isaacson and Walmsley, 1995; Ferragamo et al., 1998; *lateral superior olive*: Caspary and Faingold, 1989; Wu and Kelly, 1992; *medial superior olive*: Smith et al., 2000; MNTB: Forsythe and Barnes-Davies, 1993; Hamann et al., 2003; *midbrain*: Faingold et al., 1989; Feldman and Knudsen, 1994; Zhang and Kelly, 2001; Wu et al., 2002; Sanchez et al., 2007). Given ketamine's known effects on NMDARs, it's plausible that *in-vivo* responses of SPON neurons reported previously may not accurately represent the activity of this nucleus in the normal waking state.

Single-units were recorded in the mouse SPON, both in the absence and presence of ketamine, and each units' characteristic frequency, threshold, response map, sharpness of frequency tuning, and the acuity with which they phase-locked to SAM stimuli was determined. Quantitative analyses were performed to determine whether administration of ketamine anesthesia was accompanied by changes in these response properties.

This study represents the first characterization of the mouse SPON, but this species is becoming an increasingly common experimental animal for future auditory studies because it affords two unique opportunities. Unlike the rat, where removal of cerebellum – which requires anesthesia- is necessary to make the brainstem practically accessible to micropipettes, the small head size of the mouse is compatible with microelectrode penetrations through the intact brain, so that recordings from the auditory brainstem are possible without anesthesia (Portfors and Felix, 2005; Felix and Portfors, 2007; Bryant et al., 2009). Beyond addressing anesthesia-related concerns, establishing the mouse as an experimental model for brainstem recordings opens future avenues for investigating the consequences of targeted genetic alterations.

## Methods

Sound-evoked responses of single neurons in the SPON of 29 female CBA/CaJ mice (Jackson, Bar Harbor, ME, USA) were recorded. This strain has been established as a normal-hearing control in presbycusis studies, and its audiogram has been well-studied (Willott, 1983). All mice were housed in the vivarium at the West Virginia University Health Sciences Center and were eight to twelve weeks of age at the time of testing. Experimental procedures conformed to the National Institutes of Health Guide for the Care and Use of Laboratory Animals and were approved by the Institutional Animal Care and Use Committee of West Virginia University.

### *Surgical procedure*

Mice were initially anesthetized with isoflurane gas (1.5%; IsoFlo, Abbott, North Chicago, IL, USA) and placed in a stereotaxic apparatus using blunt ear bars to prevent damage to the tympanic membrane. Once the animal was determined to be areflexic, the scalp was incised and reflected laterally. A fine tungsten grounding pin was inserted through the skull overlying the cortex contralateral to the recording site and cemented into place. To immobilize the head during recordings, a lightweight hollow metal head-pin was glued to the exposed skull using dental cement cured with ultraviolet light (Charisma, Heraeus Kulzer, Armonk, NY, USA). A small (1-2 mm diameter) craniotomy was then opened over the right hemisphere of cerebellum without penetrating the dura mater; this procedure was performed while the mice were still under isoflurane anesthesia to eliminate pain associated with the craniotomy. Local anesthetic (5% Lidocaine gel, Teva, Sellersville, PA, USA) was applied topically to the margins of the open wound at this time and reapplied every two hours thereafter. The animal was returned to its cage and given one to two hours to recover from the isoflurane. During this period the mouse regained normal activity and resumed exploratory behavior within the cage.

### *Preparation for recordings*

The mouse was moved to a sound-attenuated chamber and placed in a molded foam “sandwich” to support its trunk while leaving the limbs unencumbered, and the previously attached head-pin was mounted onto a custom-designed stereotaxic attachment to maintain a fixed head position during the recording session (Portfors and Felix, 2005; Felix and Portfors, 2007). To minimize the potential for distress, animals assigned to recording in the absence of ketamine were acclimated by placement in the foam support for increasing durations over a period of several days prior to the recording session. In order to minimize stress related to the head restraint, animals assigned for recording in the awake state were habituated by first attaching the head-pin briefly (5 minutes), and gradually building up to successively longer intervals of head restraint on the day of the experiment.

#### *Manipulation of anesthetic state*

In order to ascertain the influence of ketamine on SPON response properties, recordings were conducted in either the unanesthetized state (i.e., in the absence of ketamine) or under the influence of ketamine anesthesia. Typically, recordings began in the unanesthetized state. After performing the recording protocol for several unanesthetized units, the animals (while remaining in the head restraint) were administered ketamine (70 mg/kg, i.p.). Approximately 15 minutes later, a foot pinch was given to confirm the absence of a nociceptive reflex. If no reflex was elicited, the animal was considered to be in the anesthetized state and recordings commenced. Using this approach, we obtained data from independent groups of unanesthetized and ketamine-anesthetized units.

In a second set of experiments, the recording protocol was refined to include paired recordings conducted in both unanesthetized and anesthetized states in the same units. To control for sequence effects, it is desirable to alternate or randomize the sequence of anesthesia states, such that some units would be recorded prior to and then following administration of ketamine, whereas other units would be recorded first under ketamine anesthesia and then again after complete recovery. Unfortunately, the recovery period from the systemic delivery of ketamine was too long to permit recordings before and after recovery. As a consequence, all units were recorded first in the unanesthetized

state. The long recovery time also limited the number of units that could be recorded in both unanesthetized and anesthetized states to one per animal.

For paired recordings, the unit was presented with a CF pure tone (20 dB above threshold) following completion of the recording protocol in the unanesthetized state, immediately following the ketamine injection and during the subsequent transition to the anesthetized state. The unit's response was continually monitored to be sure it was not altered by movement of the animal. Once the animal ceased to respond to the foot pinch, the complete recording protocol was repeated on the same unit in the anesthetized state.

### *Sedation*

Some animals exhibited excessive movement following recovery from the initial surgery and were lightly sedated with the phenothiazine sedative acepromazine maleate (1 mg/kg, i.p.; Henry Schein, Melville, NY, USA) to facilitate placement in the restraining device (Portfors and Felix, 2005). Acepromazine inhibits dopaminergic receptors (Feinberg and Snyder, 1975; Seeman and Lee 1975), and is recommended at a dosage of 1.0-5.0 mg/kg body weight for laboratory mice (Hawk et al., 2005). Although dopamine receptors have not been localized to the mouse brainstem (Camps et al., 1990), there is evidence that tyrosine hydroxylase, an enzyme necessary for dopamine synthesis, is present in the superior olivary complex (Darrow et al., 2006). Thus, the potential exists for acepromazine to alter SPON responses through modulatory inputs originating from neurons that are innervated by dopaminergic centers but are not dopaminergic themselves. With this possibility in mind, quantitative analyses were performed to determine whether acepromazine affected SPON responses, either alone or in combination with ketamine anesthesia.

### *Animal monitoring during recordings*

In the case of anesthetized animals, the depth of anesthesia was assessed by attending to the level of reflex activity and supplemental doses of ketamine were administered as needed. In animals that were either sedated or awake during recordings, stress and

discomfort were closely monitored for ethical reasons and also because any body or limb movements would interrupt the neuronal recordings; i.e., physical movements or vocalizations would cause large shifts in the baseline of the recordings. Even when such baseline modifications were not detected in the recording traces, each time the experimenter entered the booth to reposition the recording electrode (maximally at 15-20 minute intervals), the mouse was examined directly for signs of distress. Our experience with this restraint procedure is that with habituation performed as described, the mice remained essentially motionless and without apparent signs of distress for periods of up to 2 hours. If signs of distress were noted, at any time, either ketamine was administered and data were obtained in the anesthetized condition, or the experiment was terminated and the animal was euthanized. Mice were offered water with a small dropper after each electrode penetration.

#### *Acoustic stimulation and data acquisition*

Acoustic stimulus generation and data acquisition were controlled outside the recording chamber by a PC running custom-written software (BATLAB, Donald Gans, Northeast Ohio Universities College of Medicine, Rootstown, OH). To avoid unwanted onset and offset clicks, stimuli were generated with  $2 \text{ ms } \cos^2$  ramps. The digital waveforms were output through a 16-bit digital-to-analog converter (Microstar Laboratories, Bellevue, WA, USA; model DAP521a, 400,000 samples/second). The analog signals were fed to an anti-aliasing filter (Tucker Davis Technologies (TDT), Alachua, FL, USA, model FT6-2), and attenuation of the acoustic signals was controlled by a programmable attenuator (TDT, model PA-5). Signals were then routed to a speaker driver (TDT, model ED1) and presented to the animal through free field speakers (TDT, model ES1) placed 5 mm from the opening of the external auditory meatus. Speaker output was calibrated offline using a  $\frac{1}{4}$  inch condenser microphone (Brüel & Kjær model 4939, Norcross, GA), connected to a measuring amplifier (Brüel & Kjær model 2610). Acoustic cross-talk between the ears was estimated by presenting pure tones (0.5-60 kHz) from one speaker and comparing recordings of the tones obtained with a condenser microphone located in the positions of

the ipsilateral and contralateral ears. The recorded sound level was consistently ~35-40 dB lower in the contralateral location relative to the position of the ipsilateral ear.

#### *Data collection and analysis procedures*

The dura overlying the exposed brain surface was opened in preparation for recordings. Electrode penetrations through the SPON were guided by coordinates provided in the atlas of the mouse brain (Paxinos and Franklin, 2001). Responses from single neurons were recorded using micropipette electrodes filled with 1.5% biocytin dissolved in 0.5 M NaCl (tip diameter 2-4  $\mu\text{m}$ , 10-30 M $\Omega$  resistance), and advanced through the brain using a hydraulic micropositioner (David Kopf Instruments, Tujunga, CA, USA, model 650). Action potentials were amplified (Dagan Corporation, Minneapolis, MN, USA, model 2400), and passed through a band-pass-filter (Krohn-Hite, Brockton, MA, USA, model 3364) and then to a spike enhancer (Fredrick Haer, Bowdoinham, ME, USA). The output was digitized by a 16-bit high speed analog-to-digital converter at a rate of 42 kHz (Microstar Laboratories, model DAP5216a). Individual neural waveforms, raster plots, peristimulus time histograms (PSTHs) and statistics were displayed by BATLAB software during data acquisition, and raw waveforms were stored for offline analysis. Homogeneity of sound-evoked spike waveforms and the separation of action potential waveforms from background noise by a trigger window were required for classification as a single unit recording.

For recordings using broadband noise and pure tone stimuli, analysis windows for determining evoked spiking rates began at the stimulus onset and ended 50 ms after the stimulus offset. For the majority of units, this time window contained no spontaneous spiking. Bursts of broadband noise (50 ms duration, ~80 dB SPL, 4 presentations/second) were used as search stimuli. Once a single unit was isolated, its characteristic frequency (CF), defined as the frequency requiring the lowest intensity to elicit stimulus-evoked spikes to at least 50% of the presentations, and its minimum threshold, defined as the lowest intensity that elicited a consistent spike response, were determined and the neuron's frequency response area was mapped. Excitatory frequency ranges were first determined by presenting pure tones covering the most sensitive region of the mouse's hearing range (1-60 kHz at 20 dB attenuation, corresponding to 70-85 dB SPL,



depending on the frequency presented). A series of automated tests were then performed in which the predetermined excitatory frequency range of tone responses was presented in increments of 1 or 2 kHz, beginning at 10 dB below threshold and extending to 50 dB above threshold intensity in steps of 10 dB. From these tests Q values were determined for responses observed at 10 and 30 dB above threshold as a measure of the sharpness of frequency tuning. The aurality of each unit was determined by presenting 20 repetitions of broadband noise bursts at 5 dB above threshold, first monaurally to each ear, then binaurally. Sinusoidally amplitude-modulated (SAM) tones of 500 ms duration and 100% modulation depth were presented using the unit's CF as the carrier frequency at 20 dB above threshold (1 presentation/second). The analysis window for SAM tests began at the stimulus onset and ended at the offset. Each SAM stimulus was presented eight times, and modulation frequencies (MFs) were varied from 40 to 600 Hz in 40 Hz increments. The fidelity of phase-locking at each MF was quantified by calculating the vector strength (VS):

$$VS = \frac{1}{n} \sqrt{[\sum \sin(a_i)]^2 + [\sum \cos(a_i)]^2}$$

where  $a_i$  is the phase angle of spike  $i$  relative to the modulation cycle of the stimulus, and  $n$  is the total number of spikes in the analysis window (Goldberg and Brown, 1969). A VS of 1 indicates perfect entrainment between spiking to a given phase angle of stimulus modulation cycles, whereas a VS of 0 indicates no correlation. In cases where responses contained two or fewer spikes per stimulus presentation, VS was set to 0 to reduce the influence of isolated spikes that were time-locked to the stimulus onset and therefore occurred at a constant phase angle (Kadner and Berrebi, 2008). The Rayleigh test (Batschelet, 1981) was used to determine whether spike distributions relative to phase angles of stimuli differed from randomness. As with VS, responses that had  $\leq 2$  spikes per stimulus were considered unsynchronized and excluded from Rayleigh test analyses.

#### *Histological localization of recording sites*

To confirm that single unit recordings were located in the SPON, the neural tracer biocytin (Sigma Chemical, St. Louis, MO) was deposited during an electrode penetration

in each animal. Confined tracer deposits were achieved using a current generator to deliver 1  $\mu$ A of positive ejection current (Stoelting Co., Wood Dale, IL, USA; model 51413; 5 minute duration, 50% duty cycle). Detailed descriptions of histological processing techniques and reconstruction of electrode tracts were previously described for SPON recordings in the rat (Kulesza Jr. et al., 2003; Kadner and Berrebi, 2008) and were readily applied to the mouse. Briefly, at the conclusion of each recording session, mice were perfused through the ascending aorta with phosphate-buffered 4% paraformaldehyde. Brainstems were removed from the calvaria, cryoprotected overnight in 30% sucrose, and sectioned transversely at 40  $\mu$ m using a freezing microtome. Alternating sections were either mounted and counterstained for Nissl substance to reveal the boundaries of superior olivary nuclei, or processed to reveal biocytin deposits following the Avidin:Biotinylated enzyme complex procedure (Vectastain ABC, Vector Laboratories, Burlingame, CA, USA) using diaminobenzidine (Sigma-Aldrich, St. Louis, MO, USA) as chromogen. Photographs of adjacent tissue sections stained for Nissl substance and biocytin, respectively, were overlaid, using tissue landmarks to guide alignment, and the locations of tracer deposits within the superior olivary complex were determined.

## Results

A total of 83 single units were recorded from the SPON. Of these, 70 units were recorded either with (n=34) or without (n=36) ketamine, and were therefore referred to as *independent* groups. The remaining 13 units were recorded both before and after ketamine administration. Data from these 13 sets of *paired* recordings are presented separately at the end of the results section.

Localization of one recording site per animal was achieved by ejecting biocytin from the electrode tip immediately following completion of the recording protocol for a single unit response (Fig. 3.1). The remaining recording sites were inferred by calculating their distances from tracer deposit site taken from movements of the electrode with both the stereotaxic apparatus (x and y planes) and the micropositioner (z plane).

### *Effects of acepromazine sedation*

To determine if administration of acepromazine maleate sedation altered neuronal response properties, a factorial ANOVA was employed with sedative state and anesthetic state as grouping factors to compare spontaneous spiking rates, evoked spiking to CF tones, CF tone thresholds, first spike latencies, and Q10 values between neurons recorded with or without acepromazine in unanesthetized (n=28 and 8 units, respectively) and ketamine-anesthetized (n=12 and 22 units, respectively) conditions. None of the comparisons revealed a significant main effect of acepromazine (spontaneous spiking,  $p = 0.83$ ; evoked spiking,  $p = 0.17$ ; threshold,  $p = 0.48$ ; latency,  $p = 0.14$ ; Q10,  $p = 0.56$ ) nor a significant interaction effect between acepromazine and ketamine (spontaneous spiking,  $p = 0.51$ ; evoked spiking,  $p = 0.41$ ; threshold,  $p = 0.26$ ; latency,  $p = 0.82$ ; Q10,  $p = 0.09$ ). Because each of the response properties recorded in the presence of acepromazine was statistically equivalent to that obtained in the absence of acepromazine, the effects of sedation will not be considered further.

### *Responses to pure tones*

Characteristic frequencies (CFs) for independent recordings of SPON units were distributed from 2 to 41 kHz for unanesthetized units and from 5 to 41 kHz for anesthetized units, covering the most sensitive area of the mouse's audible range (Fig. 3.2). CFs increased when the electrode was positioned medially and decreased as the electrode was shifted laterally, consistent with the known topographic arrangement of the SPON in the rat, where high CF neurons are located medially and progressively lower CF neurons are positioned laterally (Kulesza Jr. et al., 2003). All units exhibited offset responses with little or no spiking during the presentation of tone stimuli (Fig. 3.3). Three offset response sub-types previously described in the rat SPON were identified (Kulesza Jr. et al., 2003). One type commonly observed were *offset-transient* responses consisting of one or two well-timed action potentials (Fig. 3.3A); these were recorded in 31% of unanesthetized and 35% of anesthetized units. Units that responded with bursts of regularly spaced offset spikes were termed *offset-choppers* (Fig. 3.3B). The regularity of these units' spiking was assessed by analysis of the first-order interspike intervals. To be classified as an offset chopper, a unit's interspike interval histogram had to show a well-defined peak (Fig. 3.3B, inset); 31% of unanesthetized and 44% of anesthetized units met this criterion. *Offset-sustained* units were characterized by at least 20 milliseconds of spiking after termination of the stimulus (Fig. 3.3C) and accounted for 38% and 21% of unanesthetized and anesthetized responses, respectively.

First spike latencies were significantly shorter for unanesthetized units ( $6.8 \pm 0.2$  milliseconds) compared to anesthetized units ( $9.5 \pm 0.3$  milliseconds;  $p < 0.001$ , Mann-Whitney U test). Moreover, unanesthetized units had significantly higher evoked spiking rates ( $2.2 \pm 0.2$  spikes/stimulus) and spontaneous spiking rates ( $3.0 \pm 0.6$  spikes/second) compared to anesthetized units ( $1.2 \pm 0.1$  spikes/stimulus and  $1.1 \pm 0.3$  spikes/second, respectively; Mann-Whitney U test,  $p < 0.001$  and  $0.001$ , respectively).

#### *Aurality and responses to broadband noise*

All SPON units responded with evoked spiking to contralateral broadband noise stimulation alone, but not to ipsilateral stimulation alone. One-way ANOVAs using each of the broadband noise stimulus conditions as factors (i.e., no sound, contralateral,

ipsilateral or bilateral), returned significant results for both independent unanesthetized and anesthetized groups ( $F(3,144) = 31.93, p < 0.001$  and  $F(3,136) = 20.47, p < 0.001$ , respectively). In each case, spiking in response to contralateral noise was significantly higher than to ipsilateral noise (Fig. 3.4; Tukey post hoc test,  $p < 0.001$  for both group comparisons), but statistically equivalent to bilateral stimulation (Tukey,  $p > 0.99$  for both groups). Furthermore, there was no significant difference in response magnitude between the “no sound” and “ipsilateral noise” conditions (Tukey,  $p > 0.99$  for both groups). Thus the mouse SPON is monaurally driven by input to the contralateral ear.

With respect to anesthetic state, there was no significant difference between responses recorded with and without ketamine, in either the “no sound” or the “ipsilateral” stimulation conditions (Mann Whitney U test,  $p = 0.26$  and  $0.19$ , respectively). However, anesthetized units had lower spiking rates than unanesthetized units when presented with contralateral and bilateral noise (Fig. 3.4; Mann Whitney U test,  $p < 0.01$  for both stimulus conditions). Overall, the aurality of responses remained unchanged regardless of anesthetic state (i.e., all responses were monaural and contralaterally-driven).

An unexpected result of the aurality testing was the presence of two distinct spiking patterns in response to broadband noise stimuli. One type was characterized by an offset response with very little or no spiking during the stimulus, similar to the typical response to a pure tone (Fig. 3.5A). Thirty-six percent of unanesthetized and 47% of anesthetized units displayed this first response type. A second response type, observed in the majority of both unanesthetized and anesthetized units (64% and 53%, respectively), was marked by substantial spiking during the stimulus, in addition to offset spiking. For both types of noise responses, spiking rates reached their peaks shortly after the stimulus offset. It is noteworthy that for units with this second response type, spiking during the stimulus was observed only in response to noise stimuli; when CF pure tones were presented to the same units, only offset spikes occurred (Fig. 3.5B). To assess whether units that displayed peristimulus spiking to broadband noise represented a subtype of SPON unit separate from those that responded strictly to the stimulus offset, we compared their pure tone thresholds, spontaneous spiking rates, sharpness of frequency tuning, as well as spiking rates and vector strengths in response to SAM stimuli. No

significant differences were observed between any of these measures (Mann Whitney U test,  $p > 0.05$  in all cases).

### *Frequency response maps*

Complete response maps were obtained for 31 unanesthetized and 33 anesthetized units, with CFs ranging from 6 to 41 kHz and 5 to 41 kHz, respectively. Thresholds for unanesthetized units averaged  $37.1 \pm 1.3$  dB SPL for tones and  $48.8 \pm 1.4$  dB SPL for noise, and were significantly lower than thresholds for anesthetized units (tones:  $57.8 \pm 2.0$  and noise:  $63.7 \pm 2.1$  dB SPL;  $p < 0.001$  for each case, Mann Whitney U test; Fig. 3.2). Both unanesthetized (Fig. 3.6) and anesthetized units had response maps that were consistently V-shaped with low-frequency tails. Moreover, for all units tested, offset response patterns did not change throughout the response maps. Q values were calculated to assess the sharpness of tuning for each unit. Unanesthetized units had sharper frequency tuning compared to anesthetized units, as demonstrated by significantly higher Q10 ( $3.5 \pm 0.3$  versus  $2.6 \pm 0.3$ ) and Q30 values ( $1.5 \pm 0.1$  versus  $1.1 \pm 0.1$ ; Mann Whitney U tests;  $p = 0.003$  and  $p < 0.001$ , respectively). In general, response thresholds to tone and noise stimuli in the anesthetized state are similar to those reported for anesthetized rat SPON units (Kulesza Jr. et al., 2003).

### *Responses to sinusoidally amplitude modulated tones*

Responses to the full sequence of SAM stimuli (40-600 Hz modulation frequency (MF)) were recorded for 26 unanesthetized and 30 anesthetized units. CFs for these units ranged from 7 to 41 kHz for unanesthetized units and 5 to 39 kHz for anesthetized units. In addition, all offset response types were represented within each group. PSTHs for SAM tones clearly showed periodic spiking, indicating a response to individual modulation cycles, particularly at lower MFs (Fig. 3.7A). Analysis of first-order interspike intervals for phase-locked responses showed that at low MFs, a large proportion of spikes were separated by the duration of one modulation cycle, but interspike intervals representing multiples of the cycle duration also occurred, indicating that the responses skipped

modulation cycles (Fig. 3.7B). Unanesthetized units displayed phase-locking to SAM stimuli ranging from 40 to 440 Hz (Rayleigh test performed for each MF,  $p < 0.05$ ), with VSs steadily decreasing with increasing MF (Fig. 3.8A). Responses of anesthetized units were also highly synchronized to low MFs, but phase-locked to a more limited range of MFs compared to unanesthetized units (40 to 160 Hz, Rayleigh tests, all  $p$  values  $< 0.05$ ). For MFs between 40 and 520 Hz, unanesthetized units displayed significantly higher VSs than anesthetized units (Mann Whitney U test, all  $p$  values  $< 0.05$ ; Fig. 3.8A). SPON neurons consistently showed high VSs to SAM tones at MFs where a robust response was elicited, particularly for unanesthetized units. The low VSs observed at higher MFs, in both unanesthetized and anesthetized units, resulted in large part from the paucity of spiking during the stimulus presentation ( $\leq 2$  spikes/stimulus), resulting in the VSs being set to zero, rather than a decrease in response synchronicity in those units that still produced more than 2 spikes per presentation (Fig. 3.8B).

#### *Effects of ketamine during paired recordings*

For a subset of SPON recordings, data were collected before and after ketamine administration in the same units (i.e., paired recordings;  $n = 13$ ). All three pure tone response types (*offset-transient*, *offset-chopper*, and *offset-sustained*) were represented in this sample. Following ketamine treatment, two offset-sustained responses changed to offset-choppers, and one offset-chopper response changed to an offset-transient (Fig. 3.9A). Consistent with this finding, pre-ketamine evoked spiking ( $2.0 \pm 0.3$  spikes/stimulus) and spontaneous spiking ( $4.2 \pm 1.4$  spikes/s) were significantly decreased after ketamine treatment ( $1.2 \pm 0.2$  spikes/stimulus,  $p = 0.002$  and  $1.9 \pm 0.8$  spikes/s,  $p = 0.039$ , respectively; Wilcoxon matched-pairs test). In addition, both the first spike latencies ( $7.1 \pm 0.4$  ms) and response thresholds ( $40. \pm 4.4$  dB SPL) of unanesthetized responses to CF pure tones increased significantly in the presence of ketamine ( $9.2 \pm 0.5$  ms,  $p = 0.003$  and  $58.7 \pm 4.7$  dB SPL,  $p = 0.001$ ; Wilcoxon matched-pairs tests). Furthermore, Q10 ( $3.2 \pm 0.4$ ) and Q30 ( $1.5 \pm 0.2$ ) values from response maps of unanesthetized units significantly decreased after ketamine treatment ( $2.1 \pm 0.3$ ,  $p = 0.034$  and  $1.0 \pm 0.1$ ,  $p = 0.28$ , respectively; Wilcoxon matched-pairs test; Fig. 3.9B).

In response to broadband noise stimuli, spiking rates decreased for all but two paired recording units following ketamine administration. Responses of five of the ten units that exhibited spiking during noise stimuli were transformed, such that only offset spiking was observed following the administration of ketamine anesthesia (Fig. 3.9C). Aурality tests revealed that spiking rates were significantly different in response to the various noise delivery conditions (repeated measures ANOVA,  $F(3,52) = 19.4$ ,  $p < 0.001$ ). Spiking in response contralateral and bilateral noise was significantly greater in the unanesthetized state compared to the anesthetized state (Tukey post hoc,  $p < 0.05$  for both cases). However, like units in the independent recording groups, spiking to no sound and to ipsilateral noise presentation did not change in paired units upon induction of ketamine anesthesia (Tukey post hoc,  $p > 0.05$  for both cases).

When units in the paired recording group were presented with SAM tones, their pre-ketamine responses phase-locked over a range of MFs from 40 to 440 Hz (Rayleigh test,  $p > 0.05$  in all cases). After ketamine treatment, both VSs and spike rates for all MFs dropped (Figs. 3.9D, 10). Specifically, the units' post-ketamine responses phase-locked from 40 to 160 Hz, and VSs were significantly lower than pre-ketamine responses for all MFs tested apart from 560 Hz (Fig. 3.10A; Wilcoxon matched-pairs test,  $p < 0.05$  in all cases). In addition, spiking rates were lower for each MF after ketamine administration, but these differences were only significant ( $p < 0.05$ ) for MFs below 240 Hz (Fig. 3.10B; Wilcoxon matched-pairs test).

### *Ketamine anesthesia effects in independent and paired recordings*

In summary, the effects of ketamine on SPON response properties for units recorded in only one anesthetic state (i.e., independent recordings, Table 3.1) were consistent with those observed in units for which paired recordings were made (Fig. 3.11). Specifically, *i*) both evoked and spontaneous spiking were significantly lower in the anesthetized state (Fig. 3.11A, B), *ii*) first spike latencies and thresholds increased significantly under ketamine anesthesia (Fig. 3.11C, D), *iii*) frequency tuning in the unanesthetized state was significantly sharper than after ketamine treatment (Fig. 3.11E), and *iv*) the magnitude of the response to contralaterally or bilaterally presented noise decreased significantly under



ketamine administration (Fig. 3.11F). Finally, VSs significantly decreased following ketamine application for all MFs below 560 Hz (Figs. 3.8A and 3.10A), and spiking rates in response to SAM stimuli significantly decreased in the presence of ketamine for all MFs below 240 Hz (Figs. 3.8B and 3.10B).

## Discussion

The motivation for the present study was twofold: first, to characterize response properties of SPON neurons in the mouse and to compare our findings to what has been reported previously in other species. Our results demonstrate that responses of SPON neurons in the mouse are most similar to those in the rat, the species in which the SPON has been most extensively studied.

Our second goal was to answer whether ketamine anesthesia substantially alters SPON response properties. In the presence of ketamine, response thresholds and latencies were significantly elevated, while spontaneous and evoked spiking rates, as well as sharpness of frequency tuning, were significantly decreased. In addition, ketamine altered the spiking patterns of some units enough to result in the reclassification of the response type. Ketamine also had two significant effects on the responses of SPON neurons to SAM stimuli, namely decreasing both the spike count and the response synchronization.

### *Comparison of mouse SPON physiology with previous studies in the rat*

This study represents the first investigation of the physiological characteristics of mouse SPON neurons *in vivo*. Herein several defining features of these responses have been identified. First, all units exhibited offset spiking in response to acoustic stimuli, with the majority of responses consisting of only one to three spikes per stimulus. In addition, all units responded exclusively to monaural stimuli presented to the contralateral ear. Frequency response maps were generally V-shaped with low frequency tails and thresholds were roughly 15-20 dB higher than principal cells of the neighboring MNTB (Sonntag et al., 2009), which represents a substantial input to the SPON (Morest, 1968; Bledsoe et al., 1990; Banks and Smith, 1992). Furthermore, under all conditions studied, mouse SPON units responded with a high degree of synchronicity to low MF (40-160 Hz) SAM tones. Each of the SPON characteristics mentioned above is in agreement with what has been reported previously in the rat SPON (Kulesza Jr. et al., 2003; Kadner and Berrebi, 2008).

Units in both the mouse and rat SPON have similar proportions of offset spiking patterns, with offset-transient, -chopper, and –sustained types making up 33%, 37%, and 30% of mouse and 41%, 23%, and 22% of rat responses, respectively (Kulesza Jr., et al. 2003). In the rat, offset spiking is thought to be created in part by a post-inhibitory rebound caused by the release from persistent glycinergic inhibition originating in the MNTB during the stimulus (Kulesza Jr. et al., 2007). In addition to a rebound mechanism, excitatory inputs from multipolar and octopus cell of the contralateral cochlear nucleus, which appear to be largely masked by inhibition during presentation of stimuli, likely play a role in forming the offset response (discussed in Kulesza Jr. et al., 2003; 2007). Thus, SPON neurons in mice and rats might receive similar weights of inputs from the MNTB and cochlear nucleus, resulting in similar evoked spiking patterns that exhibit a high degree fidelity with regard to spike timing (e.g., offset-transient and offset-chopper responses). In accord with the general uniformity of their reported spiking patterns, previous anatomical studies indicate morphological similarities of neurons in the mouse and rat SPON. In both species, SPON neurons are described as morphologically homogeneous large multipolar cells (Ollo and Schwartz, 1979; Saldaña and Berrebi, 2000; Kulesza Jr. and Berrebi, 2000).

A notable difference between these species is the presence in mouse recordings of action potentials during the presentation of broadband noise stimuli, but not in response to pure tones. Because the broadband noise stimulus used in this study is repeated and not randomly generated for each presentation, it is possible that amplitude fluctuations introduced by the “frozen” nature of the noise might account for the observed peri-stimulus spiking to this stimulus. The presence of well-defined peaks with variable interspike intervals in our recordings seems to support this idea, as repetitive envelope fluctuations might increase the likelihood that a spike will occur at certain times relative to the stimulus onset. However, it is difficult to resolve the absence of peri-stimulus spiking in the rat SPON, where frozen noise was also used. Among *paired* mouse recordings, approximately half of peri-stimulus responses to noise were abolished following ketamine delivery. Thus, perhaps differences in the relative strength or mechanism of action of the drug may underlie the occurrence of peri-stimulus spiking. Specifically, for units where the weight of excitatory inputs from multipolar cells of the

cochlear nucleus is high, peri-stimulus spiking may be present, whereas, for units where this excitatory input is less prominent, inhibition from the MNTB completely masks spiking during the noise presentation. In this scenario, fewer cases of peri-stimulus spiking are seen in anesthetized animals because activation of NMDA receptors decreases, making inhibition during the stimulus more prominent by effectively shifting the balance of excitatory and inhibitory inputs.

#### *Comparison of brainstem offset responses*

The majority of brainstem offset units have been reported in the SPON and its presumed homologue in some mammals, the dorsal-medial paraolivary nucleus (DMPO; discussed in Saldaña and Berrebi, 2000). The bat medial superior olive (MSO) resembles the SPON/DMPO in several respects, including receiving its primary excitatory and inhibitory inputs from the contralateral cochlear nucleus and ipsilateral MNTB, respectively (Cant and Casseday, 1986; Covey et al., 1991), and the presence of offset responses that synchronize to SAM stimuli, particularly at low MFs (Grothe, 1994). Thus, the bat MSO is included in our discussion of offset responders.

Many notable features of offset responses are shared across mammalian species. For instance, most studies in the superior olivary complex (apart from Behrend et al., 2002, in the gerbil) reported that the majority of offset responses were monaural, with ~10-15% of units having binaural properties. In addition, the cat DMPO (Guinan et al., 1972) and bat MSO (Grothe, 1994) exhibited low rates of spontaneous activity, similar to responses in the mouse SPON. Units in the cat DMPO also displayed offset-transient spiking patterns, while gerbil SPON units possessed patterns resembling offset-transient and offset-chopper types (Dehmel et al., 2002), as in the mouse. Offset-sustained units were also reported in the presumed DMPO of the rabbit (Kuwada and Batra, 1999), but had a much more robust sustained component compared to the mouse. Furthermore, responses of gerbil SPON units had V-shaped frequency tuning curves and elevated thresholds, relative to the behavioral audiogram (Dehmel et al., 2002). Despite the similarities of offset responses in these studies, several confounding differences exist (discussed in: Behrend et al., 2002; Kulesza Jr. et al., 2003; Kadner and Berrebi, 2008;

Pollak et al., 2010) and likely reflect evolutionary pressures that caused certain species to develop specializations for hearing at high (e.g., mice, rats, bats) versus low (gerbils; Rosowski et al. 1999) frequencies.

Properties of neurons in the bat MSO resemble those of the SPON in rodents. Mammals that possess fine low frequency hearing contain MSO neurons stimulated by binaural stimuli, whereas bat MSO cells are primarily monaural and respond phasically, either to the sound onset or offset (Covey et al., 1991). It was thought that these differences between bats and other mammals were due to specializations for echolocation (Covey et al., 1991; Grothe et al., 1992), but based on recent characterizations of the SPON in mice and rats, a more general explanation is that differences result from the bat being a high frequency hearing animal (Pollak et al., 2011). Thus, evolutionary constraints likely determine whether neurons located in the brainstem region between the MNTB and LSO are involved in binaural sound localization, as in low frequency hearing mammals, or are monaural and possibly part of a pathway specialized for the encoding of fine temporal information, as in high frequency hearing animals. Responses to SAM stimuli in accord with those reported herein were observed by Grothe (1994) in the bat MSO, and were explained by the timing of excitatory and inhibitory inputs relative to the occurrence of modulation cycles. According to this model, cycles of SAM modulations elicit responses in the MNTB, which then cause spiking in the SPON via a post-inhibitory rebound mechanism. When the modulation frequency reaches an upper limit, overlapping inhibition from the previous cycle suppresses rebound spiking, and the SPON ceases to respond. The same type of low-pass SAM modulation transfer function seen in the bat MSO has also been described in the rabbit (Kuwada and Batra, 1999) and rat (Kulesza Jr. et al., 2003; Kadner and Berrebi, 2008). Thus, offset responses to SAM stimuli in the mouse SPON are in agreement with other species, suggesting that there may be a conserved role for this type of neuron in temporal processing (discussed in: Grothe, 1994; Kuwada and Batra, 1999; Kadner and Berrebi, 2008).

*Effects of ketamine anesthesia on SPON response properties*

Previous recordings of offset responses in the brainstem were conducted either in anesthetized (Guinan et al., 1972; Behrend et al., 2002; Dehmel et al., 2002; Kulesza Jr. et al., 2003; 2007; Kadner and Berrebi, 2008) or unanesthetized states (Grothe, 1994; Kuwada and Batra, 1999). In all but one study of anesthetized animals (Guinan et al., 1972), ketamine was the agent used. The present study in the mouse enabled us to characterize both anesthetized and unanesthetized responses, in the same units in some cases. Our goal was to determine the degree to which ketamine anesthesia affects SPON offset responses and whether ketamine-induced changes, if found, could explain any of the variability in response properties observed in previous studies. Spontaneous and evoked spiking rates were both low for SPON neurons in the absence of anesthesia compared to the neighboring MNTB (Kopp-Scheinflug et al., 2008), and decreased further following ketamine application. During paired recordings, where responses were directly observed before and after ketamine treatment in the same units, two of six offset-sustained responses changed into offset-transients and one of five offset-chopper responses changed into offset-transient patterns. After ketamine delivery, the short-latency phasic component of offset spiking, which was relatively robust in pre-ketamine recordings, remained, whereas spiking later in the response which was comparatively weaker prior to ketamine, was abolished in many anesthetized units. Thus, ketamine seems to partially block excitation in the SPON, as evidenced by a reduction in both spontaneous and evoked spiking, particularly during the latter part of the response. However, ketamine likely acts on only a subset of neurotransmitter receptors. For example, glycine receptors, thought to be largely responsible for rebound spiking (Magnusson et al., 2010; Kopp-Scheinflug et al., 2010), might not be affected substantially by ketamine, as offset spiking remains following anesthesia administration. The most dramatic changes in pure tone responses observed with ketamine treatment were increases in thresholds and first spike latencies. Both of these properties may be altered due to a shift in the balance of the strength of excitatory and inhibitory neurotransmission the SPON. Although a shift in thresholds was observed throughout the units' response maps following ketamine treatment, they retained their broad shape (see Fig. 3.9B). Effects of ketamine on presynaptic nuclei, such as the MNTB, cannot be ruled out, although preliminary studies of local NMDAR blockade in the rat MNTB suggest

ketamine may have only a subtle impact on the spiking of neurons (Berrebi lab, unpublished observations).

In the absence of ketamine, mouse SPON neurons exhibited low-pass modulation transfer functions in response to SAM tones, and generally responded with a high degree of synchronicity to every MF to which there was reliable spiking. Following ketamine application, the low-pass shape of SAM modulation transfer functions remained unchanged, with units responding with a high degree of phase-locking to low MFs, although the upper limit of modulation frequencies to which units phase-locked was greatly reduced. As the reduction in SPON unit spiking presumably causes VSs to drop, the introduction of ketamine may cause phase-locking units that normally respond weakly to SAM tones in the unanesthetized state to cease spiking altogether. This lack of spiking would result in VSs of zero and a reduction in the range of modulation frequencies to which anesthetized SPON units display phase-locked responses. As mentioned above, ketamine-mediated partial blockade of NMDA receptors may account for the silencing of neurons that would otherwise produce a weak response to a given auditory stimulus.

#### *Effects of ketamine on NMDA receptors*

Any account of ketamine's effects on mouse SPON response properties requires consideration of the NMDAR. Ketamine is a non-competitive antagonist of ionotropic NMDARs (Anis et al., 1983; Harrison and Simmonds, 1985) and it acts by both blocking open NMDAR channels and by reducing the opening frequency of closed channels (Macdonald et al., 1987; Orser et al., 1997). Because glutamate is the primary ligand for NMDARs, ketamine acts to decrease the excitability of neurons that possess these channels (Ozawa et al., 1998). Even in the presence of glutamate, activation of NMDARs first requires depolarization of the membrane, resulting in the characteristic late onset portion of the neuronal response mediated by NMDARs (Lester et al., 1990). The NMDAR has been localized throughout the auditory brainstem, including in the SPON (Petralia et al., 1994; Watanabe et al., 1994), as well as in nuclei providing synaptic input to the SPON; the cochlear nucleus and medial nucleus of the trapezoid body (Bledsoe et

al., 1990; Smith and Banks, 1992; Schofield and Cant, 1995; Bilak et al., 1996; Smith et al., 1998; Petralia et al., 2000; Sato et al., 2000). Thus, ketamine effects on SPON responses may be either pre- or post-synaptic.

The general reduction in spiking observed upon ketamine treatment in the mouse SPON is greater than that observed in our preliminary rat recordings in which NMDARs were reversibly blocked *in vivo* with a selective antagonist. In these recordings, spiking of SPON units decreased, but only by 20% in contrast to the 35% decrease in spiking following ketamine treatment in the mouse. To account for the amplified decrease in ketamine-induced spiking, it is plausible that in addition to blocking NMDARs, ketamine may also act to potentiate certain subunit combinations of GABA<sub>A</sub> receptors (Hevers et al., 2007). Ketamine has not been traditionally viewed as a GABA<sub>A</sub> receptor agonist, but a recent study of the auditory cortex has provided evidence contrary to this view (Kurt et al., 2008). Specifically, systemic ketamine application acted to limit the effects of GABA<sub>A</sub> receptor antagonists in the anesthetized state compared to the unanesthetized state in the gerbil (Kurt et al., 2008). Based on previous studies in the rat (Kadner and Berrebi, 2008; Saldaña and Berrebi, 2000), GABAergic synapses provided by axonal collaterals within the nucleus are thought to contact other SPON neurons and serve to limit the magnitude and duration of responses. Thus, ketamine may exert the dual effects of blocking NMDAR-mediated excitation and increasing GABA<sub>A</sub> receptor-mediated inhibition, thereby further reducing the excitability of SPON neurons compared to what is achieved by selectively blocking NMDARs locally.

### *Functional considerations*

In previous studies, a common feature of offset responses is that they precisely respond to temporal sound features, such as SAM stimuli (Kuwada and Batra, 1999; Behrend et al., 2002; Dehmel et al., 2002; Kulesza Jr. et al., 2003; Kadner and Berrebi, 2008) and small gaps between sounds (Grothe, 1994; Kadner and Berrebi, 2008). Kadner and Berrebi (2008) proposed that the SPON acts as a discontinuity detector that enhances the segmentation of ongoing responses in its primary target, the inferior colliculus (IC). This idea is based on the finding that SPON neurons are very sensitive to periods of low



stimulus energy in ongoing sounds. One possible role of the SPON in line with this idea is that the nucleus serves to shape SAM modulation transfer functions in the IC by providing GABAergic inhibition at the offset of modulation cycles, up to roughly 200 Hz. In contrast to this view, the shapes of SAM transfer functions remained unchanged when GABA<sub>A</sub> receptors were blocked locally in the IC of the mustached bat (Burger and Pollak, 1998). This finding indicates that IC unit responses to SAM stimuli are not created locally but suggests that they may be inherited from a brainstem source or sources. Apart from the SPON few, if any, brainstem nuclei that project to the IC do not contain neurons possessing SAM modulation transfer functions similar to those in the IC (discussed in: Burger and Pollak, 1998). Thus, while the SPON may play a sizable role in SAM processing in the midbrain, global blockade of all GABAergic inputs to the IC may make its specific contribution difficult to detect.

The SPON may also contribute to the tuning properties of a specific subpopulation of IC neurons in the bat whose inputs are heavily influenced by inhibition (Pollak et al., 2010). These inhibited IC neurons possess prominent IPSPs that are triggered by the offset of stimuli and appear at intensity levels above 25-30 dB SPL, consistent with the elevated thresholds observed in the SPON. Lastly, the SPON may contribute to forward masking in the midbrain. Forward masking is a well-described psychoacoustic phenomenon in which the presence of a leading “masker” sound acts to elevate the detection threshold of a trailing “probe” sound. Perceptual masking is thought to be important in segregating multiple sound streams in complex listening environments (discussed in Chapter 6; Jesteadt et al., 1982; Plack and Oxenham, 1998). A recent study suggested a role for SPON-like inhibitory inputs to the IC that acted at the offset of sounds and exhibited broad tuning (Nelson et al., 2009). Continuing investigation is needed to determine whether this particular type of offset inhibition is mediated by the SPON.

## **Acknowledgements**

I gratefully acknowledge Dr. Alexander Kadner for providing data analysis routines and for assistance with crafting the manuscript. I thank Dr. Christine Portfors for aiding in development of the unanesthetized recording preparation. I also thank Dr. Aric Agmon for helpful pre-submission critiques. In addition, I acknowledge Mr. Dennis Cole for assistance with tissue processing and histology.

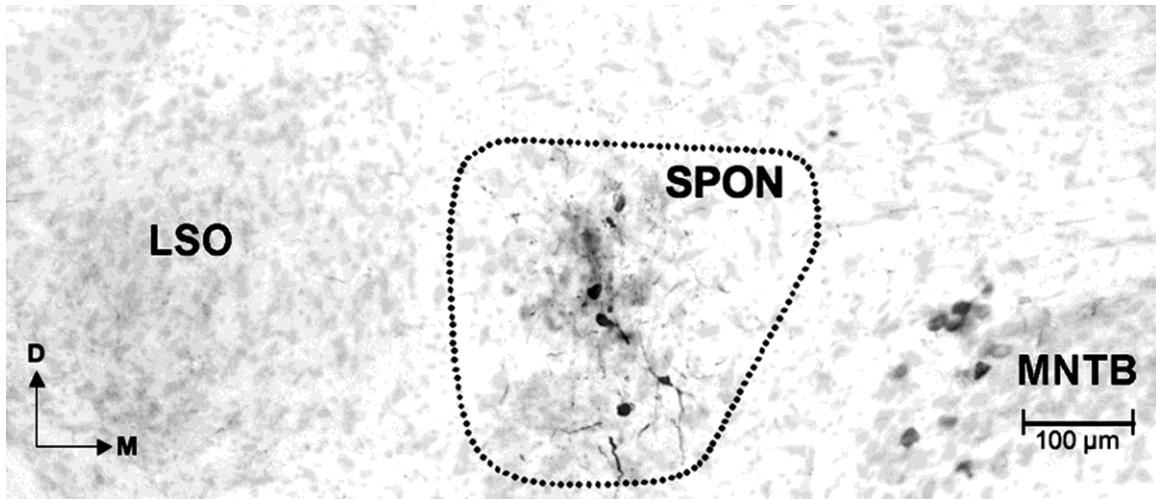


*Figure 3.1.* SPON recording sites were marked by ejecting biocytin from recording pipettes during each experiment. Counterstaining with Neutral Red facilitated accurate delineation of the boundaries of nuclei within the superior olivary complex. Retrogradely labeled neuronal cell bodies were often seen in the ipsilateral MNTB. Abbreviations: M, medial; D, dorsal; MNTB, medial nucleus of the trapezoid body; LSO, lateral superior olive.

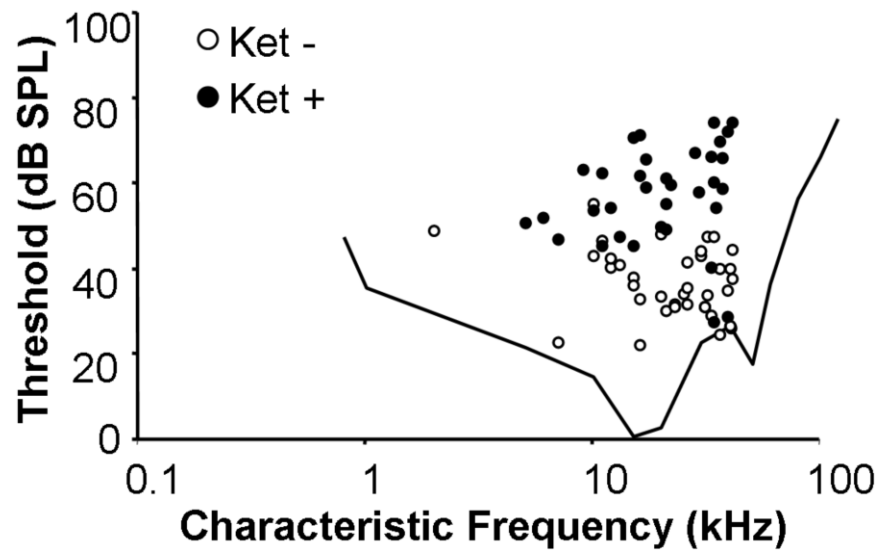


*Figure 3.2.* Distribution of thresholds and characteristic frequencies of independent single units recorded either with ketamine (Ket +) or without ketamine anesthetic (Ket -) in the mouse SPON. A behavioral audiogram of the mouse is outlined for comparison (from Ehret, 1976).

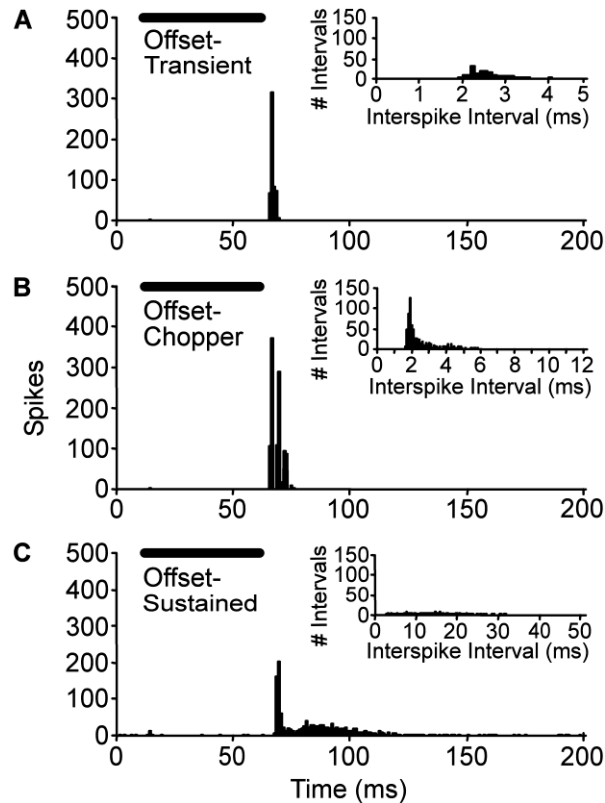


*Figure 3.3.* Classification of the main response types observed in the mouse SPON. All units responded with offset spiking, with very little or no response during the presentation of CF tone stimuli. Insets in each panel show the corresponding first order interspike interval histograms. *A*: The most common response type (31% of units) was termed *offset-transient* and consisted of well-timed spiking triggered by the stimulus offset. The corresponding ISI shows that when offset-transient units generate multiple spikes, the interspike interval is variable. *B*: Example of a response consisting of a burst of offset spikes, with moderately consistent timing between spikes, as shown by the defined peak and Poisson-like distribution in the corresponding interspike interval plot. These units were classified as *offset-chopper* (31%). *C*: A third type of discharge pattern was characterized by transient offset spiking followed by a sustained response. The time course of the response always exceeded 20 ms; these responses were classified as *offset-sustained* (38%). Offset-sustained responders did not generate regularly spaced action potentials, as shown in the corresponding interspike interval plot. Horizontal bars in each plot represent the time course of the pure tone stimulus.

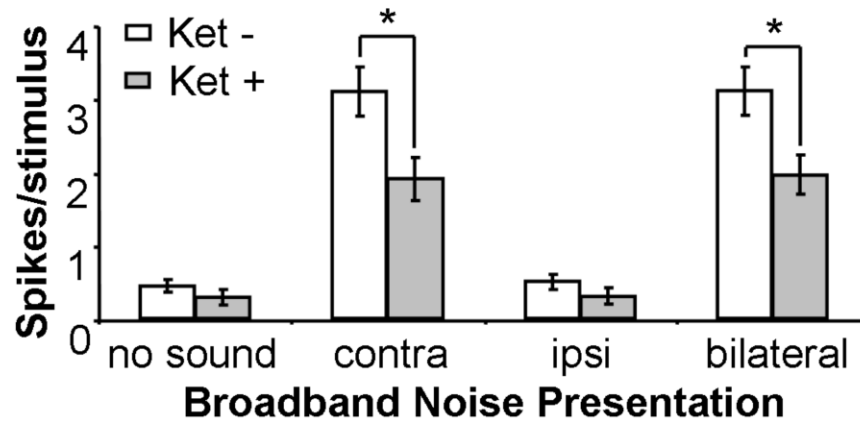


*Figure 3.4.* Auality of independent mouse SPON responses. Responses to broadband noise were recorded to assess the auality of each unit in our sample. Mean spike rates are shown for four stimulus presentation conditions: in the absence of stimuli (no sound), stimuli presented to the contralateral ear alone (contra), stimuli presented to the ipsilateral ear alone (ipsi), and stimuli presented to both ears (bilateral). Responses recorded both in the absence and in the presence of ketamine exhibited monaural, contralaterally-driven responses. In addition, units in ketamine-anesthetized mice showed lower spike rates in response to contra and bilateral stimulation compared responses recorded in the absence of ketamine. Error bars represent the standard errors of the means (\* $p < 0.05$ , Mann Whitney U test).

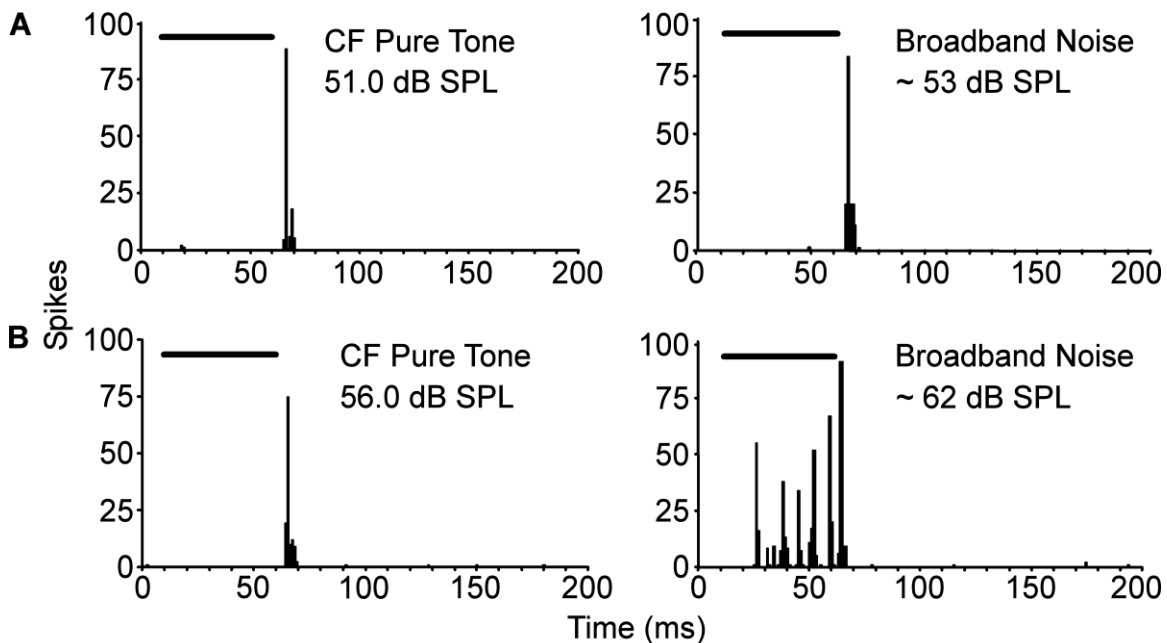


*Figure 3.5.* Comparison of SPON responses to pure tones and broadband noise. *A:* A typical SPON response to a pure tone, marked by an absence spiking during the stimulus and a transient offset response (*left panel*). This unit also responded to a broadband noise stimulus with a similar offset-transient response (*right panel*) *B:* However, the majority of SPON responses (~60%), regardless of anesthetic state, exhibited robust spiking during the presentation of broadband noise, in addition to a typical transient offset response (*right panel*). The response during the noise stimulus was characterized by a long latency relative to the stimulus onset and an intermittent spiking pattern. When units that responded during noise stimulation were presented with CF pure tones, spiking during the stimulus ceased and only the offset response was elicited (*left panel*). Horizontal bars represent the time course of stimuli. Sound levels for broadband noise are approximations based on the characteristics of the speakers.

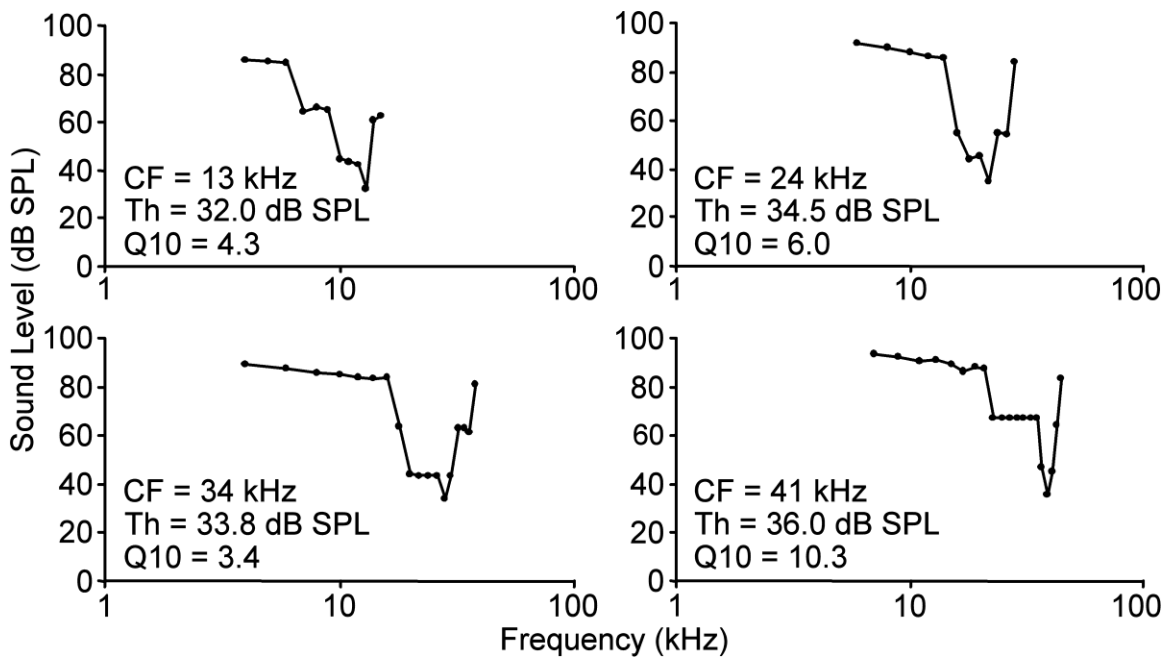


*Figure 3.6.* Typical frequency response maps of unanesthetized mouse SPON units. CFs from the sample shown ranged from 13-41 kHz, spanning most of the range of CFs recorded in our population of units. With few exceptions, response maps were broadly tuned and V-shaped near CF. Prominent low-frequency tails and sharp slopes at the high frequency ends of response maps were also typical.



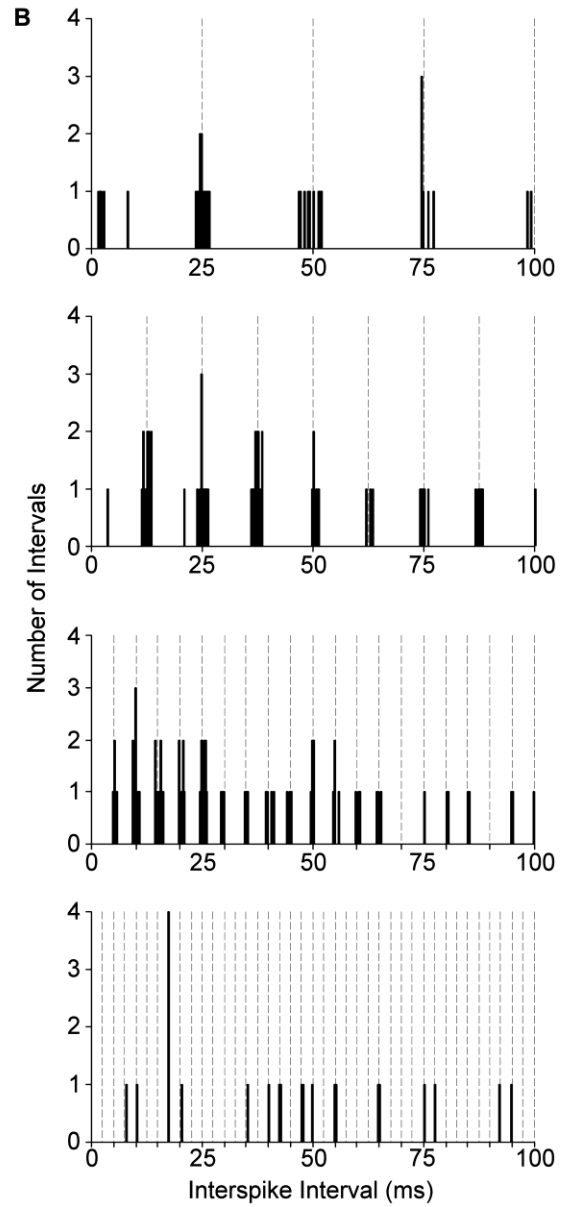
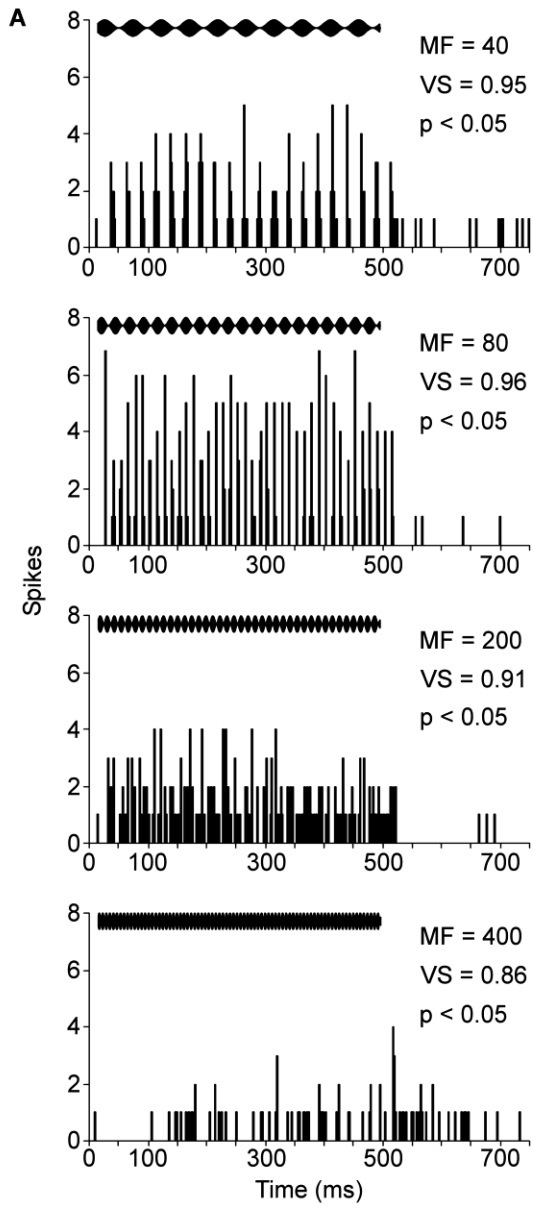


*Figure 3.7.* SPON responses to sinusoidally amplitude-modulated (SAM) tones. *A:* Peristimulus time histograms (PSTHs) of responses to SAM tones at varying modulation frequencies (MFs). Vector strengths (VSs) to all MFs were high in this example, although spiking decreased in response to the highest MF SAM tone (*bottom panel*). *B:* First order interspike interval histograms are shown beside corresponding PSTHs. Horizontal waveforms in *A* indicate the time course of SAM stimuli within the recording window. Vertical dashed lines in *B* denote multiples of the duration of the amplitude modulation cycle. P values in PSTH plots were generated using the Rayleigh test (Batschelet, 1981).; values  $< 0.05$  indicate significant phase locking.

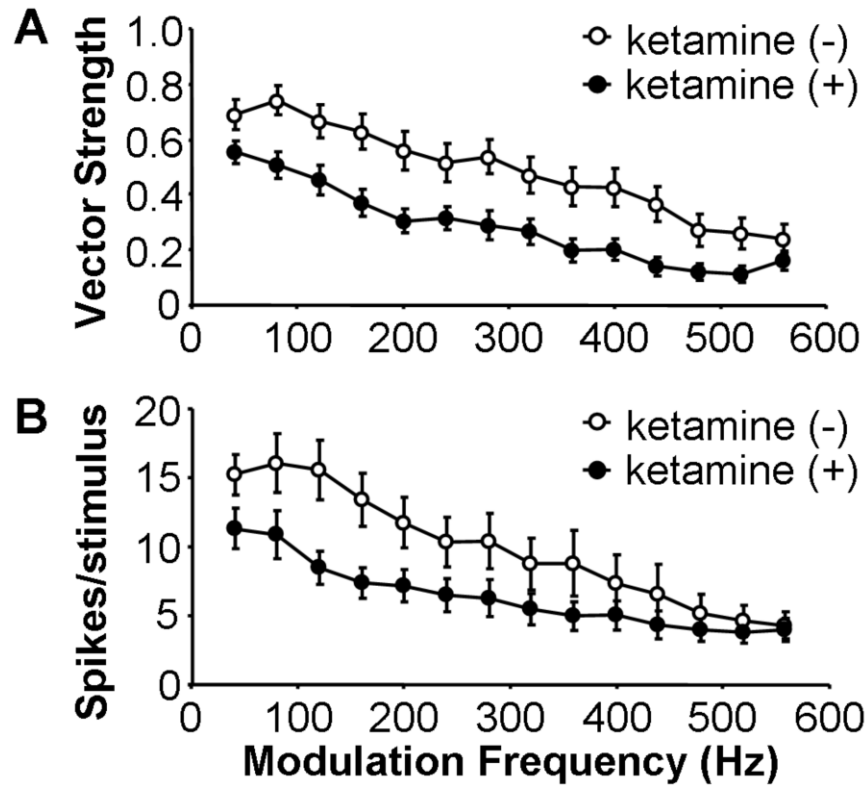


*Figure 3.8.* Responses to SAM tones for independent groups of unanesthetized (Ket -) and ketamine-anesthetized (Ket +) units. *A:* Mean vector strengths are shown as a function of modulation frequency. *B:* The mean number of spikes per stimulus presentation is shown as a function of modulation frequency. Error bars represent the standard errors of the means.

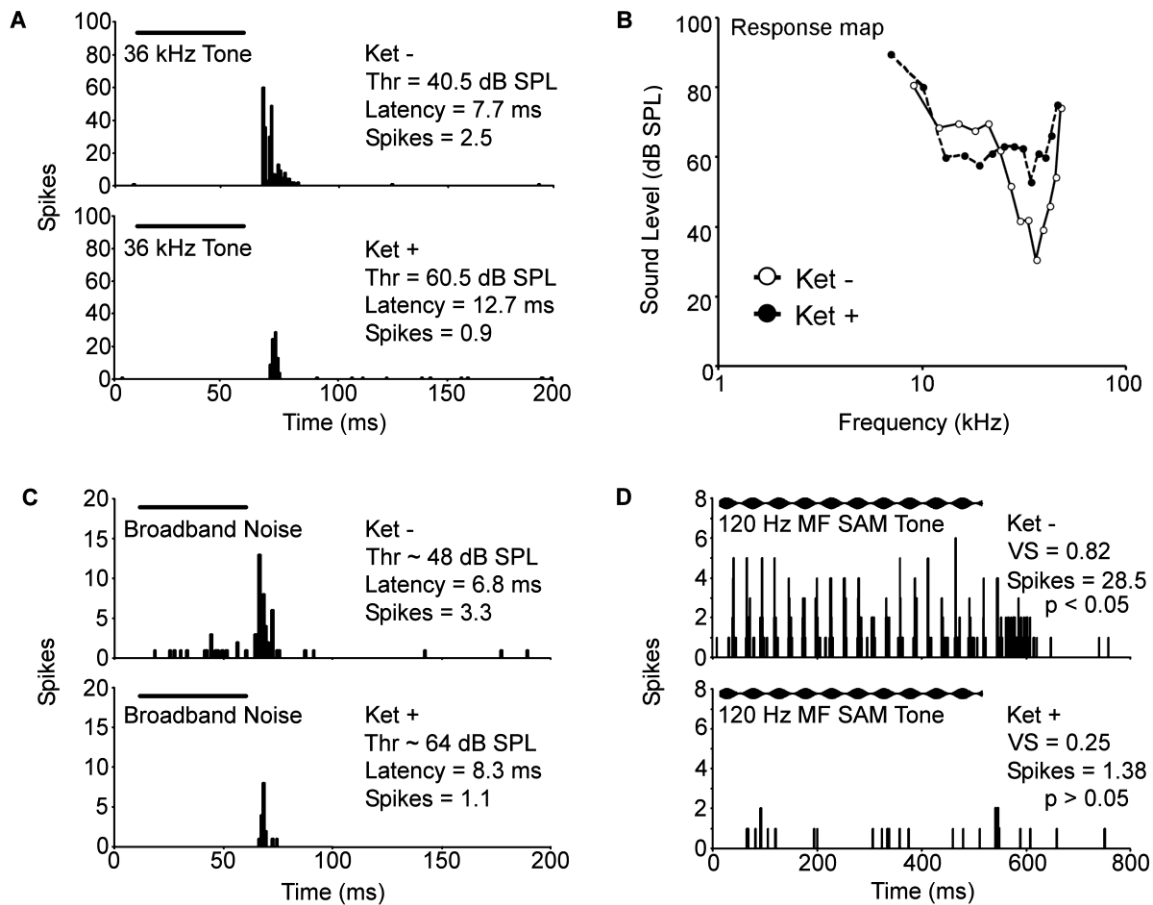


*Figure 3.9.* Examples of responses of paired SPON units directly before and after ketamine administration. *A:* Response to a CF pure tone prior to (*top panel*; Ket -) and following ketamine injection (*bottom panel*; Ket +). *B:* Response maps for a single-unit response before and after the introduction of ketamine anesthesia. *C:* Responses to broadband noise before and after ketamine delivery. *D:* A response to a SAM tone (120 Hz modulation frequency) decreased following ketamine treatment, accompanied by a substantial decrease in the vector strength. Abbreviations: Th, minimum threshold; Latency, first spike latency; Spikes, mean spikes per stimulus presentation. Horizontal bars in *A*, *C*, and *D* represent the time course of stimuli in the recording window. Sound levels of thresholds for broadband noise in *C* are approximations based on the speaker characteristics.

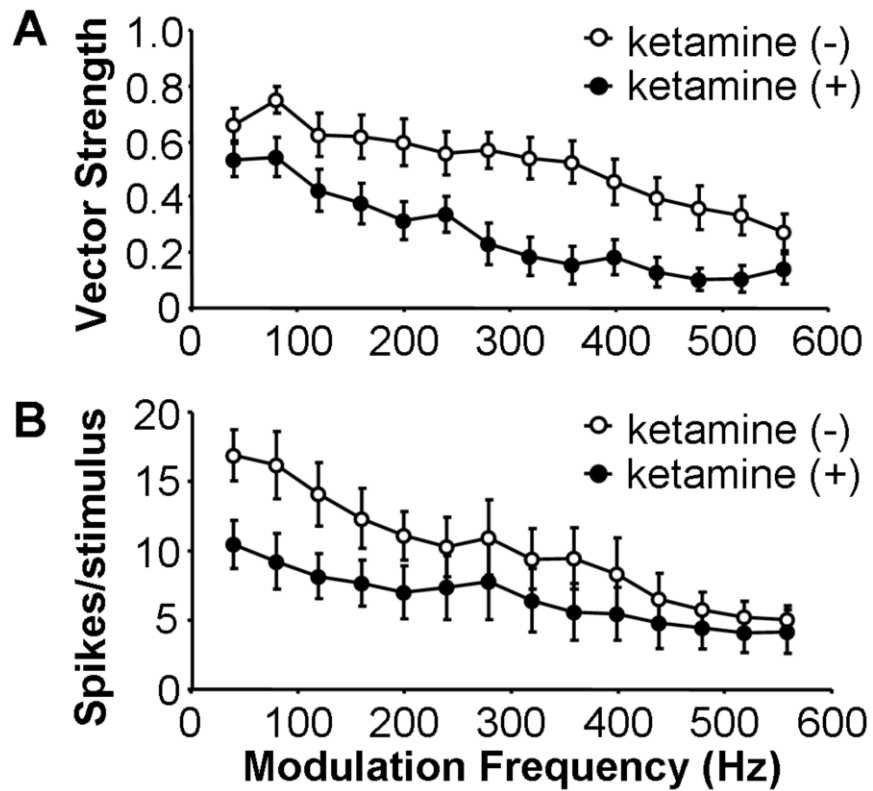


*Figure 3.10.* Responses to SAM tones for paired units recorded before and after ketamine was administered. *A*: Mean vector strengths are shown as a function of modulation frequency *B*: The mean number of spikes per stimulus presentation is shown as a function of modulation frequency. Error bars represent the standard errors of the means.

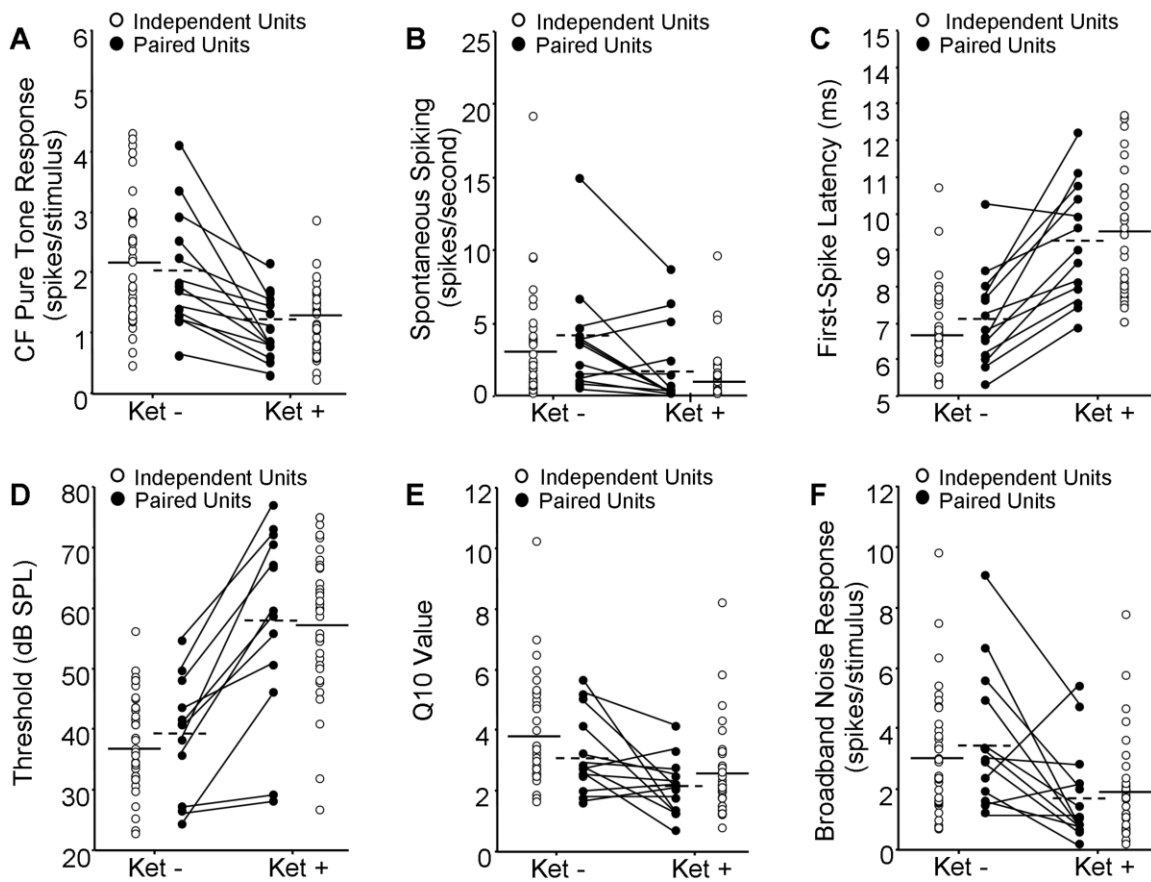


*Figure 3.11.* Population data for response properties of SPON units before and after ketamine administration. In each plot, values for individual units are represented for both independent (open circles) and paired (filled circles) pre-ketamine (Ket -) and post-ketamine (Ket +) recordings. Group means are represented by solid and dashed horizontal lines for independent and paired groups, respectively. Values for units in the paired recording group are connected by solid lines. *A, B:* Spike rates are shown for responses evoked by CF pure tone stimuli and for spontaneous activity, respectively. *C, D:* Plots of mean first spike latencies (*C*) and thresholds (*D*) of units in response to CF pure tones. *E:* Values for sharpness of tuning represented by Q10 values. *F:* Spike rates in response to broadband noise stimuli.

TABLE 1. *Summary of comparisons between independent SPON unit responses recorded with and without ketamine anesthesia*

Anesthetic State	FSL (ms)	Evoked Spikes (sp/stim)	Spontaneous Spikes (sp/sec)	Threshold (dB SPL)	Q10	Q30
Ket -	6.8 ± 0.2	2.2 ± 0.2	3.0 ± 0.6	37.1 ± 1.3	3.5 ± 0.3	1.5 ± 0.1
Ket +	9.5 ± 0.3	1.2 ± 0.1	1.1 ± 0.3	57.8 ± 2.0	2.6 ± 0.3	1.0 ± 0.1

FSL, first spike latency. All comparisons between unanesthetized (Ket-) and anesthetized (Ket +) conditions were significantly different (Mann-Whitney U test,  $p < 0.05$ ).

## **Chapter Four**

### **Ion channels and transmitter receptors shape responses to sinusoidally amplitude-modulated tones in the rodent superior paraolivary nucleus**

Part of this work was submitted for publication to the Journal of Neuroscience.



## **Abstract**

The superior paraolivary nucleus (SPON) is a prominent structure in the auditory brainstem. A defining characteristic of SPON neurons is their ability to precisely signal changes in temporal features of acoustic signals. Although neuronal responses to periodic stimuli such as amplitude-modulated tones have been described in some detail, it is not known how inputs to SPON neurons shape these responses. Both ionic currents and synaptic transmitter systems have been implicated in forming the hallmark offset spiking of SPON neurons to pure tone stimuli. A combined study of recordings in the mouse and rat used selective blockers of the  $I_h$  and T-type calcium currents, as well as antagonists of glycine, GABA<sub>A</sub>, AMPA/kainate and NMDA receptors to dissect the roles of each system on responses to amplitude modulated tones. The results demonstrate that blocking  $I_h$  and T-type calcium currents and glycine receptors has a large impact on responses to periodic stimuli, while blocking GABAergic and glutamatergic receptors has more subtle effects. Overall, the findings provide insight into how responses to temporally-rich stimuli are built and lend evidence for a functional role for the SPON in encoding periodic sound patterns. Such temporal periodicity information is likely important for detection of communication cues, such as the envelopes of animal vocalizations and speech signals.

## Introduction

The superior paraolivary nucleus (SPON) is located within the superior olivary complex in the mammalian auditory brainstem. While most nuclei in this area are associated with the processing of spatial acoustic information (e.g. reviewed by: Grothe et al., 2010; Tollin, 2003), the function of the SPON has yet to be fully resolved. Structures homologous to the SPON have been identified in all species studied thus far, including humans (Bazwinsky, et al., 2003; Kulesza Jr., 2008; Schmidt et al., 2010; Kulesza Jr. et al., 2011), suggesting that this structure has been preserved in mammalian evolution to fulfill a fundamentally important role in audition.

The hallmark of SPON neuronal responses is well-timed spiking triggered by the stimulus offset (Kuwada and Batra, 1999; Behrend et al., 2002; Dehmel et al. 2002; Kulesza et al., 2003). It has been shown *in vitro* that offset spiking is mediated by two currents active at subthreshold voltages, the hyperpolarization-activated inward cation current (I<sub>h</sub>) and the low voltage-activated (LVA) calcium current (Kopp-Scheinflug et al., 2010; Magnusson et al., 2010). It is thought that I<sub>h</sub> currents set the latency and duration of SPON offset spiking, while the both the I<sub>h</sub> and LVA Ca<sup>2+</sup> currents are necessary for responses to reach the threshold for generating action potentials (Felix II et al., 2011). In addition to subthreshold ion channels, synaptic neurotransmitter systems also shape SPON responses. Release from glycinergic inhibition (derived from the medial nucleus of the trapezoid body) has been shown to be the main generator of SPON offset spiking *in vivo* (Felix and Berrebi, 2010; Kulesza et al., 2007), and it is thought that GABAergic inhibition from within the SPON acts to limit the duration of responses, enabling neurons to signal rapid changes in temporal sound features (Kadner and Berrebi, 2008; Saldana and Berrebi, 2000). Although excitatory inputs to the SPON from octopus and multipolar cells of the ventral cochlear nucleus are also present, their role in shaping responses is not well-understood (Kuwabara et al., 1991; Friauf and Ostwald 1988; Saldaña et al., 2009; Schofield and Cant, 1995; Thompson and Thompson, 1991).

In addition to their characteristic offset spiking, another defining property of SPON neurons is their ability to respond with high precision to individual cycles of sinusoidally amplitude-modulated (SAM) sounds (Kadner and Berrebi, 2008), making

them well-suited for encoding fine temporal properties of acoustic signals, such as those associated with communication cues (e.g. Rosen 1992). Although several studies have characterized SPON responses to amplitude-modulated stimuli (Kuwada and Batra, 1999; Behrend et al., 2002; Kulesza et al., 2003; Kadner and Berrebi, 2008), the contributions of individual ion channels and transmitter systems to shaping SAM responses are unknown. Furthermore, nearly all animal studies that have investigated SAM encoding in the auditory system have used modulation frequencies above 20 Hz, even though many natural signal fluctuations shown to be important for human speech and animal vocalizations occur below this range (Langner 1997; 2005; Geissler and Ehret, 2002; Liu et al., 2006; Portfors, 2007).

In order to determine how ion channels and transmitter systems shape neuronal responses to SAM stimuli, recordings were conducted in the mouse and rat SPON prior to and following the use of various pharmacologic blockers. Experiments conducted in the mouse represent an extension of basic response properties to sound stimuli reported in Chapter 2, whereas rat experiments expand on previous findings regarding responses to temporal stimulus features (Kadner and Berrebi, 2008; Kadner et al., 2007; Kulesza Jr. et al., 2007). The results demonstrate that responses to SAM tones are affected to varying degrees by each of the receptor and channel manipulations that were conducted. Due to a substantial decrease in spiking, blocking  $I_h$  and LVA  $Ca^{2+}$  channels, as well as blocking glycinergic inhibition, greatly altered SAM responses, while blocking GABAergic inhibition and glutamatergic excitation had more subtle effects. A subset of SPON neurons also showed preferential entrainment to low frequency (1-20 Hz) SAM tone envelopes. Therefore, the findings suggest that SPON neurons encode a wider range of SAM modulation frequencies than previously thought, and, in addition to being shaped by synaptic transmitter systems, responses to temporal sound features are also governed by subthreshold ion currents *in vivo*.

## Methods

Twenty female CBA/CaJ mice aged three to twelve weeks (Jackson Laboratories, Bar Harbor, ME, USA) and fifteen sprague-dawley rats aged six to twenty weeks (Harlan, Indianapolis, IN, USA) were used for recordings. All animal care and use procedures were in accordance with the National Institutes of Health Guide for the Care and Use of Laboratory Animals and were approved by the West Virginia University Institutional Animal Care and Use Committee.

### *Surgical procedure*

*Mice:* Animals were anesthetized with a mixture of ketamine (70 mg/kg) and xylazine (5 mg/kg) prior to surgery and placed in a stereotaxic frame where the scalp overlying the skull was cut and reflected laterally. A tungsten grounding pin was inserted into the cortex on the side opposite the recording location. Then, a lightweight metal head-post was attached to the skull using dental cement, and a craniotomy, approximately one to two millimeters in diameter, was made over the cerebellum in order to gain access to the brainstem. Following the surgery, animals were moved to a sound-attenuated chamber where the head-post was connected to a stereotaxic device that rendered the head immobile during recordings. The core body temperature was maintained at 37° C throughout the experiment using a thermostatically controlled heating pad (FHC, Bowdoinham, ME, USA). The depth of anesthesia was carefully monitored each time the electrode was repositioned by observing the response to a foot pinch. In rare cases when the anesthetic state became light, an injection of ketamine at one-third the original dose was administered. Topical lidocaine (5%) was applied to the wound margins every two hours.

*Rats:* Prior to experiments, animals were anesthetized with a mixture of ketamine (70 mg/kg; i.m.) and xylazine (5 mg/kg). The head was then mounted in a stereotaxic frame and the scalp was reflected laterally to expose the skull. A custom-made head post was secured to the skull with screws and dental cement. A craniotomy (~3x7 mm) was performed with a drill, with the rostral edge of the bone defect extending to the posterior

aspect of the transverse sinus. The dura mater was penetrated and the cerebellum was aspirated to expose the floor of the fourth ventricle, whose midline was used to guide electrode penetrations. The rat was then transferred to a sound-attenuated booth for recordings. Body temperature was maintained at 37° with a heating pad. Supplemental injections of the anesthetic were administered as needed at one-third the original dose.

### *Acoustic stimulation*

Stimulus generation and data acquisition were controlled by custom-written software (BATLAB, Donald Gans, Northeast Ohio Universities College of Medicine, Rootstown, OH, USA). Stimulus waveforms were output through a 16-bit digital-to-analog converter (400,000 samples/second; model DAP521a; Microstar Laboratories, Bellevue, WA, USA), and analog signals were sent to an anti-aliasing filter (FT6-2; Tucker-Davis Technologies (TDT), Alachua, FL, USA), then fed to a programmable attenuator (PA-5; TDT). Signals were then routed to speaker drivers (ED1; TDT) and presented to the animal through free-field speakers (ES1; TDT) placed 5 millimeters from the opening of each ear. The speaker output was calibrated offline over a range of 0.5-60 kHz using a measuring amplifier (model 2610; Brüel & Kjær, Norcross, GA, USA) connected to a condenser microphone (model 4939; Brüel & Kjær) positioned at the location normally occupied by the animal's head.

### *Recording procedure*

Single-unit extracellular recordings were conducted with glass pipettes (2-4 µm tip diameter) filled with 0.5 M NaCl recording solution (10-20 MΩ resistance). The SPON was targeted using stereotaxic coordinates obtained from an atlas of the mouse or rat brain (Paxinos and Franklin, 2001; Paxinos and Watson, 1986). Once the electrode penetrated the brain, neuronal activity was amplified (model 2400; Dagan Corporation, Minneapolis, MN, USA), band-pass filtered (200-3000 Hz; model 3364; Krohn-Hite, Brockton, MA, USA), and digitized by a 16-bit analog to digital converter (42 kHz;

DAP5216a; Microstar Laboratories). Individual raw waveforms were recorded in BATLAB and stored for offline analysis.

Bursts of broadband noise (50 ms duration, ~80 dB SPL, 4 presentations/second) were used as search stimuli. Based on previous anatomically-verified recordings in the SPON of mice (Felix II and Berrebi, 2007) and rats (Kulesza Jr. et al., 2003; Kadner and Berrebi, 2008), only responses that were driven by contralateral stimulation and triggered by the stimulus offset were considered to be from the SPON. Once a single-unit was isolated, its characteristic frequency (CF; the frequency requiring the lowest intensity to elicit an evoked response), and its minimum threshold (the lowest intensity required to elicit a response) were determined. Peri-stimulus time histograms (PSTHs) were constructed by presenting 100 repetitions of a pure-tone (50 ms duration) at the unit's CF 20 dB above threshold. When spikes triggered by the stimulus onset and offset were examined independently, the time window for capturing spikes that occurred during the tone presentation was set at 0-50 milliseconds from the onset of the stimulus, while the offset response was windowed from 5-35 milliseconds from the end of the stimulus.

For experiments involving manipulation of the sound envelope, neurons were presented with sinusoidally amplitude-modulated (SAM) tones that were either two seconds (mouse experiments) or 0.5 seconds (rat experiments) in duration, using the unit's CF as the carrier frequency at 20 dB above threshold. The analysis window for SAM tests began at the stimulus onset and ended at the offset. Each SAM tone was presented either 20 times (mouse) or 8 times (rat) at modulation frequencies (MFs) that were varied from 1-600 Hz (mouse) or from 10-1200 Hz (rat) at 100% modulation depth. The fidelity of phase-locking at each MF was quantified by calculating the vector strength (VS):

$$VS = \frac{1}{n} \sqrt{\left[ \sum \sin(a_i) \right]^2 + \left[ \sum \cos(a_i) \right]^2}$$

where  $a_i$  is the phase angle of spike  $i$  relative to the modulation cycle of the stimulus, and  $n$  is the total number of spikes in the analysis window (Goldberg and Brown, 1969). A vector strength of 1 indicates perfect synchronization between the neuronal response and the modulation phase, whereas a vector strength of 0 indicates no correlation. The Rayleigh test (Batschelet, 1981) was used to determine whether spike distributions

relative to the phase angles of stimuli differed significantly from randomness. To minimize the influence of isolated action potentials that were time-locked to the onset of the SAM tone (and therefore occurred at a constant phase angle), the vector strength was set to 0 if the unit's spike count fell below 2 spikes per presentation (Kadner and Berrebi, 2008). In cases where transient onset spiking was observed, the first 10 ms of the analysis window was excluded from the vector strength calculation.

### *Pharmacologic receptor blockade*

For iontophoresis experiments, recordings were made with “piggyback” electrodes (Havey and Caspary, 1980; Kulesza Jr. et al., 2007) consisting of a single-barrel recording pipette glued onto a five-barreled glass pipette used for drug delivery (15-25  $\mu\text{m}$  total tip diameter). One barrel of the electrode was used as a sum channel, while the remaining four barrels were loaded with either ZD7288 (30 mM, pH 4.0; Sigma, St. Louis, MO, USA), Mibefradil (10 mM, pH 3.5-4.0; Sigma), strychnine (10 mM, pH 3.0; Sigma), SR95531 (Gabazine) (3 mM, pH 4.0; Tocris, Ellisville, MO, USA), 1,2,3,4-tetrahydro-6-nitro-2,3-dioxobenzo[f]quinoxaline-7-sulfonamide (NBQX) (5 mM, pH 9.0, Sigma), or ( $\pm$ )3-(2-carboxypiperazin-4-yl)-propyl-1-phosphonic acid (CPP) (10 mM, pH 8.0; Sigma). All drugs were dissolved in 0.165 M NaCl, and retention and ejection currents for each drug solution were controlled by a micro-iontophoresis unit (model 6400; Dagan) located outside the recording chamber. While searching for SPON neurons, a retention current 10 nA in magnitude and of opposite polarity of each drug's net charge was continually applied to prevent leakage from the electrode tip. Following the isolation of a unit and the recording of baseline activity, drugs were ejected with the following current ranges (in nA): ZD7288 +25-40, Mibefradil +25-60, strychnine +10-40, Gabazine +3-30, NBQX -40-60, CPP -20-80. Drugs were typically applied for a period ranging from 10-25 minutes. Maximal drug effects were signaled by changes in the neuron's spiking pattern that remained stable for three consecutive minutes. After data were collected for the drug conditions, the ejection current was terminated, the retention current was re-applied, and the drugs were allowed to wash out, followed by collection of

data in the recovery condition. In cases where a unit was lost prior to recovery, 30 minutes elapsed before the electrode was moved to search for another neuron.



## Results

Findings from two sets of experiments are presented here; both united by a focus on responses of SPON neurons to sinusoidally amplitude-modulated (SAM) tones before and after various pharmacologic blockers were applied. The first set of experiments was designed with parameters that corresponded to *in vitro* recordings that utilized “chirp” stimuli (see Chapter 1 and Felix II et al., 2011). Thus, these experiments included young mice (roughly three weeks of age) in addition to adults, and used SAM stimuli that had relatively low modulation frequencies (MFs; 1-20 Hz) and long durations (2 seconds). In addition, blockers of subthreshold ion channels were utilized in mouse experiments in order to expand on studies of the effects of these blockers on SPON responses *in vitro* (Felix II et al., 2011; Magnusson et al., 2010). The second set of experiments was designed with parameters that corresponded to those used in previous *in vivo* studies that focused on SPON SAM responses (Kadner et al., 2007; Kadner and Berrebi, 2008), and thus utilized adult rats as the animal model, higher stimulus MFs (up to 1200 Hz) and shorter durations (0.5 seconds). For rat experiments, each major transmitter system known to provide input to SPON neurons (Fig. 4.1) was blocked pharmacologically, and resulting SAM responses were examined. All experiments were conducted with “piggyback” electrodes that consisted of a single-barreled recording pipette glued to a multibarrel drug delivery pipette. To be sure that neither the pH of drug solutions nor the current used for drug ejection affected neuronal responses, vehicle solutions administered by iontophoresis in the absence of drugs were used as a control. No appreciable effect on SPON spiking was observed following the application of vehicle solutions (Fig. 4.2).

### *SPON neurons in the mouse are tuned to low-rate modulated stimuli*

In order to assess the ability of SPON neurons to encode low frequency periodic stimuli, responses were recorded from neurons in young (p20-p22, n= 13) and in adult (p58-p80, n= 19) mice, with CFs ranging from 11-40 kHz. Each unit was presented with SAM tones; with the carrier frequency set to the unit’s CF and the MF systematically varied from 1-20 Hz.

Two types of SAM responses were frequently observed for neurons in both young and adult animals. One type was marked by significant phase-locked spiking to SAM tones with low MFs ( $p < 0.05$ , Rayleigh test) and a pronounced decrease in entrainment to cycles of MFs above approximately 15 Hz; this type of modulation transfer function was observed in 38% of units in young animals (Fig. 4.3A) and in 42% of units in adult animals (Fig. 4.3B). A second type of SAM response, seen in 62% and 58% of units in young (Fig. 4.3C) and adult (Fig. 4.3D) animals, respectively, displayed significant phase-locking to all MFs presented. In addition, all neurons that responded to low MFs did so with clustered spiking restricted to roughly one-third of each modulation cycle, as shown by period histograms (Fig. 4.3A-D, PSTH insets).

In both young and adult animals, the highest percentage of phase-locked responses for SPON neurons occurred from 5-15 Hz (Fig. 4.3E). Overall, phase-locking for units in young and adult animals did not significantly differ for responses to any of the MFs tested (1-600 Hz; Mann-Whitney U test,  $p = 0.07-0.95$ ). However, at very low MFs (1-5 Hz), vector strengths of units in young animals were higher than in adults, although these differences did not reach significance (Mann-Whitney U test,  $p = 0.07-0.13$ ; Fig. 4.3F). In all but two cases, neurons that phase-locked to MFs up to 20 Hz (e.g., Figs. 4.3C, D) continued to exhibit significant entrainment to SAM modulations up to 200-400 Hz (Fig. 4.3G), as previously reported for the rat SPON (Kulesza Jr. et al., 2003; Kadner and Berrebi, 2008).

#### *Ih and LVA Ca<sup>2+</sup> currents shape mouse responses to tone and SAM stimuli*

*Pure tone responses:* Neuronal responses were recorded from seven units in the SPON of young mice (p21-p24) to determine the degree to which Ih and LVA T-type Ca<sup>2+</sup> currents contributed to sound-evoked spiking. Due to the low number units that were recorded, statistical verification of drug effects on tone and SAM responses was not conducted. After obtaining responses to a CF pure-tone under baseline conditions, either the Ih current blocker ZD7288 or the LVA Ca<sup>2+</sup> current blocker Mibefradil was administered alone, followed by the addition of the second drug. The order of drug application was alternated in order to assess the actions of each drug in isolation. After responses were

obtained with both drugs delivered simultaneously, the neuron was allowed to recover. The complete recording procedure, from baseline to recovery, was completed for four neurons, with ZD7288 applied first in two cases and Mibefradil first in the other two cases. A partial protocol was run for an additional three units, in which data from baseline conditions and either ZD7288 (n= 1) or Mibefradil (n= 2) conditions were collected. However, in these cases, single-unit isolation was lost prior to application of the second drug.

SPON neurons showed distinct changes in spiking behavior following ZD7288 and Mibefradil application (Fig. 4.4). In one example, a robust offset response was observed with little spiking during the stimulus under baseline conditions (Fig. 4.4A), but upon ZD7288 application, the magnitude of offset spiking decreased and spiking that occurred during the stimulus presentation increased substantially, particularly near the onset of the tone (Fig. 4.4C). When Mibefradil was added along with ZD7288, nearly all spiking was abolished, apart from a well-timed onset response (Fig. 4.4E). After the drugs were allowed to wash out, a large portion of the offset component recovered, but the response duration remained truncated compared to baseline (Fig. 4.4A, G). For a second representative SPON unit, Mibefradil was applied first, followed by the addition of ZD7288. In this case, Mibefradil acted to reduce the magnitude and duration of offset spiking, and decreased the onset response seen in the baseline condition (Fig. 4.4B, D). When ZD7288 was added the offset response was abolished and the onset response that was reduced by Mibefradil increased (Fig. 4.4F). After both drugs were removed, both onset and offset responses for this unit recovered to near-baseline levels (Fig. 4.4H).

On average, action potentials occurring in the offset time window (5-35 ms post-stimulus) decreased by 53% in the presence of ZD7288 compared to baseline conditions (Fig. 4.4I). The application of Mibefradil alone resulted in an even larger reduction (78%) in offset spiking. Moreover, although both ZD7288 and Mibefradil applied in isolation acted to substantially limit the offset response, the combination of both drugs nearly eliminated all post-stimulus spiking, with less than 2% of baseline spikes remaining after the combined drug application. In addition to the offset response, drugs also affected spiking during the stimulus presentation, particularly near the tone onset. The application of Mibefradil alone or ZD7288 plus Mibefradil decreased onset spiking by 91% and 77%,

respectively, compared to baseline, similar to what was observed for offset responses (data not shown). However, when ZD7288 was applied alone, spiking during the stimulus presentation increased by 152% (e.g., Fig. 4.4A, C). Overall, compared to the offset response, onset spiking for SPON neurons was unreliable, with only three of seven units exhibiting a clear evoked response (defined as  $> 0.5$  spikes/stimulus).

In addition to spike counts, mean first-spike latencies were also measured to determine the impact of each drug on the temporal precision of SPON offset responses (Fig. 4.4J). The application of ZD7288 alone elevated offset response latencies by 21% compared to baseline conditions, while Mibefradil alone resulted in an increase of only 6%. When ZD7288 and Mibefradil were combined, latencies increased to 18% above baseline. For onset responses, latencies were highly variable, ranging from 6.1 to 17.0 ms, compared to offset latencies which ranged from 7.9-10.3 ms. In all drug conditions, onset response latencies were elevated compared to baseline conditions, even for ZD7288, which caused a substantial increase in onset spiking.

*SAM responses:* To further assess the effects of  $I_h$  and LVA  $Ca^{2+}$  currents on the behavior of SPON neurons, responses to SAM stimuli were recorded before, during and after the application of ZD7288 and/or Mibefradil (Fig. 4.5 and 4.6). In an example where ZD7288 was applied, we observed decreases from baseline in both spiking and phase-locking (Fig. 4.5A, B). In addition, ZD7288 acted to reduce the range of MFs over which the neuron phase-locked, limiting entrainment to MFs of 1-4 Hz, down from 1-15 Hz in baseline recordings. When Mibefradil was added along with ZD7288, spiking was dramatically reduced, and in turn, phase-locking to all MFs was abolished (Fig. 4.5C). After allowing the drugs to wash out for one hour, both vector strengths and spiking partially recovered (Fig. 4.5D). For a second unit, Mibefradil was applied first, resulting in decreased spiking and entrainment to SAM tones (Fig. 4.6A, B). Although vector strengths of responses to MFs of 6-12 Hz were lower in the presence of Mibefradil, they were still significant ( $p = 0.01-0.001$ , Rayleigh test). However, when ZD7288 was combined with Mibefradil, the spiking rate of the neuron was further reduced and phase-locking was abolished at all MFs presented (Fig. 4.6 C). Following an hour-long period of recovery from the drugs, vector strengths returned toward baseline levels, but spiking remained depressed (Fig. 4.6D).

*Inhibitory transmitter systems shape phase-locking properties in the rat*

Although SPON neurons receive both excitatory and inhibitory synaptic input, their responses to acoustic signals have been shown to be mediated primarily by inhibition (Kulesza Jr. et al., 2007; Kadner and Berrebi, 2008). While offset responses to pure-tones are created in large part by release from MNTB-derived glycinergic inhibition (Kulesza Jr. et al., 2007), it has been proposed that GABAergic inhibitory inputs that originate within the SPON may contribute to generating the temporal precision required to faithfully encode modulations of low-rate SAM stimuli (Kadner and Berrebi, 2008). To investigate the role of inhibitory transmitter systems on SPON response properties, blockers for both glycine and GABA<sub>A</sub> receptors were applied while presenting pure-tone and SAM tone stimuli. A total of 24 units were recorded in the SPON, with CFs ranging from 1-42 kHz, covering the majority of the rat behavioral audiogram (Kelly and Masterton, 1977).

Following the recording of a typical SPON unit's response to a CF pure tone (Fig. 4.7A), the GABA<sub>A</sub> receptor blocker Gabazine was applied continuously for 25 minutes. Compared to baseline, the response for the Gabazine condition had a similar magnitude of spiking in the onset window (39 and 32 spikes for baseline and Gabazine, respectively); however, spiking was not well-timed to the stimulus onset and was intermittent for the duration of the tone presentation, in contrast to the baseline condition (Fig. 4.7B). By removing GABAergic inhibition with the application of Gabazine, the response magnitude of neurons would be expected to increase. Thus, it was unexpected when both spiking and the response duration in the offset window decreased following Gabazine treatment, albeit by small amounts (39 vs. 32 spikes and 27 vs. 24 ms for baseline and Gabazine conditions, respectively). Conversely, after 10 minutes of strychnine application, the baseline offset response was abolished and prominent spiking in the onset window was observed (Fig. 4.7C). When strychnine and Gabazine were both applied simultaneously for 15 minutes, the response in the onset window increased twofold (205%) compared to the response when strychnine was applied alone (Fig. 4.7D). In addition, the combination of strychnine and Gabazine resulted in a bimodal

distribution of spike times centered on 18 and 31 ms from the stimulus onset. One hour after the termination of drug application, the response recovered to resemble the baseline condition. However, the response did not fully recover, as the small onset response observed in the baseline condition did not reappear and the offset response was not as precisely triggered by the stimulus offset in the recovery condition (Fig. 4.7E). In summary, strychnine dramatically alters spiking to pure tones by eliminating the offset response and unmasking spiking during the stimulus, while Gabazine has modest effects when applied alone, but enhances spiking during the stimulus presentation when combined with strychnine (Fig. 4.7F).

Although Gabazine alone did not substantially alter SPON responses to pure tones, it did have a more pronounced effect on responses to SAM tones. Gabazine administration increased the offset response to a 60 Hz MF SAM tone (0.5 second duration), but spiking to individual modulation cycles during the stimulus presentation decreased, opposite the expected result of blocking a source of inhibition (64 and 37 spikes for baseline and Gabazine conditions, respectively; Fig. 4.8A, B). In addition, the vector strength of the response to the sound envelope dropped from 0.92 in the baseline condition to 0.56 following drug application, resulting in a loss of phase-locking (from  $p < 0.01$  to  $p = 0.78$ , Rayleigh test). Despite the observed decrease in spiking to the 60 Hz MF stimulus, Gabazine elevated the response magnitude at other rates of modulation (Fig. 4.8G), resulting in significant phase-locking at 260 and 300 Hz ( $p = 0.02$  and  $0.01$ , respectively, Rayleigh test), in contrast to the baseline condition, where phase-locking only occurred at very low modulation rates (20-100 Hz; Fig. 4.8F). The application of strychnine alone caused an even greater decrease in spiking and entrainment to the 60 Hz SAM tone (64 vs. 27 spikes and 0.92 vs. 0.44 VS for baseline and Gabazine, respectively), with spiking primarily restricted to the onset of the stimulus (Fig. 4.8C, F, G). Strychnine limited the range over which the unit phase-locked, from 20-100 Hz MF in the baseline condition to only 20 Hz after drug application. Although the strychnine-influenced response phase-locked to 20 Hz MF, the vector strength was lower (0.65) compared to baseline (0.83) (Fig. 4.8F). Gabazine and strychnine applied concurrently elevated spiking to near-baseline levels at 60 Hz modulation (53 and 64 spikes, respectively), although spikes were clustered near the on- and offset of the stimulus,

resulting in the majority of modulation cycles eliciting no response and leading to a vector strength of only 0.34 (Fig. 4.8D). The highest VSs for the drug combination were 0.48 and 0.54 for 20 and 40 Hz, respectively, although phase-locking was not significant ( $p= 0.16$  and  $0.09$ , Rayleigh test; Fig. 4.8F). For higher MFs ( $>60$  Hz), the combination of Gabazine and strychnine elevated spiking above levels observed in the baseline condition, but this effect did not result in phase-locking at any of the MFs tested (Fig. 4.8F, G). Following washout of the drugs, phase-locking returned to baseline levels, although spiking was depressed, perhaps due to an incomplete recovery (Fig. 4.8E, F, G).

In order to further explore the effects of glycine receptor blockade, strychnine alone was applied to 23 SPON neurons in order to characterize changes in responses to SAM tones. Neurons exhibited significantly synchronized spiking in the baseline condition to MFs below 160 Hz ( $p < 0.01$ , Rayleigh test), and all VS values in this range were greater than 0.7 (Fig. 4.9A, C, E). At higher MFs, neurons ceased spiking during the stimulus, and thereby lost synchronization (Fig. 4.9E, F). Excitatory input to the SPON, which was unmasked by strychnine application, was characterized by VS values below 0.6 (Fig. 4.9E), indicating a lack of phase-locking at all MFs tested, even though response magnitudes increased after strychnine application (Fig. 4.9F).

#### *Effects of excitatory transmitters on responses to SAM tones in the rat*

Changes following inhibitory receptor blockade revealed an excitation-driven response of SPON neurons to pure tones. To directly assess the nature of this excitatory input, we recorded from a neuron while blocking NMDA receptors with CPP and by blocking AMPA/kainate receptors with NBQX (Fig. 4.10). Blockade of NMDA neurotransmission led to a 22% reduction of a pure tone response without changing its temporal characteristics; additional blockade of AMPA/kainate receptors did not lead to a further reduction in spike counts (Fig. 4.10A-C, top panels). In response to SAM tones, application of CPP alone did not alter VSs from baseline levels (Fig. 4.10B bottom panel and Fig. 4.10 D), although spiking was reduced for nearly all MFs at which spiking was evoked (Fig. 4.10E). When NBQX was applied simultaneously with CPP, spiking was substantially reduced at all MFs to which the unit phase-locked in the baseline condition

(Hz; Fig. 4.10C bottom panel and Fig. 4.10E). In addition, the range of MFs where significant phase-locking occurred was shortened from 20-250 Hz in the baseline and CPP conditions to 20-120 Hz with CPP+NBQX (Fig. 4.10D).



## Discussion

The studies presented here demonstrate that the blockade of subthreshold ionic currents, as well as synaptic inputs to the SPON, alter neuronal responses to both pure tones and SAM tones. Each system that was investigated contributed in some way to shaping response properties, with relative contributions ranging from major involvement of  $I_h$  and LVA  $Ca^{2+}$  currents and glycinergic input to more subtle contributions from GABAergic and glutamatergic inputs. In addition, SPON neurons exhibited highly synchronous responses to very low rates of sound envelope modulation. Of particular interest was a subset of neurons that appeared to be sensitive to envelope modulation frequencies under 20 Hz. In general, rodent SPON neurons are particularly well-suited for encoding the timing and shape of periodic acoustic signals, such as SAM stimuli. This sensitivity is primarily mediated by a combination of inhibitory synaptic inputs that hyperpolarize the cell membrane and membrane-bound ion channels that set the magnitude and precision of spiking responses. Although experiments were conducted using both mice and rats, response properties of SPON neurons in both animal models are similar, and therefore, species differences will not be discussed further (see Chapter 3 Discussion).

### *SPON neurons respond to a wide range of sound envelope modulation frequencies*

Previous studies of neuronal responses to SAM stimuli in the SPON were limited to modulation frequencies (MFs) ranging from 20-1000 Hz (Behrend et al., 2002; Kadner and Berrebi, 2008; Kulesza Jr. et al., 2003; Kuwada and Batra et al., 1999). For mouse experiments in the current study, the range of MFs was expanded to include 1-20 Hz modulation in addition to the more commonly presented 20-600 Hz range. The rationale for focusing on very low rates of modulation rates was twofold: first, many conspecific vocalizations, including those of mice, possess envelope modulations below 20 Hz (Geissler and Ehret, 2002; Liu et al., 2006). Thus, the sensitivity to low MFs exhibited by SPON neurons suggests a potential role in encoding natural sounds that low rates of envelope fluctuations. Second, *in vitro* experiments conducted on SPON neurons in similarly aged mice revealed sharp tuning to frequency-modulated oscillating current

injections (“chirp” stimuli; Felix II et al., 2011; Magnusson et al., 2010). The present study lends additional evidence that low MF periodic stimuli evoke robust and temporally-precise responses from SPON neurons *in vivo*.

Although some SPON neurons preferred very low rates of envelope modulations, the majority of units demonstrated phase-locking up to roughly 400 Hz. This broader range of MFs corresponds closely to modulations of SAM tones that neurons in the target of the SPON, the inferior colliculus, respond to most faithfully (Frisina, 2001; Joris et al., 2004). Therefore, the SPON likely contributes to shaping responses to periodic stimuli in the inferior colliculus, as both nuclei exhibit precise responses over similar ranges of MFs. However, one notable difference between the SPON and inferior colliculus exists; whereas neurons in the SPON respond to very low rates of envelope modulation, modulation transfer functions for units in the inferior colliculus have been described as bandpass; that is, their responses do not generally synchronize to MFs below ~50 Hz, nor above ~400 Hz (Krishna and Semple, 2000). Entrained responses of SPON neurons cover a broad enough range of MFs that the nucleus could be involved in the representation of one or more distinct sound percepts. For example, it is possible that at very low MFs the SPON is involved in rhythm detection. At higher MFs, it may have a role in the perception of roughness, and at the upper range of preferred MFs the role may be that of resolving pitch, either of which could be encoded by way of the SPON-inferior colliculus circuit. These perceptual ranges correspond to human psychoacoustics, where below 20 Hz listeners hear rhythm, as each SAM cycle is perceived as a separate stimulus; between 20 and 200 Hz the perception is of roughness, and at MFs above 200 Hz, the perception changes to periodicity-driven pitch (discussed in Kadner and Berrebi, 2008).

#### *Ih and LVA Ca<sup>2+</sup> currents underlie spiking to pure tone and SAM stimuli*

The characteristic offset spiking observed in the SPON is generated when neurons are released from MNTB-derived inhibition. Following the termination of the stimulus and corresponding inhibition, Ih channels remain open for tens of millisecond (Magnusson et al., 2010). Inward current through these open channels causes the cell membrane potential to rebound (depolarize) to spike threshold with the help of LVA Ca<sup>2+</sup> currents,

resulting in a brief burst of spiking that is well-timed to the end of the hyperpolarizing stimulus. Specifically, the  $I_h$  current sets the timing window of the response, whereas both  $I_h$  and LVA  $Ca^{2+}$  currents depolarize the membrane to spike threshold. To determine whether these currents had a similar role in the response of SPON neurons *in vivo*, selective blockers for  $I_h$  and LVA  $Ca^{2+}$  currents were administered and responses to pure tones were recorded prior to and following drug delivery. When applied in isolation, each blocker decreased the spiking rate, indicating that both are necessary for normal neuronal behavior. Blockade of the LVA  $Ca^{2+}$  current reduced spiking to the stimulus onset, in addition to the offset, blocking the  $I_h$  current potentiated the onset response. Another difference between  $I_h$  and LVA  $Ca^{2+}$  currents is their effects on spike timing. In accordance with findings *in vitro*, blocking  $I_h$  caused a significant increase in first spike latencies, while blocking the LVA  $Ca^{2+}$  current had no effect on latencies. Thus, both currents are required for robust SPON spiking, but only  $I_h$  appears to be involved in spike timing.

In addition to having distinct effects on pure tone responses,  $I_h$  and LVA  $Ca^{2+}$  currents have different roles in modulating spiking to SAM tones. For instance, when  $I_h$  was blocked, synchronization to very low MFs (<5 Hz) remained intact and phase-locking to higher frequencies was abolished. This effect is likely due to the fact that entrainment to higher MFs requires precisely-timed responses (discussed in Grothe, 1994; Kadner and Berrebi, 2008) and such precision is lost when  $I_h$  is blocked. At very low MFs, spike timing is less critical and vector strengths remain high in the absence of  $I_h$ . Thus, any drop in vector strengths in this range is likely related to decreases in the overall spike rate of the neuron. Conversely, LVA  $Ca^{2+}$  current blockade resulted in a drop in vector strength for responses to all MFs presented, also presumably due to a general decrease in response magnitude, but significant phase-locking remained intact for most MFs compared to baseline. Therefore, the combined effects of decreases in the magnitude and precision of spiking that accompanied  $I_h$  blockade resulted in a more pronounced impact on responses to SAM compared to blocking LVA  $Ca^{2+}$  currents, which only affected the spiking rate. Conversely, blocking LVA  $Ca^{2+}$  currents had a slightly larger effect on pure tone responses compared to blocking  $I_h$ . It is important to note that the methods used for drug delivery almost certainly result in imperfect

channel/receptor blockade, and thus, any observed effects of blocker application likely underestimate the role of each of the systems investigated.

It is possible that the effects of both ZD7288 and Mibefradil on SPON spiking may have been overstated due to non-specific effects associated with each drug. Specifically, in addition to blocking the  $I_h$  current, ZD7288 also partially blocks T-type calcium (Sanchez-Alonso et al., 2008) and potassium currents (Do and Bean, 2003). Also, Mibefradil has been shown to block voltage-gated sodium currents in addition to T-type calcium currents (Eller et al., 2000). Therefore, decreases in spiking that were observed following application of these drugs were likely more pronounced than would be expected using blockers with higher affinity for the channels of interest in this study. However, it remains difficult to resolve why ZD7288 increased the magnitude of onset spiking in several SPON cells. One possible explanation is that a general increase in membrane input resistance caused by ZD7288 (Robinson and Siegelbaum, 2003) makes neurons more excitable near the onset of stimuli, which may alter the balance of early arriving excitatory inputs from octopus cells and inhibition from the MNTB. This possible shift toward increased subthreshold excitation at the sound onset may be large enough for onset spiking to increase.

#### *Glycinergic and GABAergic inputs contribute of phase-locking of SPON neurons*

One goal of the current study was to explore the role of GABAergic inhibition on the behavior of SPON neurons. In contrast to MNTB-derived glycinergic inhibition, which has been described in some detail (Kadner and Berrebi, 2008; Kulesza Jr. et al., 2007), far less is known of the origin and impact of GABAergic inputs on SPON properties. When  $GABA_A$  receptors were blocked with Gabazine, only subtle effects on pure tone responses were seen. Spiking during the sound presentation was unchanged, while offset spiking showed only a modest increase. This result is at odds with a study conducted by Kulesza Jr. and colleagues (2007). After blocking SPON  $GABA_A$  receptors with bicuculline, they found that, compared to baseline, roughly half of the neurons tested had dramatic increases in spiking during the tone presentation, with no difference in spiking observed for the remaining units. In addition, a 36% increase in offset spiking was seen

following the application of bicuculline. Differences between these studies may be due to effects of bicuculline that are not specific to GABA<sub>A</sub> receptors because bicuculline can also block potassium channels in a dose-dependent manner (Kurt et al., 2008). Thus, it is likely that when high drug ejection currents were used for bicuculline, large increases in SPON spiking were observed, caused by blockade of both GABA receptors and potassium channels. In contrast, Gabazine is highly selective blocker of the GABA<sub>A</sub> receptor, and is thus preferred for exploring the role of GABAergic neurotransmission on pure tone responses. When glycine receptors were blocked with strychnine, offset spiking was abolished and spiking increased substantially during the stimulus presentation, similar to what has been previously shown (Kulesza Jr. et al., 2007). And although GABA receptor blockade had little effect on pure tone responses when applied alone, it did considerably augment the spiking magnitude during the stimulus presentation when paired with strychnine. This finding is in line with previous results (Kulesza Jr. et al., 2007), and confirms that glycine receptor blockade is necessary to unmask excitatory inputs active during the stimulus presentation before the effects of blocking GABA receptors can be seen.

When SPON neurons were presented with SAM tones, baseline responses showed phase-locking to MFs only up to 100 Hz. Entrainment to higher rates of modulation ceased due to a drop in spiking rate below two spikes per stimulus (see Methods). Blocking GABA and glycine receptors independently and in combination resulted in increased spiking rates, yet phase-locking did not approach baseline levels for responses to most MFs. Therefore, the accurate encoding of periodic acoustic stimuli not only requires a robust spiking response, it also requires the relative timing of spiking events to be precise.

#### *Excitatory transmitters have subtle effects on SPON response properties*

The results described above suggest that glycine receptor blockade reveals an excitation-driven response of SPON neurons to pure tones. To directly assess the nature of this excitatory input, recordings were conducted while blocking NMDA and AMPA/kainate receptors. A reduction in spiking to pure tones was observed following blockade of

NMDA neurotransmission, although the temporal characteristics of the response were unchanged. Additional blockade of AMPA/kainate receptors did not lead to a further reduction in spike counts, presumably because AMPA-mediated excitatory post-synaptic potential terminated before the pure tone offset response began. These results are compatible with the idea that relief of the NMDA receptor's Mg block can occur via rebound depolarization in the SPON, rather than requiring AMPA-mediated excitatory post-synaptic potentials.

In response to SAM tones, the effects of NMDA receptor blockade and the combined NMDA/AMPA/kainate receptor blockade were essentially the same to MFs up to 40 Hz. However, at increasing MFs, NMDA receptor blockade in isolation did not lead to a further decrease in spiking rates compared to baseline, whereas the NMDA/AMPA/kainate receptor blockade results in dramatically reduced spiking. This suggests that at higher MFs the release from MNTB-derived glycinergic inhibition may not be strong enough to consistently trigger rebound spiking in SPON neurons, but that an excitatory input may elicit a strong enough response for phase-locking to occur.

The results of experiments involving glutamatergic receptor blockers invite discussion of two potential mechanisms for spike generation in SPON neurons. The first is rebound spiking caused by release from MNTB-derived glycinergic inhibition, and the second is from cochlear nucleus-derived excitation. Both mechanisms are likely active concurrently, but their relative contributions will vary depending on stimulus conditions; whereas rebound spiking primarily underlies the SPON pure tone response, excitation may trigger action potentials in situations where neurons spike repeatedly, as is the case with SAM stimuli. Although it is currently thought that excitatory inputs to SPON neurons are normally masked by MNTB-derived inhibition during sound stimulation, a role for synaptic excitation in SAM encoding could be imagined for SPON responses that exhibit precise phase-locking to modulation frequencies that evoke poor responses in MNTB neurons (Kadner et al., 2007).

### *Functional implications*

By discharging with precision to amplitude-modulated tones, SPON neurons transmit precise temporal information about sound envelopes to higher order brain areas (Kuwada and Batra, 1999; Kadner and Berrebi, 2008). SPON neurons respond with notable fidelity to modulation frequencies up to several hundred hertz (Kuwada and Batra, 1999; Kadner and Berrebi, 2008; Felix II et al., 2007), corresponding to the range of envelope fluctuations that convey critical information in many animal vocalizations and human speech sounds. The results of the present study confirm that SPON neurons also phase-lock to low frequency modulations of the sound envelope (<20 Hz), and that certain cells show preferential tuning to these low rates of modulation. In the mouse, the encoding of periodic low frequency modulations could be relevant for various communication calls, such as wriggling calls, characterized as single-frequency pup whistles that are vocalized at a repetition rate of 3–10 Hz (Geissler and Ehret, 2002; Liu et al., 2006; Portfors, 2007).

The high degree of precision in the response of SPON neurons to changes in the sound envelope makes them attractive candidates for involvement in temporal processing. However, little is known concerning the impact of SPON projections on their synaptic targets in the ipsilateral inferior colliculus (Kelly et al., 1998; Saldaña and Berrebi, 2000; Saldaña et al., 2009). One idea is that the SPON serves as a sensitive detector of discontinuities within ongoing stimuli; for example, by signalling troughs in amplitude-modulated sounds or brief gaps in tones (Kadner and Berrebi, 2008). Because SPON neurons are GABAergic, their offset spikes are expected to provide brief bursts of synaptic inhibition that would act to segment responses of inferior colliculus neurons to periodically modulated signals. The fact that SPON and inferior colliculus neurons are sensitive to similar ranges of envelope modulation frequencies (Kuwada and Batra, 1999; Krishna and Semple, 2000), and that pharmacological blockade of GABA receptors in the inferior colliculus can selectively affect some aspects of responses to SAM tones, (Caspary et al., 2002; Koch and Grothe, 1998; Lu et al. 1998, Zhang and Kelly, 2003), suggests that the SPON may have a role in shaping the representation of periodic stimuli in the midbrain.

## **Acknowledgements**

I thank Dr. Anna Magnusson for help designing the mouse experiments and for helpful critiques of figures and text. I also gratefully acknowledge Dr. Alexander Kadner for assistance with collection and analysis of rat data. I also thank Drs. Jeff Wenstrup and Jason Sanchez for training with piggyback electrode construction and iontophoretic drug delivery.



## The Superior Olivary Complex

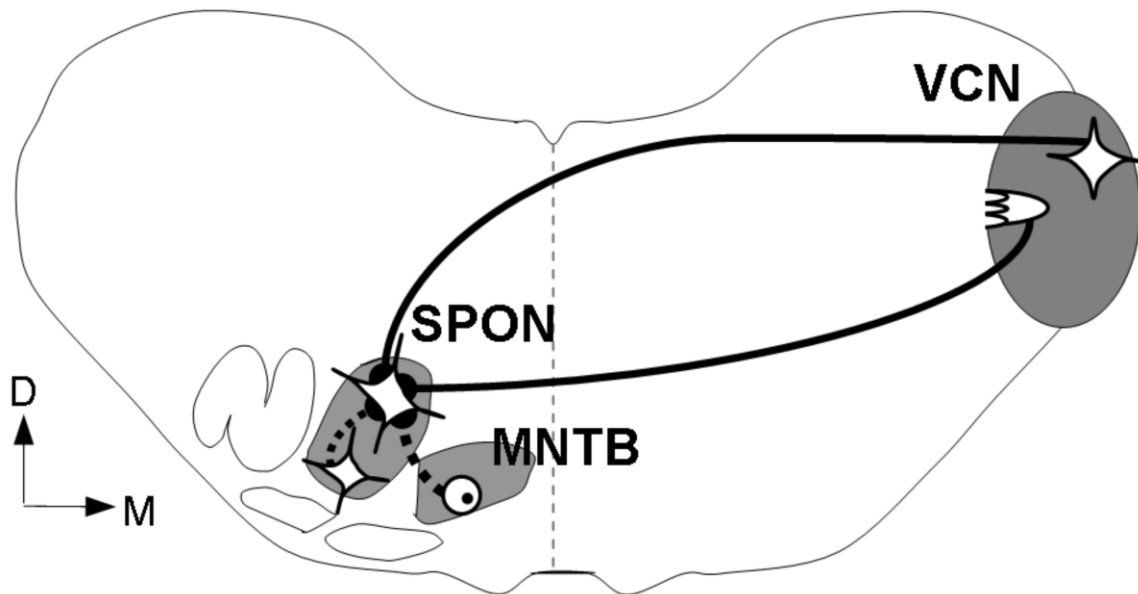


*Figure 4.1.* Schematic representation of synaptic inputs to the rodent SPON. Axons from octopus and multipolar cells in the contralateral ventral cochlear nucleus (VCN) provide excitatory glutamatergic input to SPON neurons. Inhibitory input to the SPON arises from glycinergic principal cells of the ipsilateral medial nucleus of the trapezoid body (MNTB). A second source of inhibition is likely provided by SPON neurons contacting other cells within the nucleus via GABAergic inputs. Dashed gray line represents the midline. D: dorsal; M: medial.

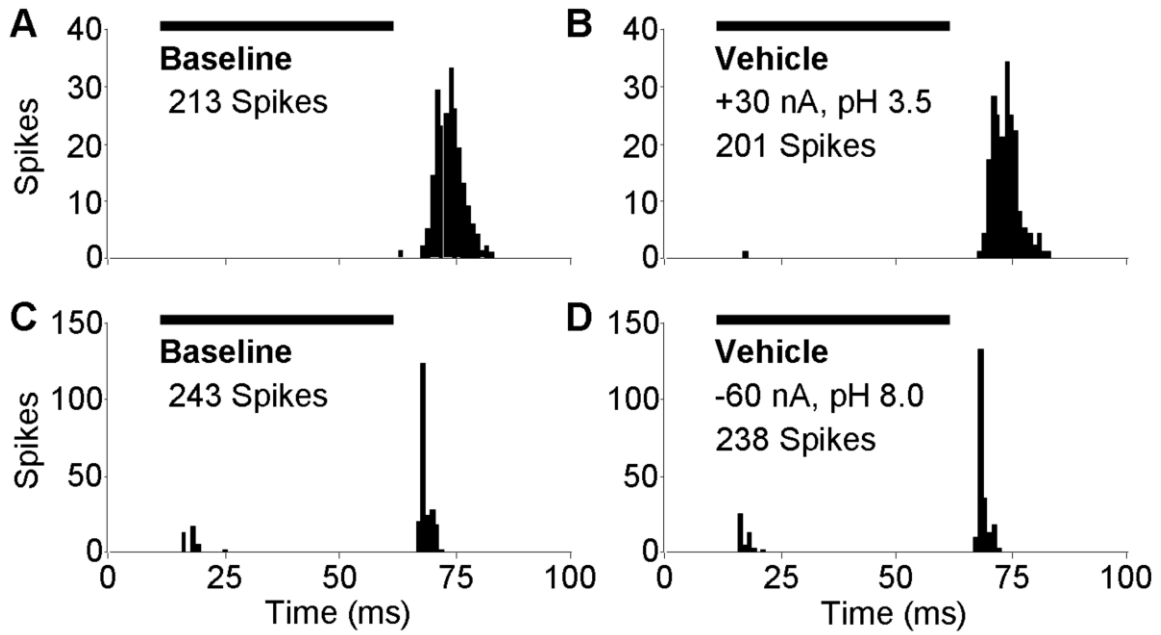


*Figure 4.2.* Neuronal responses in the SPON are not affected by the application of current or vehicle solutions. Responses of neurons to pure-tones were recorded before (A, C) and after the vehicle solutions for ZD7288, Mibefradil, strychnine and Gabazine (B), or NBQX and CPP (D) were applied with current. Horizontal bars represent the location of the stimulus in the recording window.

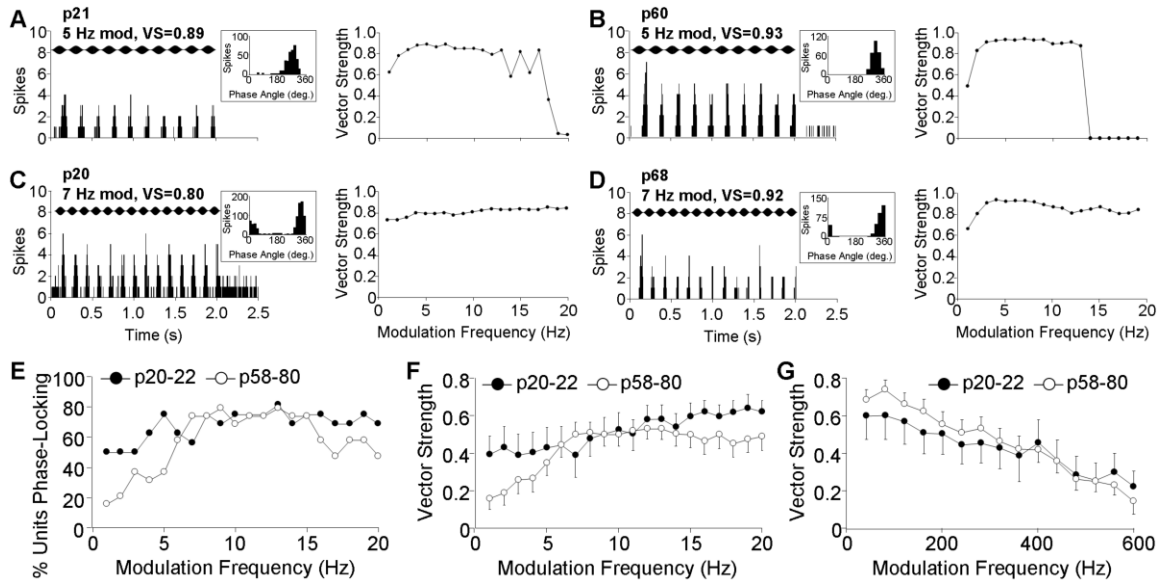


*Figure 4.3.* Mouse SPON neurons exhibited two types of modulation transfer functions in response to SAM stimuli. One response type observed in SPON neurons of both young (A) (p20-p22;  $n=5$ ) and adult (B) (p58-p80;  $n=8$ ) animals was marked by temporally-precise spiking to each modulation cycle of SAM tones ranging from 1-15 Hz, with a sharp decrease phase-locking to modulation frequencies above 15 Hz. A second type of response to SAM stimuli seen for neurons in young (C) ( $n=8$ ) and adult (D) ( $n=11$ ) animals consisted of phase-locked spiking to all modulation frequencies presented. E) Percentage of neurons in young and adult animals that demonstrated phase-locked responses to SAM stimuli as a function of modulation frequency, as indicated by a significant result of the Rayleigh test. Mean vector strengths for young ( $n=13$ ) and adult ( $n=19$ ) neurons in response to low (F) and higher (G) modulation frequencies. Horizontal rippled bars in (A – D) represent the location of the SAM tone in the recording window. Period histograms (insets) were constructed from spikes that occurred during the stimulus presentation. Error bars in (F) and (G) represent the standard errors of the means.

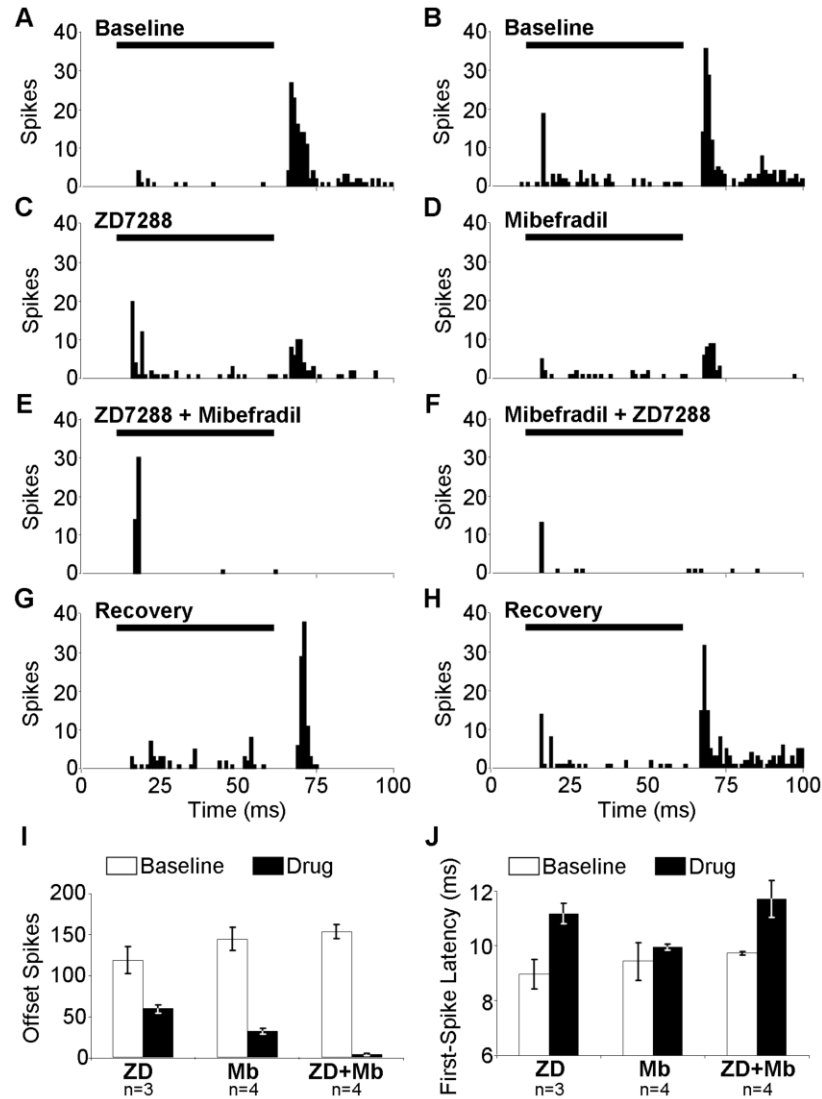


*Figure 4.4.* ZD7288 and Mibefradil alter the spiking of SPON neurons in the mouse. PSTHs were constructed for SPON units under the following conditions: baseline prior to the application of drugs (A, B), iontophoretic application of either the I<sub>h</sub> current blocker ZD7288 (C) or the LVA Ca<sup>2+</sup> blocker Mibefradil (D) in isolation, combined application of both ZD7288 and Mibefradil simultaneously (E, F), and recovery following wash out of the drugs (G, H). Spike counts (I) and first-spike latencies (J) were measured for offset responses before and during drug application. Horizontal bars in A-H show the location of the stimulus in the recording window. Error bars in I and J represent the standard errors of the means.

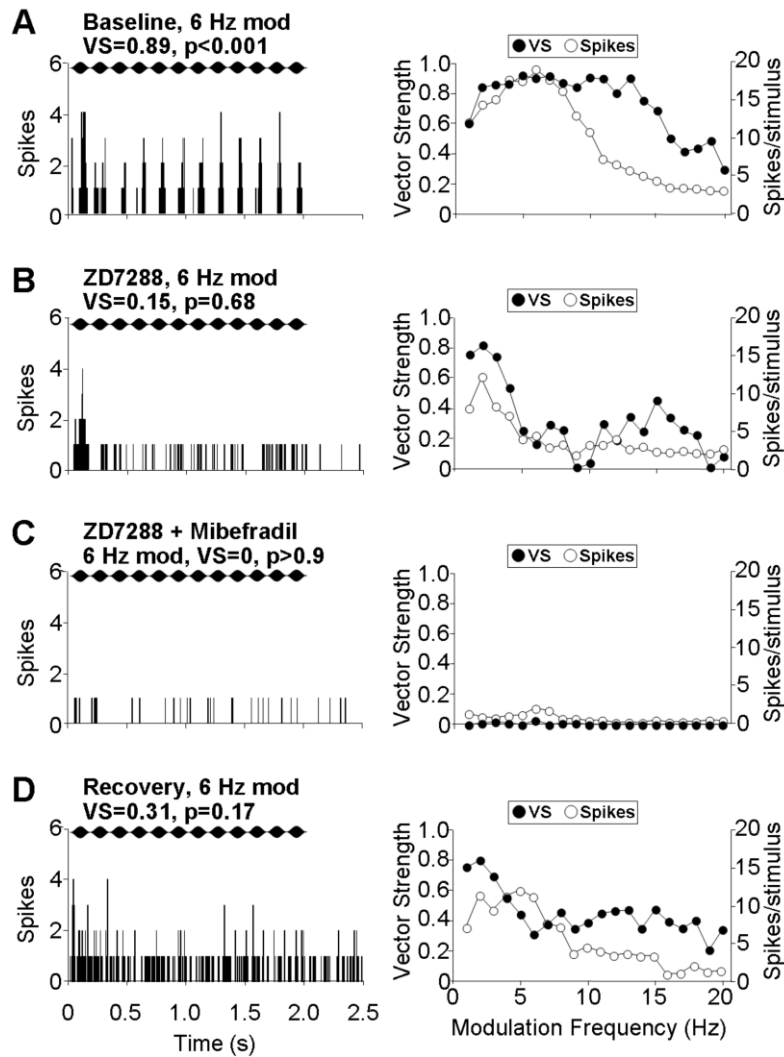


*Figure 4.5.* Ih currents contribute to SAM tuning in the mouse SPON. Spike rate and vector strength modulation transfer functions (right panels), along with representative PSTHs (left panels; p-values obtained from the Rayleigh test) are shown for responses to SAM tones recorded from units under the following conditions: baseline prior to the application of drugs (A), the Ih current blocker ZD7288 (B) applied in isolation, combined application of ZD7288 and the LVA Ca<sup>2+</sup> channel blocker Mibefradil simultaneously (C), and recovery following wash out of the drugs (D). Horizontal rippled bars in each PSTH plot represent the location of the SAM tone in the recording window. Vector strengths greater than 0.4 were significantly phase-locked to the stimulus (Rayleigh test, p< 0.05).

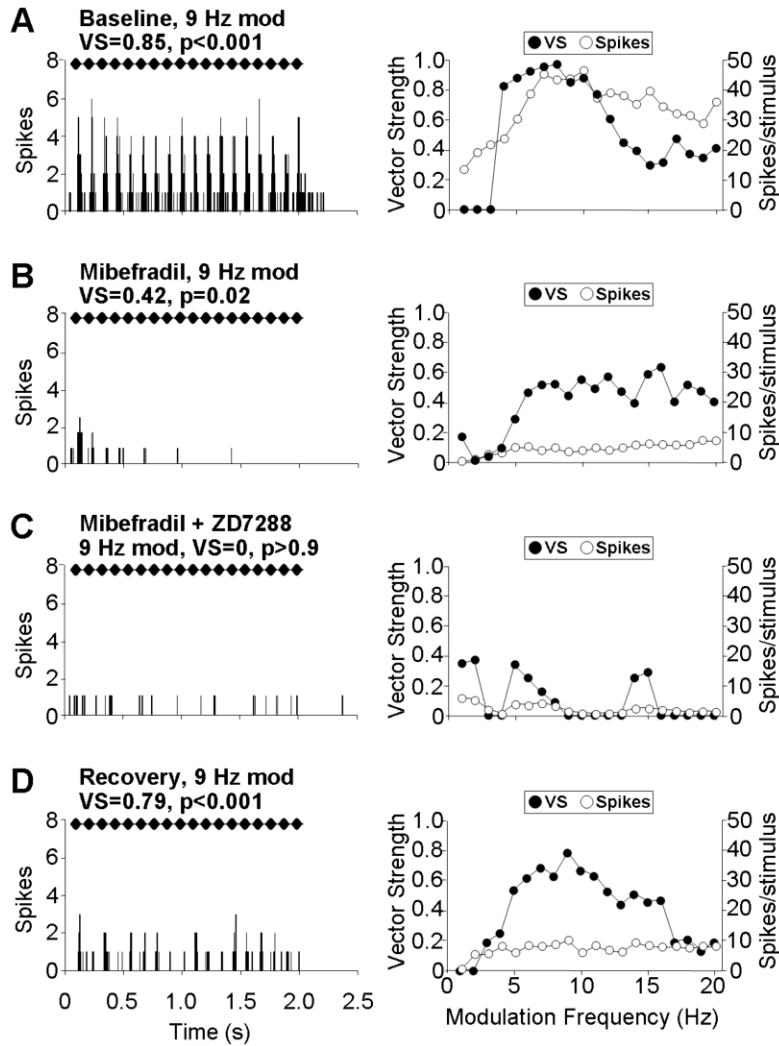


*Figure 4.6.* LVA  $\text{Ca}^{2+}$  currents contribute to SAM tuning in the mouse SPON. Spike rate and vector strength modulation transfer functions (right panels), along with representative PSTHs (left panels; p-values obtained from the Rayleigh test) are shown for responses to SAM tones recorded from units under the following conditions: baseline prior to the application of drugs (A), the LVA  $\text{Ca}^{2+}$  blocker Mibefradil (B) in isolation, combined application of Mibefradil and the Ih current blocker ZD7288 simultaneously (C), and recovery following wash out of the drugs (D). Horizontal rippled bars in each PSTH plot represent the location of the SAM tone in the recording window. Vector strengths greater than 0.4 were significantly phase-locked to the stimulus (Rayleigh test,  $p < 0.05$ ).

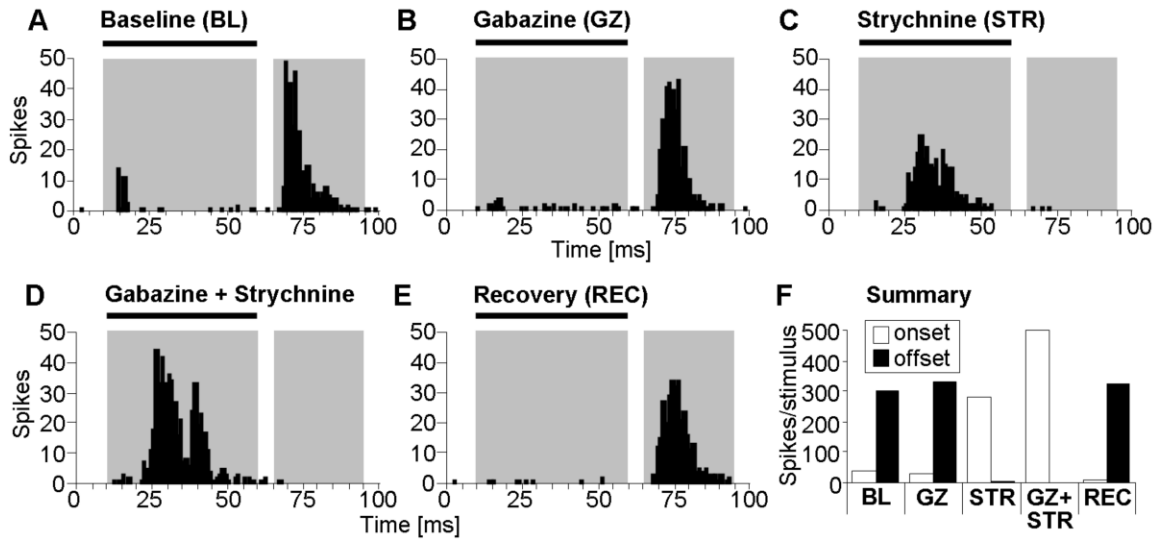


*Figure 4.7.* Blockade of glycine and GABA<sub>A</sub> receptors alters the spiking patterns of rat SPON neurons. Compared to the baseline condition (A), application of the GABA<sub>A</sub> receptor blocker Gabazine (B) resulted in a decrease in the onset response but had little effect on offset spiking. C) Blockade of glycine receptors with strychnine abolished the offset response and increased spiking during the stimulus. D) When Gabazine was applied in combination with strychnine, spiking during the stimulus increased beyond what was observed with strychnine alone. E) After the blockers washed out, the response partially recovered to resemble the baseline condition. F) Summary of spike counts for onset and offset components of the response for each of the conditions tested. Horizontal bars in the PSTH plots represent the location of the pure-tone stimulus in the recording window.

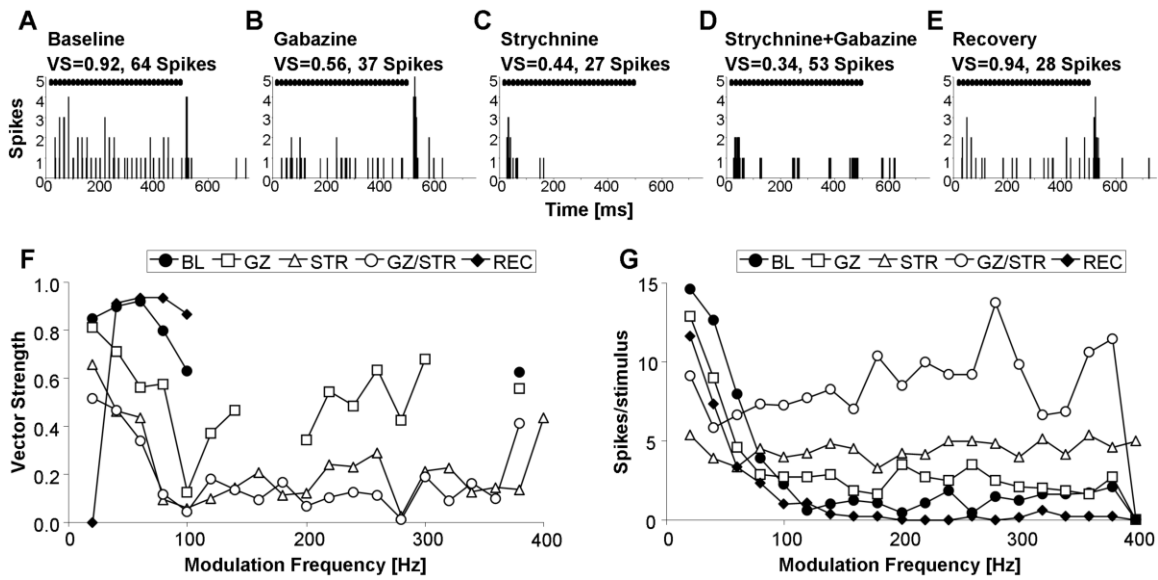


*Figure 4.8.* Inhibitory neurotransmitter systems shape phase-locking properties of rat SPON neurons. Compared to the baseline response (A), Gabazine decreased both the vector strength and spiking rate (B) in response to a SAM tone with a modulation frequency of 60 Hz. C) Application of strychnine alone resulted in a further reduction of entrainment and spiking compared to the Gabazine condition. D) Adding Gabazine along with strychnine did not cause a substantial decrease in the vector strength beyond the effects seen with strychnine alone. E) When the drugs were permitted to wash out, the resulting vector strength approximated to baseline condition, but spiking remained depressed. F) Modulation transfer function showing the vector strengths of SAM responses for the various drug manipulations. G) Spike rates for responses to SAM stimuli are shown as a function of modulation frequency. Rippled bars in A-E represent the location of the SAM stimulus in the recording window. Missing data points in F indicate when vector strength values equaled zero.



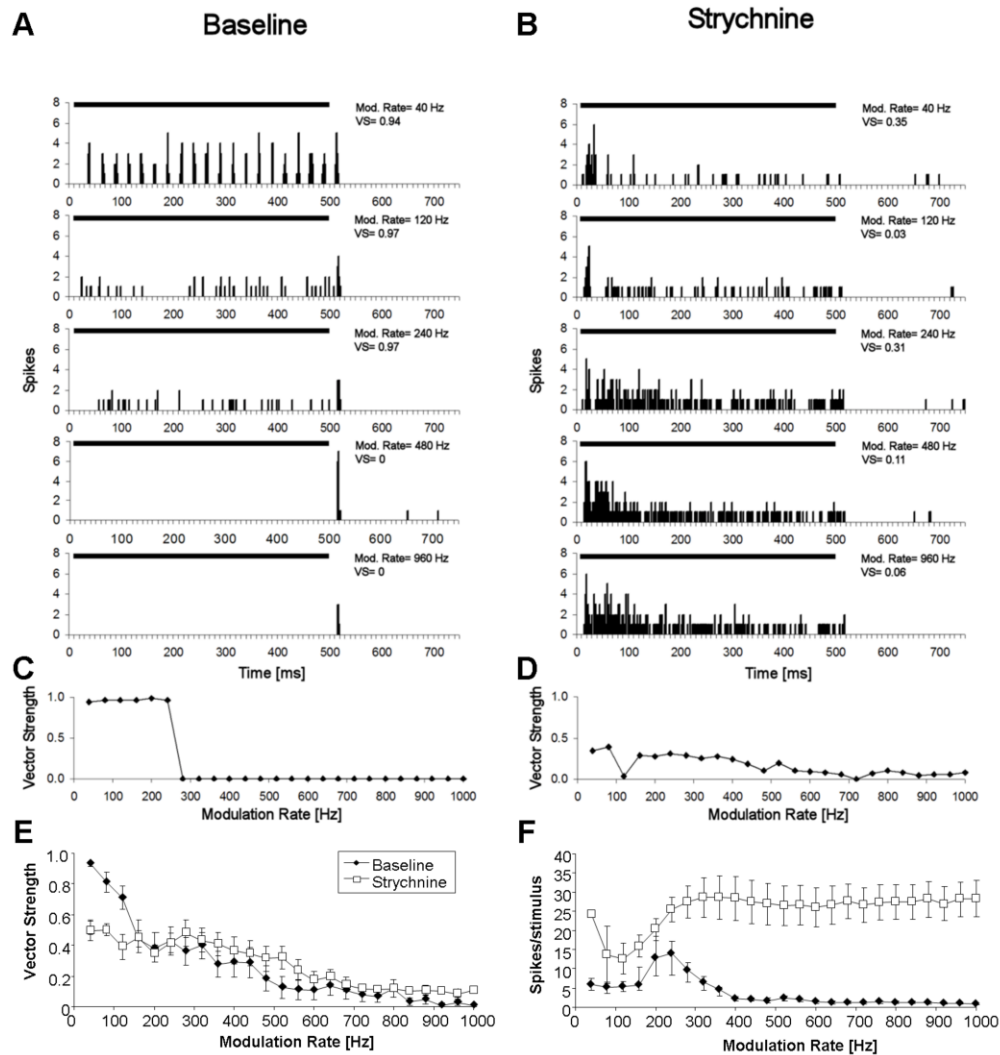


*Figure 4.9.* Glycine receptor blockade decreases phase-locking to low modulation frequency (MF) SAM stimuli and increases spiking for rat SPON neurons. Responses to a range of MF of SAM tones are shown prior to (A) and following strychnine application (B). Compared to baseline (C), strychnine decreased vector strengths (VS) at MFs less than 240 Hz (D) in the example shown in A-B. E) Mean vector strengths dropped for MFs below 160 Hz for the population of SPON neurons tested (n= 23). F) Strychnine application resulted in an increase in spiking rate to all MFs presented. Horizontal bars in A-B represent the location of the stimulus in the recording window. Error bars in E-F represent the standard errors of the means.

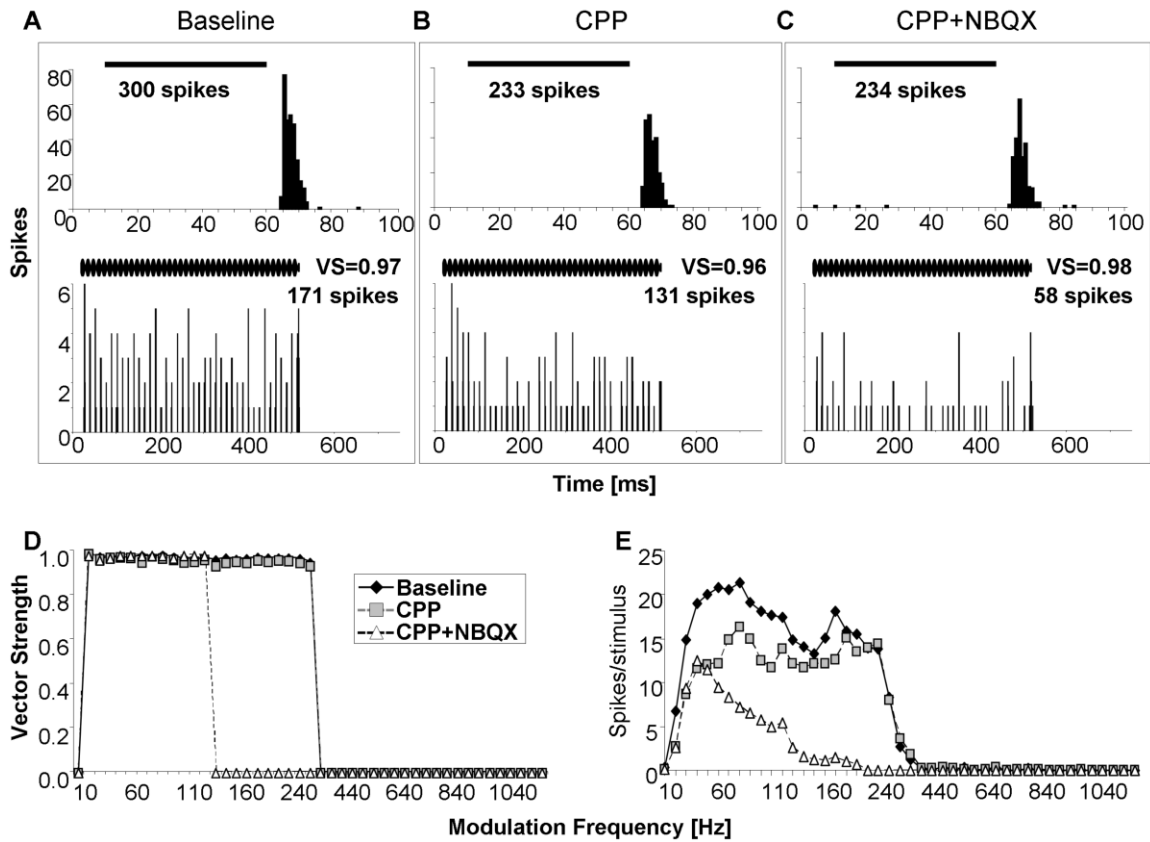


*Figure 4.10.* Excitatory neurotransmitter systems affect response magnitude and phase-locking abilities of rat SPON neurons. A) A response to a pure-tone (*upper panel*) and SAM tone (*lower panel*) was reduced by NMDA blockade with CPP (B); the addition of the AMPA/kainate receptor blocker NBQX (C) had little effect beyond the action of CPP alone in response to tones, but further decreased the magnitude of the SAM response. D) In response to SAM tones, highly synchronized responses to modulation frequencies (MFs) up to 320 Hz were observed in the baseline condition. NMDA receptor blockade with CPP had no discernable effect on vector strengths, although spike rates were reduced at most MFs (E). Concurrent application of CPP and NBQX resulted in markedly lower spike counts to all MFs tested and the range of MFs over which phase-locking occurred was truncated. Horizontal bars and rippled bars represent the location of the stimulus in the recording window for pure-tones and SAM tones, respectively. Responses  $\leq 2$  spikes per stimulus presentation are assigned VS of 0 (See Methods).

## **Chapter Five**

**The superior paraolivary nucleus shapes temporal response properties of neurons in the inferior colliculus**

## **Abstract**

The superior paraolivary nucleus (SPON) is a major source of GABAergic inhibition to neurons in the inferior colliculus (IC). The IC is a well studied nucleus in the midbrain and the site of convergence and integration for nearly all ascending auditory pathways en route to the cortex. Neurons in both the SPON and IC exhibit highly sensitive and precise responses to temporal sound features, which are important perceptual cues for naturally occurring sounds. To test whether input from the SPON contributes to the encoding of temporal information in the IC, a reversible inactivation procedure was conducted in the SPON while recording responses to amplitude-modulated tones and silent gaps between tones in the IC. The results suggest that SPON-derived inhibition shapes responses of IC onset units to amplitude-modulated stimuli and responses of sustained units to gap stimuli, to varying degrees. A functional role for the SPON in temporal processing has implications for the accurate encoding of biologically important sounds, such as animal vocalizations and human speech.

## Introduction

The superior paraolivary nucleus (SPON) is a GABAergic cell group located prominently in the brainstem within the superior olivary complex, a collection of auditory nuclei implicated in binaural sound localization (Grothe et al., 2010; Saldaña and Berrebi, 2000; Tollin, 2003). Unlike cells in neighboring nuclei, SPON neurons are monaurally stimulated by acoustic signals and do not appear to have a role in sound source localization (Behrend et al., 2002; Dehmel et al., 2002; Kulesza Jr. et al., 2003). To date, a clear functional role for the SPON in audition has been elusive, partly due to the unique properties of its evoked neuronal responses. A hallmark of the SPON response is a well-timed transient burst of spikes triggered by the offset of sound stimuli (Dehmel et al., 2002; Kadner and Berrebi, 2008; Kadner et al., 2006; Kulesza Jr. et al., 2003). Because SPON-derived GABAergic inhibition would manifest following, but not during sound stimulation, it has been difficult to propose conditions in which the SPON could shape response properties in target brain areas.

Several hypotheses regarding the role of the SPON in the auditory pathway have been proposed (sound localization: Behrend et al., 2002; rhythm coding: Felix II et al., 2011; gap detection: Kadner et al., 2006; Kopp-Scheinflug et al., 2010), but the one with the most supporting evidence is that of the SPON functioning as a discontinuity detector for temporal sound features (Kadner and Berrebi, 2008). This view suggests that SPON neurons are specialized for signaling brief periods of low stimulus energy via offset inhibition. This characterization is based on observations that SPON neurons exhibit highly synchronous responses to rapid changes in the amplitude of stimulus envelopes and are able to detect very short gaps within ongoing sounds (Behrend et al., 2002; Kadner and Berrebi, 2008; Kulesza Jr. et al., 2003; Kuwada and Batra, 1999). Although SPON neurons are well-suited to encode temporal features, it remains unclear how they impact auditory processing at their primary synaptic target in the midbrain, the inferior colliculus (IC).

Properties of neurons in the central nucleus of the IC have been studied extensively with regard to responses to temporal sound features, including those of amplitude-modulated sounds (Burger and Pollak, 1998; Caspary et al., 2002; Frisina,

2001; Joris et al., 2004; Langner, 1992; Zhang and Kelly, 2003) and gap detection (Allen et al., 2003; Barsz et al., 1998; Walton et al., 1997; Wilson and Walton, 2002). However, knowledge of how brainstem inputs are integrated at the level of the IC remains poorly understood. The SPON is a good candidate for shaping responses of IC neurons to temporal sound features based on the fact that cells in both nuclei demonstrate sensitivity to similar ranges of stimulus parameters compared to other GABAergic nuclei that provide inputs to the auditory midbrain (Kadner and Berrebi, 2008; Krishna and Semple, 2000; Walton et al., 1997; Yang and Pollak, 1997; Zhang and Kelly, 2006).

To examine the degree to which SPON input mediates responses to temporal stimulus features in the IC, an inactivation protocol was employed whereby SPON neurons were reversibly silenced via neurotransmitter receptor blockade. Responses of IC neurons to amplitude-modulated and gap stimuli were recorded before, during, and after SPON inactivation. The findings suggest that subpopulations of IC neurons are affected differently by SPON inactivation. Therefore, SPON input likely contributes to the processing of amplitude-modulated signals in some IC cells and appears to be involved in encoding gap detection in other cells. Furthermore, the sharpening of IC response properties to temporal stimulus features, provided by SPON input, is consistent with the existence of a discontinuity detector in the brainstem. Thus, the SPON is likely an important contributor to auditory pathways that extract and represent the fine temporal structure of sounds, such as those that underlie perception and comprehension of animal vocalizations and human speech (Drullman, 1995; Geissler and Ehret, 2002; Rosen, 1992).

## Methods

### *Animals and surgical procedure*

Seventeen female Sprague–Dawley rats (Harlan Sprague Dawley, Indianapolis, IN, USA) weighing between 175 and 250 g were used for this study. Animal procedures were approved by the West Virginia University Animal Care and Use Committee and conformed to the Guide for the Care and Use of Laboratory Animals.

Prior to surgery, the animal was deeply anesthetized with an injection of a mixture of ketamine (70 mg/kg) and xylazine (5 mg/kg). The animal was then mounted in a stereotaxic frame and a scalp incision was made and connective tissue removed to expose the skull. A custom-made head post was secured to the skull with screws and dental cement. To gain access to the brainstem, a craniotomy (~3x7 mm) was opened with the rostral edge of the bone defect positioned near the caudal border of the transverse sinus. The dura mater was then removed and the exposed cerebellum aspirated to uncover the floor of the fourth ventricle, whose midline was used as a landmark for electrode penetrations. A second craniotomy (~1-2 mm) was made for midbrain recordings approximately 0.5 mm lateral of the midline skull suture mark, with the caudal extent abutting the rostral border of the transverse sinus. The rat was then transferred to a sound-attenuated recording booth and placed on a thermostatically-controlled heating pad that maintained body temperature at 37°C. Depth of anesthesia was monitored frequently throughout the experiment (~15-30 minutes) by observing the breathing rate and giving a foot pinch. When necessary, a supplementary injection of ketamine was administered at one-third the original dose to maintain a deep level of anesthesia.

### *Sound generation and delivery*

Acoustic stimuli were created using BATLAB software (Donald Gans, Northeastern Ohio Universities College of Medicine, Rootstown, OH, USA). Digital signals were converted to analog by a data acquisition processor (model DAP5216a; Microstar Laboratories, Bellevue, WA, USA) and passed through an anti-aliasing filter (FT6-2,

Tucker-Davis Technologies (TDT), Alachua, FL, USA). The sound level was controlled by programmable attenuators (PA-5; TDT) and signals were sent to speaker drivers (ED1; TDT) and presented through free-field speakers (ES1; TDT) mounted in the stereotaxic frame 5 mm from the opening of the ear canal. To avoid spectral contamination of stimuli by on and offset clicks, all stimuli were phased in and out using  $\cos^2$  ramps (0.5 ms duration). The speaker output was calibrated and converted to dB SPL offline using a condenser microphone (model 4939; Brüel and Kjaer North America, Norcross, GA, USA) connected to a measuring amplifier (model 2610; Brüel and Kjaer).

### *Microelectrodes*

Single unit responses were recorded with glass pipette electrodes (tip diameters of 2–4  $\mu\text{m}$ ; 10–20 M $\Omega$  resistance) filled with 1.5% Biocytin (Sigma; St. Louis, MO, USA) dissolved in 0.165 M NaCl (pH 7.4). SPON recordings were made with “piggyback” electrodes (Havey and Caspary 1980) consisting of a single-barrel recording pipette glued onto a five-barreled pipette (20–30  $\mu\text{m}$  total tip diameter). Piggyback electrodes were constructed such that the tip of the recording electrode extended 20–40  $\mu\text{m}$  from the tip of the multibarrel pipette. Drug barrels were loaded with either strychnine (10 mM; Sigma) or kynurenic acid (100 mM; Sigma) dissolved in 0.165 M NaCl (pH 3.0 and 8.5 for strychnine and kynurenic acid, respectively). During recordings, drugs were delivered using iontophoresis (Dagan) with ejection currents of +10 to +40 nA for strychnine and -60 to -80 nA for kynurenic acid. A drug retention current opposite the net charge of the drug solutions was applied during the search for neurons and during baseline and recovery conditions of the recording protocol to prevent drug leakage from the electrode tip (described below). For all experiments, one barrel was filled with physiological saline and used as a sum channel to balance the currents of the other drug barrels.

### *Recording procedures*

The SPON and IC were localized using stereotaxic coordinates from an atlas of the rat brain (Paxinos and Watson, 1986). Electrode signals were amplified (model 2600;



Dagan Corporation, Minneapolis, MN, USA), bandpass filtered (200-3000 Hz; model 3364 Filter (Krohn-Hite, Brockton, MA, USA) and then digitized at 42 kHz (model DAP5216a; Microstar). A unit was considered well isolated if the acoustically-evoked spike waveforms were homogeneous and could be reliably separated from the background noise. A 50 ms broadband noise burst, presented at 80–100 dB SPL was used as a search stimulus. Units were presumed to be in the SPON if they responded exclusively to monaural stimuli presented to the contralateral ear and if they possessed activity evoked by the stimulus offset (Kadner and Berrebi, 2008; Kadner et al., 2006; Kulesza Jr. et al., 2003). IC neurons were identified by sound evoked responses with first-spike latencies below 15 ms and thresholds below 35 dB SPL (Palombi and Caspary, 1996). To further distinguish IC responses, units were classified as either onset cells, marked by phasic spiking (<20 ms duration) triggered by the stimulus onset, or sustained cells which responded for the entire duration of the stimulus.

#### *Histological localization of recording sites*

For each recording protocol that was successfully completed, Biocytin was deposited at recording locations in the SPON and IC by applying 1-2  $\mu$ A positive current (50% duty cycle) for 5-10 min (Fig. 5.1). Following the completion of tracer deposit, the animal was perfused through the ascending aorta with physiological saline followed by 4% paraformaldehyde in 0.12 M sodium phosphate buffer (pH 7.2). The brains was then removed from the cranium, cryoprotected overnight, and sectioned in the coronal plane (40  $\mu$ m) on a freezing microtome. Free-floating sections were processed according to the ABC method (Vector Laboratories, Burlingame, CA, USA) using diaminobenzidine as the chromogen.

#### *Experimental paradigms*

At the start of each experiment, a piggyback electrode was slowly advanced into the brainstem while a repeating broadband noise stimulus was presented. When a SPON single-unit was isolated, its characteristic frequency (CF) and minimum threshold were

determined audiovisually. The CF was defined as the frequency that evoked a response to at least half of the stimulus presentation at the lowest sound level, and the threshold was the lowest intensity that elicited a consistent spiking response. A peri-stimulus time histogram (PSTH) was then constructed for the SPON response to a CF pure tone (100 repetitions) presented 10 dB above threshold for the baseline condition, prior to delivery of inactivating drugs. Next, the combination of strychnine and kynurenic acid was applied until the spiking response observed in the baseline condition fell below 0.2 spikes per stimulus and remained consistent for five consecutive minutes. A value of 0.2 spikes per stimulus was chosen because it is less than the criterion for an evoked response (0.5 spikes/stimulus, see Chapter 3), but still allows for some spontaneous spiking to occur. The time course of drug action was noted and a second PSTH was recorded for the inactivation condition. Retention currents for drug solutions were then applied and the drugs were allowed to wash out for a period of up to one hour, with the time course for recovery noted. Following the confirmation of drug action and efficacy, the piggyback electrode was left in place in the brainstem and a second single-barrel recording electrode was advanced in the midbrain to search for neurons in the central nucleus of the IC.

Only IC units that possessed CFs matching corresponding SPON units (or within 3 kHz) were selected in order to take advantage of the highly organized tonotopic projections from the SPON to IC (Saldaña et al., 2009; Saldaña and Berrebi, 2000). Selection of closely matching CFs maximized the likelihood that projections from isolated SPON neurons were functionally connected to units recorded in the IC. Upon isolation of a single-unit in the IC, a baseline PSTH was recorded first from the previously isolated SPON unit then immediately from the IC unit in response to pure tones. Tones were 50 ms in duration and were presented at the IC unit's CF at 10 dB above the SPON unit's threshold. Next, SAM tone and gap detection tests were conducted on the IC unit in the baseline condition (described below). After the collection of baseline data, the protocol of PSTH, SAM and gap tests was repeated for the IC unit, during SPON inactivation and recovery conditions (Table 4.1).

*PSTH:* To determine how SPON offset spiking impacted spiking in the IC, an analysis window was defined and the IC neuron's offset response rate was examined before, during and following SPON inactivation (Fig. 5.2A). The 10 ms offset analysis

window was determined for each recording pair and began at the time point of the lowest first-spike latency of the SPON offset response. Spiking in this window was then measured for the IC unit's response for all conditions and compared (Wilcoxon matched-pairs signed-ranks test).

*SAM*: Stimuli consisted of a SAM tone with the carrier frequency set at the IC unit's CF (10 dB above SPON threshold) and the modulation frequency (MF) was varied from 20 to 180 Hz in 20 Hz steps. Stimuli had durations of 500 ms and were presented eight times for each MF (100% modulation depth). The analysis window for SAM tests began 10 ms after the stimulus onset and ended at the offset (Fig. 5.2B). Responses to the first 10 ms of the stimulus were excluded from the analysis in order to eliminate spikes that were triggered by the onset of the SAM tone rather than to the phase of a modulation cycle. At each MF, spiking rates were determined and the synchronization of responses to each MF was quantified by calculating the vector strength (VS) (Goldberg and Brown, 1969) using the formula

$$VS = \frac{1}{n} \sqrt{\left[ \sum \sin(a_i) \right]^2 + \left[ \sum \cos(a_i) \right]^2}$$

where  $a_i$  is the phase angle of spike  $i$  relative to the modulation cycle of the stimulus, and  $n$  is the total number of spikes in the analysis window. To minimize the influence of isolated spikes that were time-locked to the stimulus onset and thus occurred at a constant phase angle, the vector strength was set to 0 when the spike count fell to fewer than two spikes per stimulus presentation. A vector strength of 1 indicates perfect synchronization between the neuronal response and the modulation phase, while a vector strength of 0 indicates no correlation. The Rayleigh test (Batschelet, 1981) was used to assess whether the distribution of spikes relative to the phase angle of the stimulus significantly differed from randomness (i.e., whether the stimulus imparted a temporal structure on the response). Differences between spiking rate and vector strength values in baseline and SPON inactivation conditions were compared using the Wilcoxon matched-pairs signed ranks test. In addition to examining spike counts and vector strengths, period histograms were constructed for a subset of IC unit responses by plotting the phase angle of each spike relative to the amplitude modulation frequency of the stimulus (Kadner and Berrebi, 2008; Kuwada and Batra, 1999).

*Gap detection:* To characterize the gap detection abilities of each IC unit, a multi-step recording protocol was used. First, a no stimulation condition (N) test was conducted to determine the spontaneous activity rate. Next, the response to a continuous 100 ms CF tone (C), presented at 10 dB above the SPON unit's threshold was presented. This continuous stimulus was then replaced by two separate, but identical, 50 ms stimulus markers. For control purposes, responses to the two markers were recorded separately (hereafter termed leading (L) and trailing (T) marker conditions). Leading and trailing markers were then presented in succession as the duration of the gap between them was varied from 0 to 10 ms in 1 ms increments. In the 0 ms gap condition, the downward ramp of the leading marker and the upward ramp of the trailing marker abutted each other, so that only a negligible silent period existed between the stimuli. Each of the stimulus conditions was presented 20 times.

Gap detection thresholds were defined as the shortest gap between leading and trailing markers that evoked a spiking response to a quarter of the presentations of the trailing marker. Responses were considered to be elicited by the gap when spiking was triggered separately by the onset of the leading and trailing markers (i.e., the markers were recognized as distinct tones). For each IC unit response, a 10 ms analysis window was set; beginning at the time point of the lowest first-spike latency to the trailing marker presented alone (Fig. 5.2C). This window was used to count spikes in all stimulus conditions and to determine whether gap detection thresholds changed between baseline and SPON inactivation conditions (Wilcoxon matched-pairs signed-ranks test).

## Results

A total of 19 pairs of neurons were recorded in the SPON and IC of the rat. Characteristic frequencies (CFs) for units in both nuclei were between 5 and 33 kHz, which covered the most sensitive range of the rat behavioral audiogram (Kelly and Masterton, 1977). Matching the CFs of neurons in the SPON and IC within 3 kHz was the only requirement for considering the units paired. Following completion of the recording protocol, Biocytin tracer deposits were made at the recording site in each nucleus to confirm that neurons were located in the SPON and central nucleus of the IC (Fig. 5.1).

### *Control experiments*

Control experiments were conducted in the SPON prior to data collection. For a subset of units ( $n=3$ ), 0.165 M NaCl vehicle solutions for strychnine (pH 3.0) and kynurenic acid (pH 8.5) were ejected onto neurons with +40 and -80 nA current, respectively. In both cases, the vehicle solutions had no impact on SPON spiking ( $p > 0.9$ , Wilcoxon signed ranks test; Fig. 5.3A). For each experiment, the inactivation and recovery of SPON activity was achieved prior to starting the IC recording protocol. This control experiment was conducted to verify that drugs were effective and to note the time course for inactivation and recovery, which were used later during IC recordings. SPON inactivation was achieved by first blocking glycinergic inhibition with strychnine, thereby eliminating the offset response (see Chapter 4). In addition to abolishing offset spiking, glycine receptor blockade unmasked excitatory inputs active during the stimulus presentation; thus, kynurenic acid was simultaneously applied in order to eliminate residual spiking. Each of these drugs requires different current strengths and polarity for ejection from the pipette, therefore, each was loaded in separate barrels and controlled independently (see Methods). Typically, the combination of strychnine and kynurenic acid application effectively silenced SPON neurons within 10-15 minutes (Fig. 5.3B).

The degree of drug spread for SPON inactivation experiments was estimated by comparing the distance between the site of drug ejection and the recording location and the time course of the observed drug action. This was achieved by measuring the

separation of the tips of the recording and drug delivery pipettes and correlating that distance with the elapsed time from the start of the ejection current to the silencing of SPON spiking, thereby providing a measure of the rate of drug spread (Fig. 5.4). The relationship of the distance between tips and time to drug action was significantly correlated for the population of SPON neurons examined ( $n= 24$ ; Spearman's rank correlation,  $r= 0.69$ ,  $p< 0.001$ ). All verified recording sites were at least 100  $\mu\text{m}$  from the boundaries of the SPON (data not shown). Thus, an attempt was made to limit the total duration of SPON drug application and IC recordings for the inactivation condition to approximately 30 minutes to inactivate groups of SPON cells while decreasing the chances of potential drug spread into neighboring brainstem nuclei (Figs. 5.1 and 5.4).

#### *SPON inactivation increased post-stimulus spiking of IC neurons*

To assess whether SPON inactivation alters responses in the IC, spiking was measured in a pre-determined window prior to and following inactivation (Fig. 5.2A). Immediately before IC responses were recorded in the baseline condition, SPON spiking was measured (Fig. 5.4A gray PSTH) and a 10 ms offset analysis window was set, using the lowest SPON first-spike latency as the start of the time window (Fig. 5.5A- D dashed vertical lines). This analysis window was then used to measure spiking of IC neurons before and after SPON inactivation. By removing a source of inhibition, it was predicted that spiking rates near the stimulus offset, if present, would increase for IC units. Onset IC units had few spikes in the offset window under baseline conditions (Fig. 5.5A), and after SPON inactivation, IC units showed no increase in spiking in the offset window (Fig. 5.5B). However, sustained IC units had spiking patterns that persisted for the duration of the tone presentation and outlasted the stimulus offset (Fig. 5.5C). In nearly all cases, spiking for sustained units extended well into the offset analysis window. Following SPON inactivation, spiking in the offset window increased for sustained units (Fig. 5.5D). Although partial recovery from drug action was observed for some SPON units, spiking never returned to baseline levels and no recovery effects were measured for IC responses (data not shown).

Analysis of spiking rates in the offset window revealed no difference in onset IC unit responses ( $n= 8$ ) before ( $3.75 \pm 1.7$  spikes/stimulus) and after ( $4.13 \pm 1.2$  spikes/stimulus) SPON inactivation ( $p= 0.94$ , Wilcoxon signed-ranks test; Fig. 5.6). Conversely, sustained units ( $n= 9$ ) had significantly higher spiking rates in the offset analysis window following inactivation ( $40.12 \pm 9.6$  spikes/stimulus) compared to the baseline condition ( $29.83 \pm 6.5$  spikes/stimulus;  $p= 0.03$ , Wilcoxon signed-ranks test; Fig. 5.6). The latency of direct cochlear nucleus-derived EPSPs at the onset of IC responses is roughly 10 milliseconds in the mouse. Because there are and additional two synapses in the circuit from cochlear nucleus to the IC via the MNTB and SPON, a rough estimate for the latency of offset IPSPs originating from the SPON is predicted to be on the order of 15 milliseconds. This time difference is due to additional synapse in the circuit from cochlear nucleus to IC via the MNTB and SPON. Thus, the offset analysis window used for assessing offset activity in the IC (Fig. 5.2) likely includes the time frame when SPON-derived IPSPs occur.

#### *IC responses to SAM stimuli were altered after SPON inactivation*

Under baseline conditions, neurons in the IC had phase-locked responses to a limited range of SAM modulation frequencies (MFs; Fig. 5.7C). Similar to neurons in the SPON, IC units had an upper limit of phase-locked responses to MFs of 180 Hz, which is in agreement with previous reports from the rat central nucleus of the IC (Caspary et al., 2002; Zhang and Kelly, 2003). The representative onset IC unit shown in Figure 5.7A responded best to a SAM tone with a 40 Hz MF in the baseline condition (top left panel). Spiking for this unit was entrained to a very limited range of MFs (40-80 Hz), over which significant vector strengths were observed ( $VS= 0.83-0.76$ ;  $p= 0.01-0.06$ , Rayleigh test). A phase plot of the baseline response revealed that spiking was evoked roughly one-third of each modulation phase (Fig. 5.7A top right subpanel). When SPON activity was silenced, both spiking and the vector strength dropped for the IC unit, resulting in a loss of phase-locking (Fig. 5.7A middle panel). After the inactivating drugs were allowed to wash out, a partial recovery was observed, although the spiking rate and vector strength remained depressed compared to baseline (Fig. 5.7A bottom panels). Overall, vector

strengths were greatly reduced for the range of MFs at which the unit phase-locked to in the baseline condition (40-80 Hz; Fig. 5.7C). In addition, selective recovery was observed after an hour of drug wash out at 40-80 Hz MF, but the statistically significant phase-locking observed in the baseline condition was not reached (Fig. 5.7C;  $p= 0.09-0.21$ , Rayleigh test).

SAM tone responses of a representative sustained IC unit are shown in Fig. 5.7B. This cell also exhibited significant phase-locking to a limited range of MFs under baseline conditions (20-40 Hz;  $p= 0.004-0.03$ , Rayleigh test). Similar to observations of the onset unit response, sustained spiking was elicited by a specific segment of each modulation phase (Fig. 5.7B right panel). Following SPON inactivation, the response magnitude to 40 Hz MF showed little change, however phase-locking was lost ( $p= 0.31$ , Rayleigh test; Fig. 5.7B left panel). The loss of spiking precision was clearly seen in corresponding phase plots, where a loss of selectivity to the early part of the modulation phase was observed following inactivation (Fig. 5.7B right panel). Although the level of entrainment to the SAM stimulus approached significance after the recovery period ( $p= 0.06$ , Rayleigh test), the response never reached the degree of synchrony seen in the baseline condition. Overall, sustained units exhibited poor synchronization to most MFs presented, and although SPON inactivation impaired entrainment to the stimulus at 20 and 40 Hz MF in particular, only partial recovery was observed, even after one hour (Fig. 5.7D).

Across the sample of onset ( $n= 7$ ) and sustained ( $n= 6$ ) IC neurons, virtually all had bandpass modulations transfer functions; that is, spiking was not synchronized to the lowest MF presented nor at MFs above 80 Hz (Fig. 5.8). As a group, onset cells had significant phase-locking ( $p= 0.001-0.01$ , Rayleigh test) to 40, 60 and 80 Hz modulation in the baseline condition, with vector strengths averaging  $0.78 \pm 0.04$ ,  $0.73 \pm 0.07$  and  $0.70 \pm 0.07$ , respectively (Fig. 5.8A). After SPON inactivation, vector strengths for this range of MFs dropped to  $0.49 \pm 0.13$ ,  $0.50 \pm 0.13$ ,  $0.41 \pm 0.12$ , resulting in a loss of phase-locking ( $p= 0.14-0.26$ , Rayleigh test). In addition, the drops in baseline vector strength values at 40-80 Hz MF following inactivation were statistically significant ( $p < 0.05$ , Wilcoxon signed-ranks test). Although differences in vector strengths were seen for onset units following inactivation, no change in spiking was observed ( $p > 0.05$ , Wilcoxon



signed ranks test; Fig. 5.8C). For sustained IC units, no change was measured for average vector strengths to any of the MFs presented ( $p= 0.16-0.93$ , Wilcoxon signed-ranks; Fig. 5.8B). In addition, no change in average spiking rates of sustained units was observed for any MF (Fig. 5.8D).

#### *Gap detection thresholds in the IC increased following SPON inactivation*

To examine whether SPON input influences the gap detection thresholds of IC neurons, responses of IC units to gaps with systematically varying durations were recorded before and after SPON inactivation (Figs. 5.9 and 5.10). Prior to manipulating the gap duration between tone stimuli, a series of control experiments were conducted. First, spontaneous activity was measured by recording IC neuronal activity with no sound presentation. Typically, onset IC units had very little spontaneous activity ( $7.8 \pm 2.6$  spikes per second; Fig. 5.9, N plot), while sustained units had much higher levels of spiking in the no sound condition ( $169.7 \pm 27.9$  spikes per second; Fig. 5.10, N plot). After spontaneous activity was measured, responses to the leading and trailing markers presented in isolation were recorded (Figs. 5.9 and 5.10, L and T plots). The first 10 ms of the response to the trailing marker was used as an analysis window to assess gap detection (Fig. 5.2C). This window was chosen because the trailing marker remained fixed in the recording window while the delay of the leading marker was systematically reduced to create gaps of increasing duration. Following recordings for the leading and trailing marker conditions, a 100 ms CF tone was presented (Figs. 5.9 and 5.10 C plots) and responses were used to serve as a comparison to the 0 ms gap condition, where two identical 50 ms tones were separated only by their ramps; that is, end of the leading marker ramp abutted the start of the trailing marker ramp, resulting in an extremely short silent period.

After control data were collected, baseline PSTHs were generated from responses to gaps beginning at 0 ms and increasing to 10 ms in 1 ms increments. For the onset IC unit shown in the Figure 5.9, spikes were evoked by the trailing marker at 5 ms gap duration (left panel; see Methods). As the gap duration increased, increased spiking was evoked at 8 and 10 ms, respectively. The gap detection threshold for this unit had an increase from 5 to 10 ms gap duration after SPON inactivation (Fig. 5.9 right panel). In

the example of a sustained unit in Figure 5.10, the unit showed a clear response to the 0 ms gap condition in the baseline condition (left panel). Following inactivation, the gap detection threshold increased to 8 ms (Fig. 5.10 right panel).

For the sample of onset IC units recorded ( $n= 5$ ), no apparent differences in spiking were seen for any of the gap tests between baseline and SPON inactivation conditions (Fig. 5.11A). For gap durations above 3 ms, there was no difference in spiking in the inactivation condition. For sustained units ( $n= 6$ ), comparisons revealed a decrease in spiking to stimuli with small gap durations ( $< 4$  ms) following inactivation ( $p= 0.02$  to  $< 0.01$ , Wilcoxon signed-ranks test). Spiking remained depressed after inactivation at higher gap durations, although the difference became non-significant with increasing duration (Fig. 5.11B). For onset units, no significant difference was seen in gap detection thresholds (see Methods) following the SPON inactivation condition ( $5.5 \pm 2.1$  ms) compared to baseline ( $4.3 \pm 1.2$  ms;  $p= 0.125$ , Wilcoxon signed ranks test). In contrast, baseline gap detection thresholds for sustained units ( $2.4 \pm 0.9$  ms) were significantly elevated after inactivation ( $5.6 \pm 1.0$  ms;  $p= 0.03$ , Wilcoxon signed ranks test).

## Discussion

The goal of the current study was to determine the extent to which input from the superior paraolivary nucleus (SPON) influences response properties of neurons in its primary target, the central nucleus of the inferior colliculus (IC). The SPON has been implicated in processing temporal features of acoustic signals based on precise spiking to changes in the amplitude modulation of sound envelopes and its ability to signal short gaps within ongoing sounds. Thus, responses of IC units were recorded before, during and after SPON inactivation in response to the presentation of sinusoidally amplitude-modulated (SAM) tones and varying gap durations between tones. The results demonstrate that SPON inactivation significantly reduces entrainment of IC responses to SAM stimuli and gap detection thresholds. Therefore, it is likely that one function of the SPON is to enhance the ability of IC neurons to signal and encode temporal discontinuities within rapidly changing stimuli. This role for the SPON may be important for the representation of temporal attributes of behaviorally relevant sounds in the auditory pathway.

### *Methodological considerations of SPON inactivation experiments*

One concern when designing experiments in the current study was the length of the recording protocol. SPON inactivation via iontophoretic delivery of receptor blockers and accompanying IC recordings typically require a minimum of two to three hours in which isolation of a single-unit response must be maintained. Typically, single unit responses in the IC could be maintained beyond three hours; however, the length of the recording protocol was minimized to avoid drugs spreading into surrounding auditory nuclei during the SPON inactivation procedure. Thus, to limit the duration of the recording session, only three types of tests were conducted for IC units: responses to pure tones were measured to determine whether SPON-mediated inhibition was present at the termination of the sound stimulus, and SAM and gap tests were conducted to assess whether the SPON had a role in temporal processing at the level of the IC. Despite the truncated

protocol, recovery data for most IC units was not attained, either due to the loss of single-unit isolation in the IC or from incomplete wash out of inactivating drugs in the SPON.

The primary experimental aim was to record from functionally connected pairs of SPON and IC neurons. To maximize the likelihood of this outcome, the characteristic frequencies (CFs) of units in respective nuclei were closely matched. Because of the highly tonotopic organization of SPON to IC projections, it was assumed that neurons in the SPON would directly contact units in the IC that possessed a similar CF (Saldaña et al., 2009; Saldaña and Berrebi, 2000). However, we cannot rule out the possibility that SPON neurons project outside the tonotopic arrangement to frequency bands that flank the excitatory spectral range of IC units. For some recording pairs, effects of SPON inactivation on IC responses were not evident. Although it is assumed that these pairs shared no functional connection, they remained in the data set, as there was no definite way to assess connectivity; that is, recording pairs may have been connected but the stimuli were not appropriate to reveal an effect of inactivation. Thus, the size of the effects that were reported is likely underestimated.

In order to further increase the chances that recording pairs were connected we attempted to inactivate a region of the SPON rather than just a single neuron. Because neighboring neurons in both the SPON and IC respond to similar frequency ranges (Egorova et al., 2001; Kulesza Jr. et al., 2003; Stiebler and Ehret, 1985), it was likely that, given a large enough area of SPON inactivation, an effect would be observed in the IC. To achieve a larger inactivated area, the tip of the recording pipette tip typically extended 20-40  $\mu\text{m}$  beyond that of the drug delivery pipette. However, it is possible to get non-specific effects of SPON inactivation if the area of drug spread is too large, because other auditory nuclei that project either directly or indirectly to the IC are located close to its borders. Drug spread was estimated by systematically varying the distance between the recording and drug delivery pipette tips of the piggyback electrodes and measuring the time course for drug action (also see: Burger and Pollak, 2001). This approach allowed measurement of a time course during which the drugs had taken effect on the neuron under study, but had not yet spread to neighboring nuclei. Restricting drug application to this time course presumably limited confounding drug effects from areas like the medial nucleus of the trapezoid body and lateral superior olive. In cases where

the recording protocol was longer than expected and as a result, drug spread may have exceeded the borders of the SPON, it is assumed that affected areas in neighboring auditory nuclei were sensitive to frequency ranges very different than that of the SPON and IC units under investigation due to the tonotopic organization of neurons in the superior olivary complex. Specifically, SPON neurons with low CFs are located closest to lateral superior olive cells with high CFs. Similarly, high CF SPON units are closest to low CF cells in the medial nucleus of the trapezoid body (Irvine, 1992; Schofield, 2005). Thus, projections from these surrounding nuclei, either direct or indirect, are presumed to project to different areas of the IC compared to the SPON region under investigation.

*Spiking at the termination of pure tones was altered in the IC after SPON inactivation*

Neurons in the IC were selected by matching their CFs to those of corresponding SPON neurons in order to take advantage of the potential tonotopic connectivity. Because SPON unit thresholds are elevated compared to those in the IC (Felix II and Berrebi, 1997; Kopp-Scheinflug et al., 2008; Kulesza Jr. et al., 2003; Palombi and Caspary, 1996), all stimuli used during IC recordings were presented at 10 dB above the threshold of the SPON unit, regardless of the IC unit's threshold. This sound level was chosen so that sufficient SPON activity was recruited to elicit an effect in the IC. It is possible that SPON units that were within the range of drug action, but were not detected by the electrode, had thresholds that were not crossed by the stimulus level, as a previous study of rat SPON physiology found a moderate degree of variability of SPON thresholds (Kulesza Jr. et al., 2003). Thus, cases where no inactivation effect was seen may have been due to inadequate stimulation. However, the sound levels that were chosen were also meant to maximally excite IC neurons, many of which have non-monotonic rate-level functions (i.e., response magnitude decreases with increasing sound level; Egorova et al., 2001; Stiebler and Ehret, 1985).

Neurons in the IC that had sustained discharge patterns typically displayed spiking that persisted into the “offset” time window corresponding to the active period of SPON units. When SPON-derived inhibition was removed from sustained IC responses, spiking in this window increased, as predicted. Thus, SPON input limited, but did not

eliminate spiking in the offset window for IC neurons. In contrast, onset IC responses were marked by transient spiking near the start of the stimulus and had very little spontaneous activity. Therefore, it was not surprising that no increase in spiking in the offset window was seen after inactivation in these units, as excitatory inputs were likely restricted to the onset of stimuli (Peruzzi et al., 2000), and therefore could not be masked by SPON input. One method for obtaining a clearer picture of how the SPON affects pure tones responses of IC units is to artificially increase the level of spontaneous activity in the IC. Experiments are currently underway involving the delivery of a combination of glutamate and aspartate to provide a background against which SPON inhibition can be seen (Klug et al., 1999; Bauer et al., 2000). Thus, for both onset and sustained IC units, intact offset inhibition would be expected to create a notch in persistent spontaneous activity that would be abolished following SPON inactivation.

#### *Effects of SPON inactivation on IC unit responses*

A prominent feature of SPON responses is their ability to spike to modulations of SAM tones with extremely high precision (Behrend et al., 2002; Felix II and Berrebi, 2007; Kadner and Berrebi, 2008; Kulesza Jr. et al., 2003; Kuwada and Batra, 1999). In addition, IC neurons also exhibit highly selective responses to SAM stimuli, over roughly the same range of modulation frequencies as SPON units (Kadner and Berrebi, 2008; Zhang and Kelly, 2003). Thus, it was predicted that the SPON would have a prominent role in shaping responses to temporal sound features in its target neurons located in the IC. However, based on the findings of the current study, the SPON only has a modest contribution to the generation of IC responses to SAM stimuli.

While both onset and sustained IC units had lower vector strengths to most modulation frequencies (MFs) following SPON inactivation, the differences were generally not statistically significant. One exception occurred for responses to the narrow range of MFs (40-80 Hz) to which onset units phase-locked in the baseline condition. For these responses, phase-locking was abolished and vector strengths significantly decreased following SPON inactivation. It is possible that SPON-mediated inhibition is needed to segment responses of onset IC units to individual cycles of modulation. When offset

inhibition is removed, responses to neighboring cycles may blend together, thereby decreasing sensitivity. A partial explanation for decreases in vector strengths after inactivation is the corresponding drop in spiking that occurred. It is unclear why SPON inactivation decreased spiking for both onset and sustained IC units. It may be that offset inhibition is needed for onset IC neurons to respond to rapidly changing periodic stimuli via a rebound mechanism, and when this input is removed, spiking drops. Although vector strength significantly decreased for responses to a narrow range of MFs, the corresponding decreases in spiking rate were not statistically significant.

The findings presented here are in general agreement with previous studies of the effects of GABAergic inhibition on IC responses to SAM stimuli. Burger and Pollak (1998) found no significant effects on SAM tone responses after blocking GABA<sub>A</sub> receptors locally in the IC. While phase-locking to some MFs was abolished in the present study, the shapes of modulation transfer functions remained the same for all IC units following SPON inactivation. It is noteworthy that previous studies employed a local blockade of presumably all types of GABAergic input to IC neurons, including those originating from the dorsal and ventral nuclei of the lateral lemniscus and from the contralateral IC. Thus, the results of GABA receptor blockade at the level of the IC and the selective inactivation of the SPON input may have differing characteristics.

#### *SPON inactivation increases gap detection thresholds in the IC*

The ability to resolve short gaps between sound stimuli is important for the perception of speech in humans (Glasberg and Moore, 1989; Irwin and McAuley, 1987; Phillips, 1999; Snell and Frisina, 2000; Tyler et al., 1982). Neural correlates of gap detection have also been described in various mammalian species, including in the rodent IC (rat: Leitner et al., 1993; 1997; Mazelova et al., 2003; Rybalko and Syka, 2005; Syka; mouse: Allen et al., 2003; Barsz et al., 2002; Walton et al., 1997; 2002). Studies in the mouse IC have shown that very short gap stimuli are able to elicit distinct, strong responses to the onset of the trailing marker (Walton et al., 1997). Because SPON neurons also exhibit robust spiking to short gaps, it was hypothesized that they would play a role in IC gap detection (Kadner and Berrebi, 2008). In baseline recordings, sustained IC neurons had lower gap

detection thresholds, and thus, greater sensitivity for signaling stimulus discontinuities, compared to onset units. Following SPON inactivation, a significant elevation of thresholds was observed for sustained, but not for onset units. One interesting result was that for sustained IC units, spiking decreased to all gap durations after inactivation, particularly for very short gaps (< 4 ms). Even though gap detection thresholds were predicted to increase after SPON inactivation, it is difficult to resolve how spiking decreased when a source of inhibition was removed. One potential explanation is that membrane depolarization mediated by release from SPON-derived inhibition boosts responses for IC neurons to respond to short gap durations beyond the level observed when the continuous stimulus is presented. Such a mechanism would require subthreshold current that are activated or primed by hyperpolarization. In support of this idea, evidence of rebound spiking had been described in the rat IC, and is consistent with the results described here (Sivaramakrishnan and Oliver, 2001).

#### *Functional implications*

The SPON provides a major source of GABAergic inhibition to IC neurons. The hallmark of SPON neuronal responses is their ability to precisely signal discontinuities in temporal sound features. In particular, SPON responses synchronize to low MF SAM tones with very high vector strengths and recognize short gaps in stimuli with great sensitivity. The findings of the present study suggest that SPON input shapes responses to SAM and gap stimuli in the IC. Specifically, the precision of onset IC responses to SAM stimuli were diminished by inactivation, whereas effects on sustained units were most evident for responses to short gaps. Thus, a role for the SPON in the segregation of IC responses may underlie gap detection performance observed in behavioral experiments, and is consistent with the hypothesis that precisely-timed SPON inputs enhance the encoding of periodic stimuli in the IC.



## **Acknowledgements**

I thank Dr. Mike Burger for guidance and helpful suggestions regarding SPON inactivation experiments. In addition, I thank Drs. Jeff Wenstrup and Jason Sanchez for training in piggyback electrode construction and iontophoretic drug delivery. I also acknowledge Mr. Dennis Cole for assistance with the histological localization of recording sites.

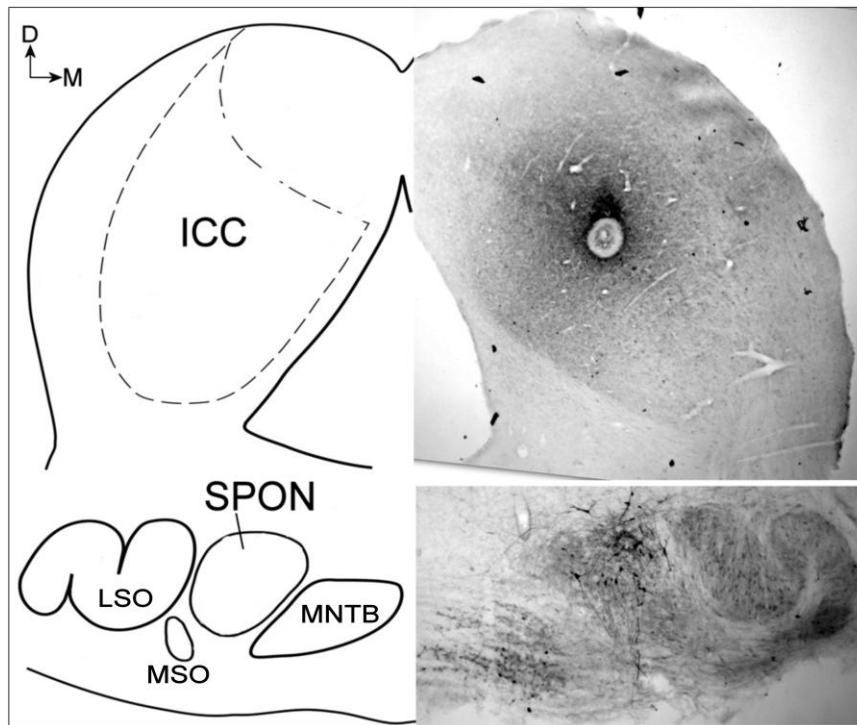


Fig. 5.1. Localization of recording sites in the Superior Paraolivary Nucleus (SPON) and central nucleus of the Inferior Colliculus (ICC). A schematic view of the brainstem and midbrain is shown in the left panel with labeled auditory nuclei (*left*). Corresponding tissue sections show Biocytin deposit sites that marked recording locations in the SPON and ICC (*right*). D: dorsal; M: medial; LSO: lateral superior olive; MNTB: medial nucleus of the trapezoid body; MSO: medial superior olive.

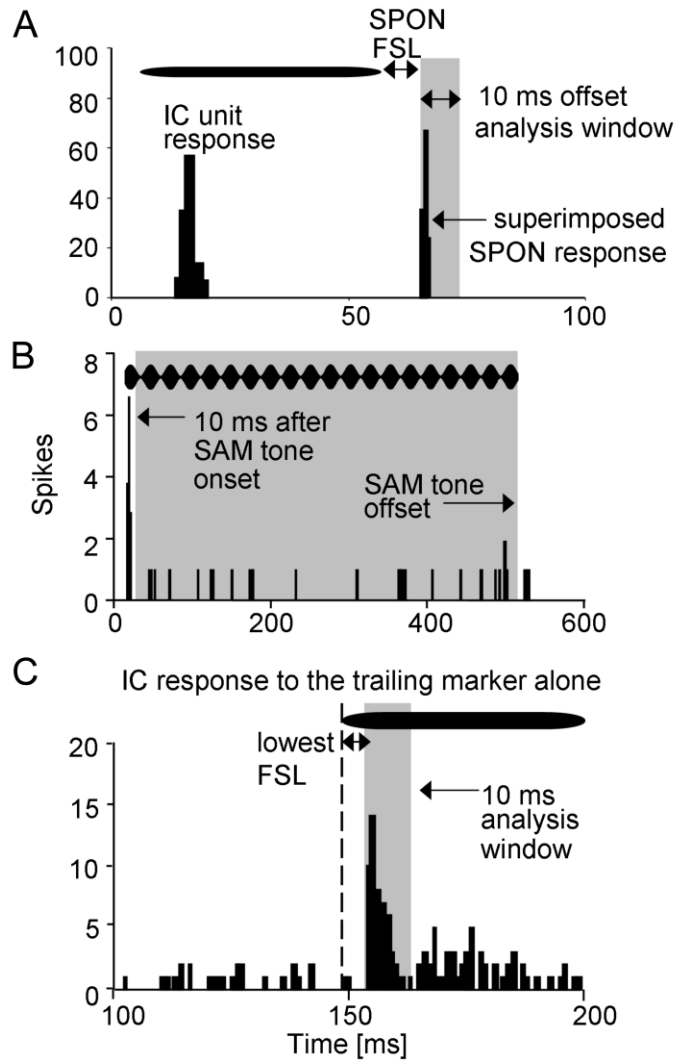


Fig. 5.2. Definitions of analysis windows for IC recordings. (A) For each recorded pair of SPON and IC neurons, spiking for the IC unit was measured in a 10 ms offset window (gray shaded area). This analysis window began at the time point of the first evoked spike of the SPON response (shown superimposed in the offset window). (B) For IC SAM responses, the analysis time window (gray shaded area) for calculating vector strengths began 10 ms after the start of the SAM tone and ended at the stimulus offset. The first 10 ms of the response was not analyzed to avoid the inclusion of spiking triggered by the stimulus onset (see Methods). In addition, all spiking triggered by the stimulus offset was excluded from the analysis. (C) The time window for gap detection tests were taken from the IC response to the trailing marker presented alone (see Methods). The 10 ms window started at the time point of the first evoked spike (gray shaded area). Spiking that occurred in each analysis window in A-C was compared for baseline and SPON inactivation conditions. Horizontal bars in A, C and the horizontal rippled bar in B represent the location of the stimulus in the time recording window. The vertical dashed line in C represents the time of the stimulus onset.

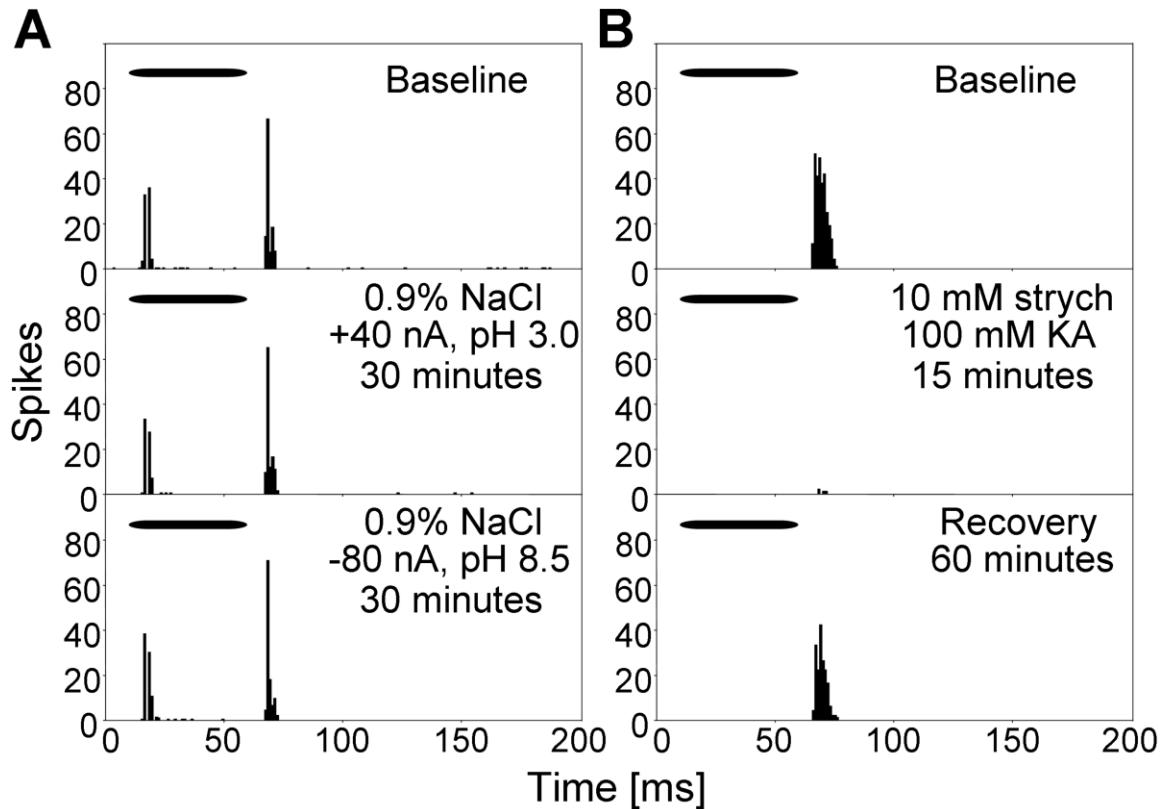


Fig. 5.3. Effective SPON inactivation was achieved using extracellular iontophoresis. (A) Compared to the baseline condition (*top*), current-applied vehicle solutions (bottom panels) had no appreciable effect on SPON spiking. (B) Robust offset spiking prior to drug application (*top*) was abolished following the application of strychnine and kynurenic acid (*middle*). The response magnitude approached baseline levels after a period of recovery (*bottom*). Horizontal bars represent the location of the stimuli in the recording windows.

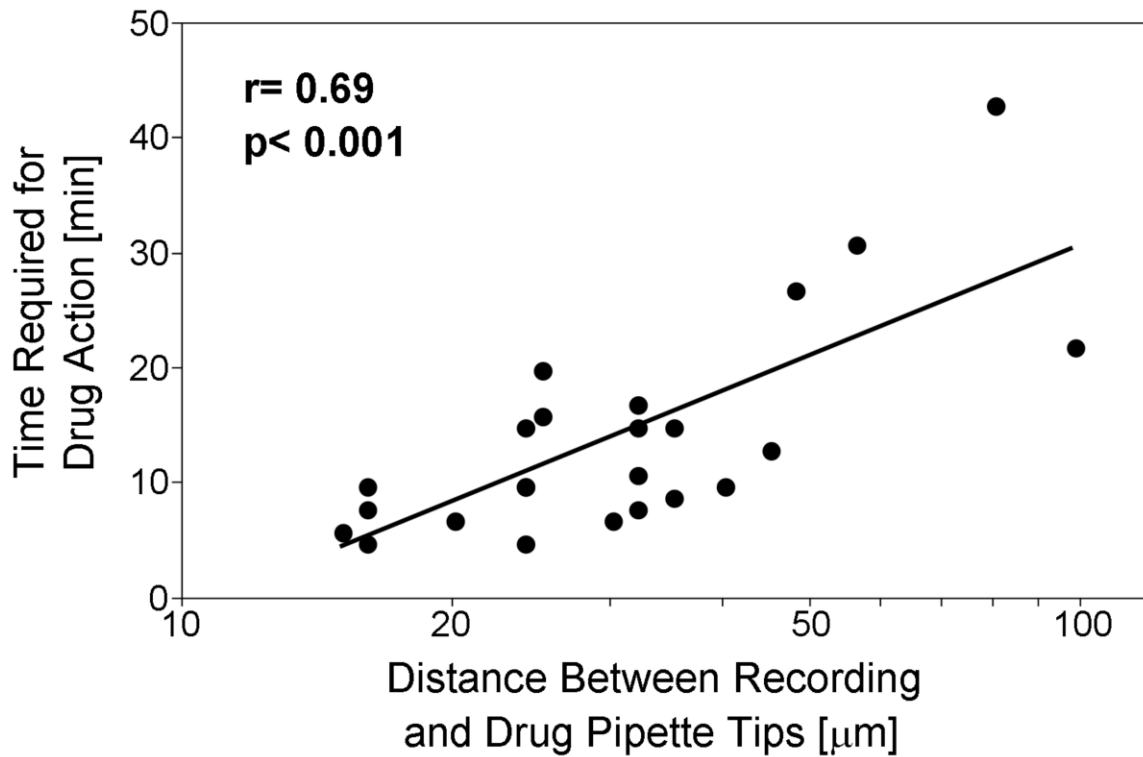


Fig. 5.4. The time course of drug action depends on the distance from the point of drug ejection to the SPON target neuron. The distance between the tip of the recording and multibarrel pipette tips was measured and correlated with the amount of time required for drug action (Spearman's rank correlation test).

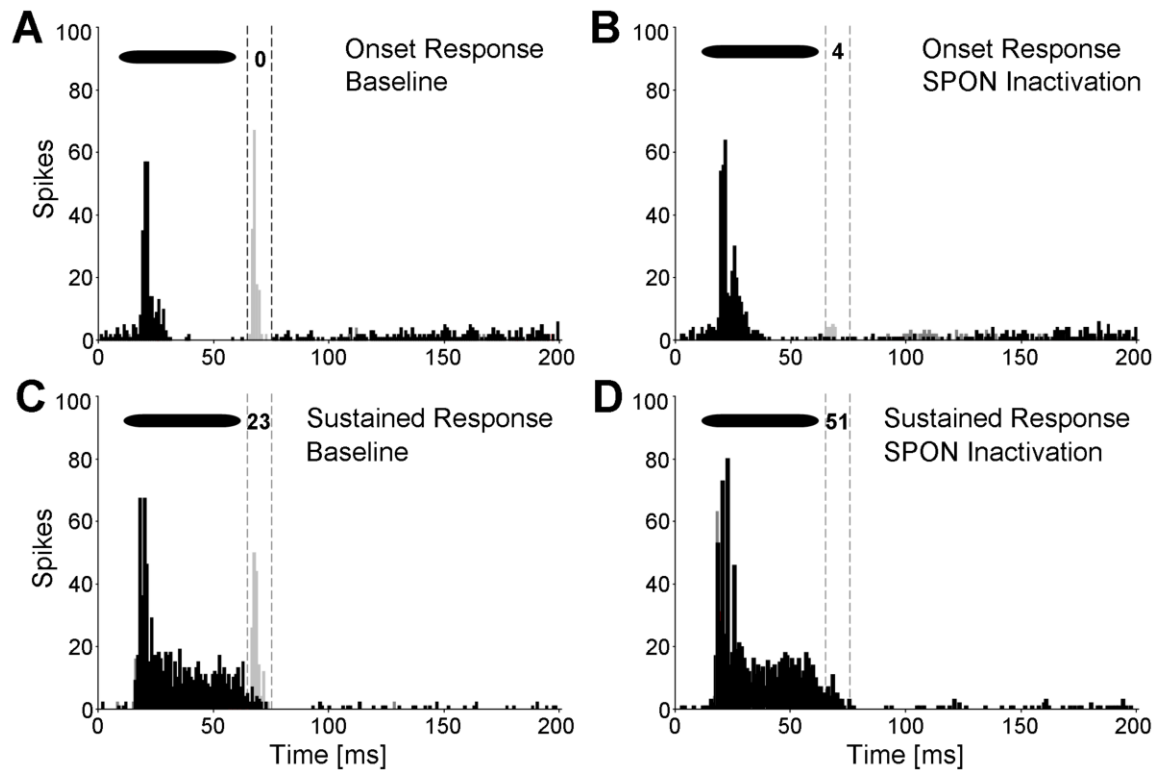


Fig. 5.5. SPON inactivation alters spiking patterns of IC neurons to pure tones. (A) A typical onset IC unit (black PSTH), marked by low rates of spontaneous activity in the time window following the stimulus offset (dashed vertical lines; see Fig. 5.2A). (B) After SPON activity (gray PSTHs) was silenced, only a small change in activity was observed in the offset window for the onset IC cell. (C+D) A sustained IC unit exhibited higher levels of spiking in the offset window in the baseline condition, whereby the effect of SPON inactivation could be seen more clearly. (D) This unit showed a substantial increase in spiking in the offset window following SPON inactivation. Gray PSTHs in the offset window of each plot represent superimposed spiking in the SPON collected 1-2 minutes prior to the IC PSTHs (black). SPON responses were recorded immediately prior to corresponding PSTHs of IC units. Values shown at the top of each offset analysis window represent IC spike counts. Horizontal bars in each plot represent the location of the pure tone stimulus in the recording window.

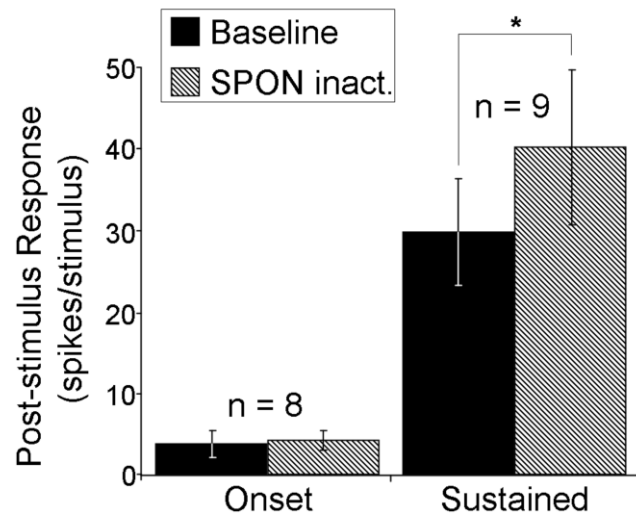


Fig. 5.6. Spiking of sustained IC neurons was altered following SPON inactivation. Inactivation had no effect on spiking for onset IC neurons in the time window (see Fig. 5.2A) in which SPON units were active. In contrast, sustained IC units had higher spiking rates in the offset window following SPON inactivation. Error bars represent the standard errors of the means. \* denotes statistical significance according to the Wilcoxon signed-ranks test,  $p < 0.05$ .



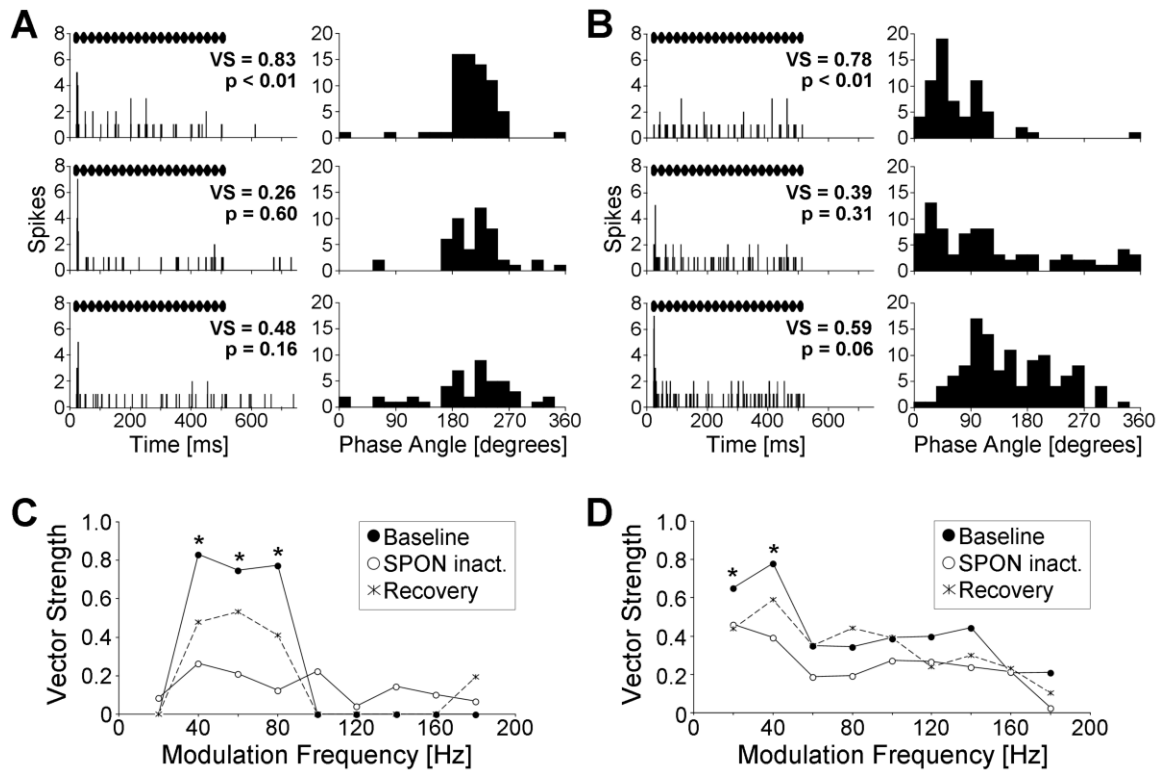


Fig. 5.7. SPON inactivation impacts phase-locking of representative IC neurons to SAM stimuli. (A) PSTHs (left subpanels) and corresponding phase plots (right subpanels) are shown for an onset IC unit's response to a SAM tone with 40 Hz modulation frequency (MF) in the baseline condition (top), following SPON inactivation (middle), and after the recovery period (bottom). (B) Responses of a sustained IC unit to a 40 Hz MF SAM tone for equivalent baseline, inactivation and recovery conditions. (C) Vector strengths (VS) are shown for the onset response in (A) for the range of modulation frequencies presented for baseline, SPON inactivation and recovery conditions. (D) Vector strengths of responses to the experimental manipulations for the sustained unit shown in (B). Horizontal rippled bars in A-B represent the location of SAM tones in the recording window. p values below 0.05 in A-B and asterisks in C-D indicate significant phase-locking of responses as determined by the Rayleigh test.

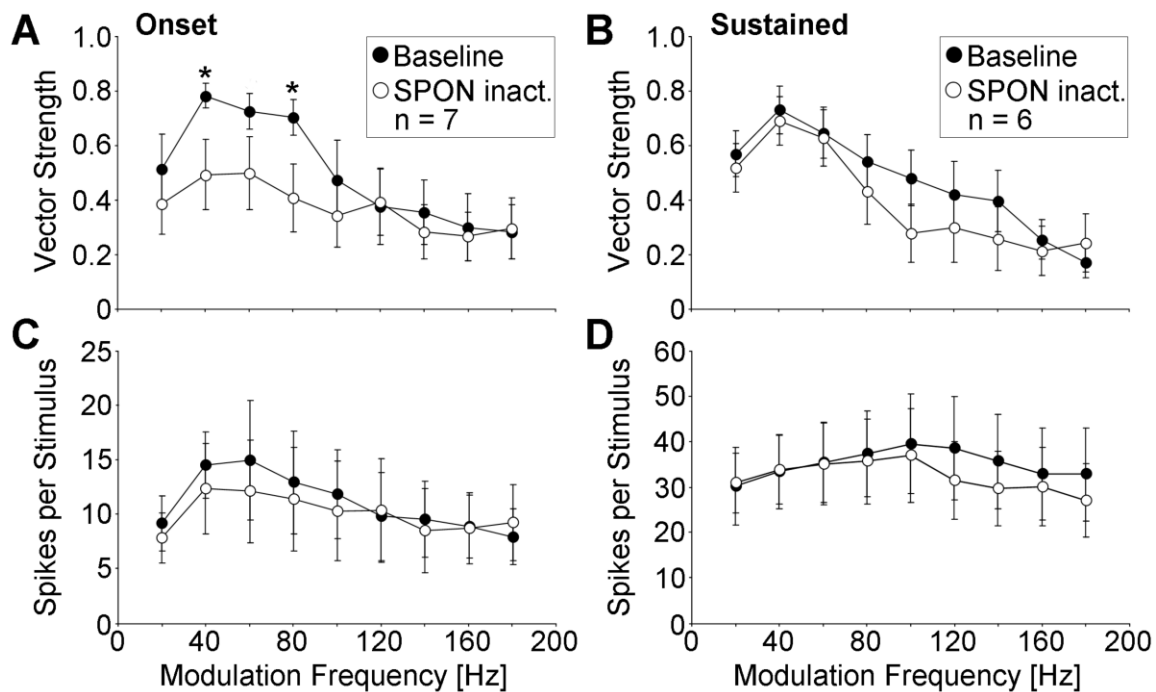


Fig. 5.8. Phase-locking to SAM stimuli was reduced for IC neurons following SPON inactivation. (A) Onset units in the IC had reduced vector strengths for low modulation frequencies after inactivation. (B) Sustained units showed a trend of lower response vector strengths at higher modulation frequencies (>60 Hz) post SPON inactivation, but these differences were not significant. (C) For onset units, spiking did not significantly decrease after inactivation for modulation frequencies that elicited the largest changes in vector strength. (D) Spiking for the sustained units also did not decrease in response to any of the modulation frequencies presented. Error bars represent the standard errors of the means. All vector strength values greater than 0.6 were significantly phase-locked to the stimulus ( $p < 0.05$ , Rayleigh test). Asterisks represent significant differences between baseline and SPON inactivation conditions ( $p < 0.05$ , Wilcoxon signed-ranks test).

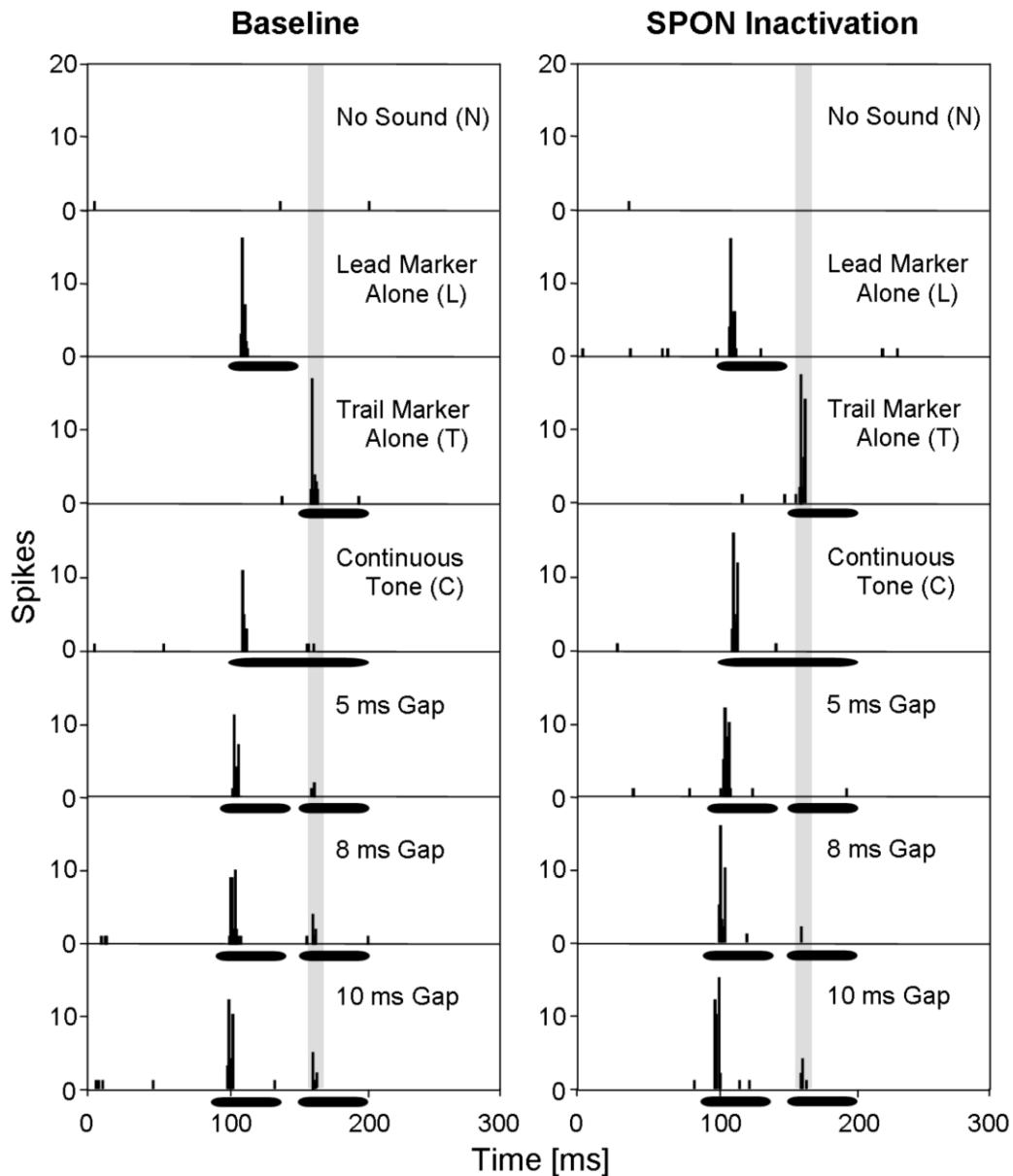


Fig. 5.9. SPON inactivation diminished the ability of a representative onset IC neuron to respond to short gaps between tones. (A) PSTHs are shown for an onset IC neuron prior to (*left panels*) and following SPON inactivation (*right panels*) for control conditions and at several gap durations. Horizontal bars represent the position of pure tone stimuli in the recording windows. Tone representations are shown below each PSTH for clarity, unlike previous figures, in which bars are located above corresponding PSTHs. Gray areas highlight the analysis window for gap detection (see Fig. 5.2C).

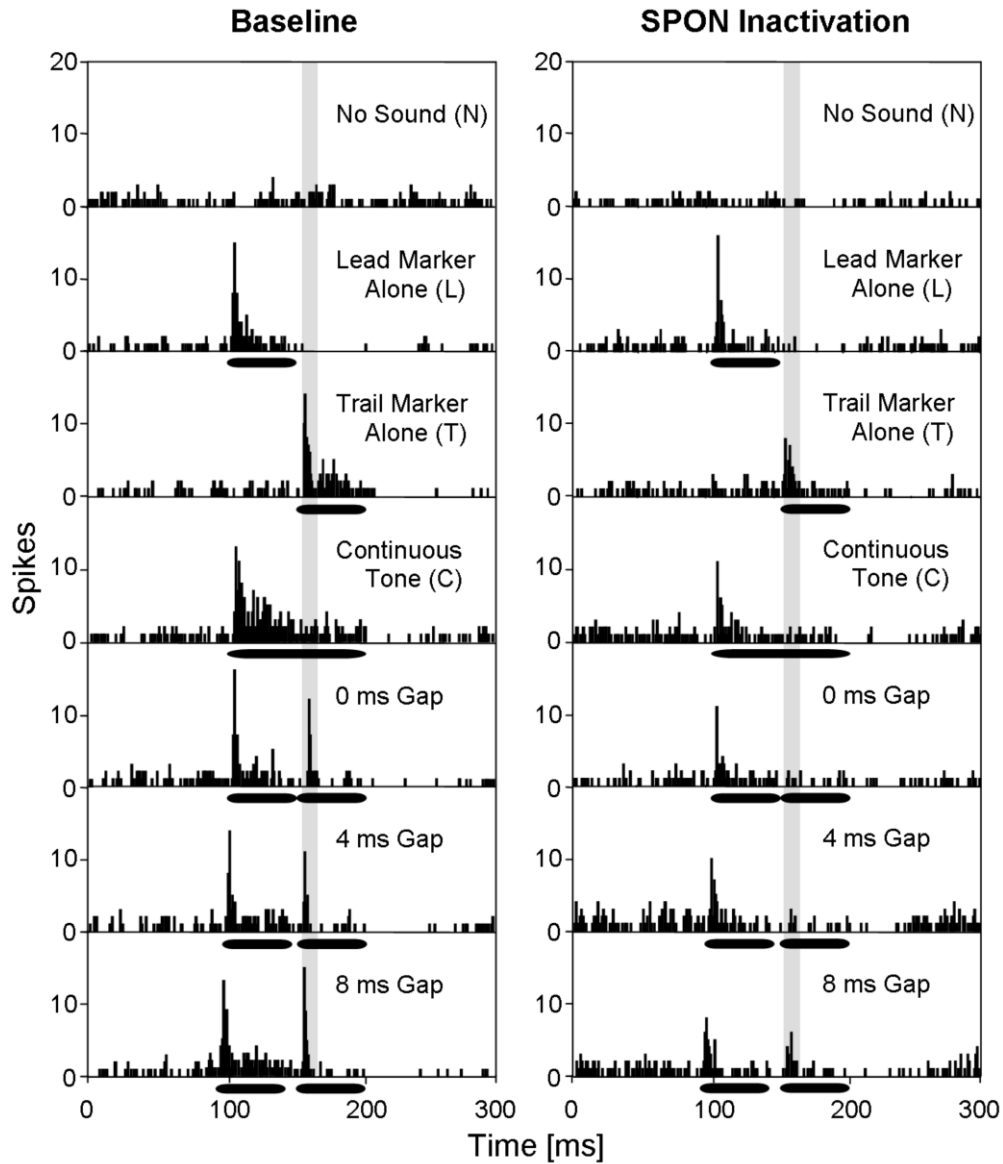


Fig. 5.10. SPON inactivation diminished the ability of a representative sustained IC neuron to respond to short gaps between tones. (A) PSTHs are shown for a sustained IC neuron prior to (*left panels*) and following SPON inactivation (*right panels*) for control conditions and at several gap durations. Horizontal bars represent the position of pure tone stimuli in the recording windows. Tone representations are shown below each PSTH for clarity, unlike previous figures, in which bars are located above corresponding PSTHs. Gray areas highlight the analysis window for gap detection (see Fig. 5.2C).

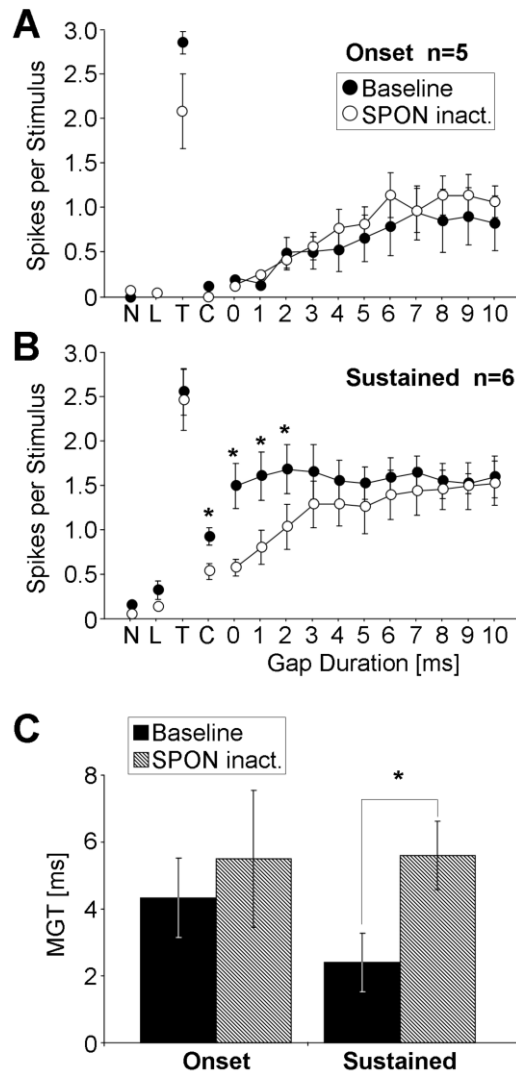


Fig. 5.11. IC neurons exhibit elevated gap detection thresholds following SPON inactivation. (A) Onset IC neurons exhibited no substantial spiking change following SPON inactivation in response to all gap durations presented. (B) Spiking for short gap durations decreased following SPON inactivation. (C) Gap detection thresholds were significantly elevated for sustained, but not onset IC units following inactivation (Wilcoxon signed ranks test). N: no sound; L: leading marker; T: trailing marker; C: 100 ms control. MGT: minimum gap detection threshold (see Methods). Error bars represent the standard errors of the means.

## **Chapter Six**

### **General Discussion**

## Summary

The purpose of this dissertation was to explore the behavior of neurons in the mouse and rat SPON using *in vitro* and *in vivo* physiological techniques. The SPON has been the subject of increasing interest among investigators due to its prominent position in the ascending auditory pathway and because its functional role in hearing has not been well established compared to other major nuclei in the auditory brainstem. The findings presented herein suggest that one role of the SPON is to provide well-timed inhibition that shapes responses to temporal features of sound in its primary target, the inferior colliculus (IC). The experiments described in the previous chapters will serve as a framework, whereby hypotheses for the SPON's role in encoding other attributes of acoustic signals may be tested. In addition, the present results add to the depth of knowledge regarding how inhibitory inputs from brainstem nuclei are integrated in higher processing centers.

### ***Study 1: Are there morphologically distinct cell types in the SPON?***

To determine whether SPON neurons in the mouse are a morphologically homogeneous population or whether distinct cell types are present, physiologically characterized neurons were filled with dye and reconstructed. The first detailed description of mouse SPON neurons is presented in Chapter 2, demonstrating that even with subtle variations in the sizes and shape of cell bodies and dendrites, morphological differences did not warrant classification into distinct cell types. These findings correspond with published data reporting homogeneous cell morphology in the rat (Kulesza Jr. and Berrebi, 2000; Saldaña and Berrebi, 2000), suggesting the mouse and rat SPON share similar structural properties which likely underlie shared functional roles. In addition to describing cell morphology, Chapter 2 provides the first classification of physiological properties of SPON neurons *in vitro*. The results confirm that the hallmark offset spiking described *in vivo* (Dehmel et al., 2002; Kulesza Jr. et al., 2003; Kuwada and Batra, 1999) is generated by a rebound from membrane hyperpolarization. Furthermore, it was determined that SPON neurons are intrinsically tuned to periodically modulated stimuli, which may

contribute to highly precise spiking to periodic sounds *in vivo* (Behrend et al., 2002; Kadner and Berrebi, 2008; Kulesza Jr. et al., 2003; Kuwada and Batra, 1999). In sum, this study represents a first step towards elucidating the biophysical properties that make SPON neurons well-suited for processing temporal information in the auditory system.

***Study 2: Does anesthesia alter the behavior of SPON neurons?***

Nearly all previous reports of SPON physiology have used ketamine-anesthetized animals, and reported neuronal responses that typically exhibited highly transient evoked spiking (Behrend et al., 2002; Dehmel et al., 2002; Kadner and Berrebi, 2008; Kadner et al., 2006; Kulesza Jr. et al., 2003; 2007). In the absence of anesthesia, the response magnitudes of SPON neurons were found to be substantially greater than those from studies using anesthetized animals (Kuwada and Batra, 1999). To characterize the behavior of SPON neurons in a more natural state and to determine the impact of anesthesia on neuronal responses, recordings were conducted in the mouse SPON with and without ketamine anesthesia. In the first characterization of *in vivo* response properties in the mouse SPON, the results of Chapter 3 show that ketamine acts to lower the general excitability of neurons, but does not affect tuning to periodically fluctuating stimuli. Thus, previous reports from anesthetized animals likely provide an accurate description of neuronal selectivity for temporal sound features, although the magnitude of the potential impact that SPON inputs have on their targets may have been underestimated.

***Study 3: How do ion currents and transmitter systems shape neuronal responses?***

A defining characteristic of SPON neurons is their ability to precisely signal changes in temporal features of acoustic signals. Although the major inputs to the SPON are known, it remains unclear how each transmitter system contributes to responses during the presentation of rapidly fluctuating sound envelopes. To explore the roles of inhibitory and excitatory inputs and ionic currents in shaping responses to amplitude modulated tones, neurons were recorded from before and after blockade of neurotransmitter



receptors and ionic current channels. The results shown in Chapter 4 demonstrate that glycinergic input, in addition to hyperpolarization activated outward cation and low voltage-activated calcium currents, have large impacts on neuronal responses to periodic stimuli. In addition, blocking GABA<sub>A</sub>, NMDA and AMPA/kainate receptors had more subtle effects on responses. Moreover, this study provides a first report of highly synchronous responses of SPON neurons to very low amplitude modulation frequencies (< 20 Hz), which are thought to be important for rhythm perception (Zwicker and Fastl, 1990).

***Study 4: What is the functional role of the SPON in forming properties of IC neurons?***

To test how responses to temporal features of stimuli are shaped by SPON-derived inhibition in the IC, neurons in the IC were recorded before and after inactivation of SPON inputs. The results presented in Chapter 5 suggest that SPON inputs contribute to shaping responses of onset cells in the IC to amplitude modulated tones. Furthermore, IC units that discharge with sustained responses rely on offset inhibition from the SPON to sharpen gap detection. These findings represent the first direct evidence that the SPON has a role in encoding temporal sound information at the level of the IC.

The data presented in this dissertation support previous studies that implicate the SPON in the processing of temporal information contained in acoustic signals. This work has led to the hypothesis that at least one role of the SPON is to faithfully signal both periodic (e.g., SAM stimuli) and singular (e.g., gaps) discontinuities within ongoing sounds. Although this role for the SPON has been discussed previously (Kadner and Berrebi, 2008), this dissertation provides the first direct evidence that the SPON transmits its unique properties to higher processing areas to create novel response types. Additional potential roles for the SPON in auditory processing are discussed in the following section.

## Discussion

### *Other potential functional roles for the SPON in hearing*

There is evidence that the SPON has functional roles in the encoding of temporal sound features (Behrend et al., 2002; Kadner and Berrebi, 2008; Kulesza Jr. et al., 2003; Kuwada and Batra, 1999) and in stimulus duration tuning (Kadner et al., 2006). However, SPON neurons may also participate in other aspects of sounds processing. Recently, it has been proposed that SPON-like responses may contribute to shaping selectivity to frequency modulated sweeps in the IC, and the SPON has also been implicated in creating “growth of masking” in the central auditory system. These proposed circuits involving the SPON are the subjects of the following sections.

### *Frequency modulated sweeps*

Acoustic signals that are modulated in the frequency domain are common among natural communication sounds (Fuzessery and Hall, 1996; Klug et al., 2002). In the IC, a subpopulation of neurons shows selectivity to frequency modulated (FM) stimuli (Xie et al., 2007; 2008). At low sound levels (< 25-30 dB), these cells exhibit spiking responses to pure tones and to both downwardly sweeping FM stimuli that decrease in frequency over time, and to upward FM sweeps which progressively increase in frequency. However, at higher sound levels (> 25-30 dB), tone-evoked spiking ceases and neurons become dominated by inhibition. This inhibition consists of transient inhibitory postsynaptic potentials that arrive shortly after the onset and offset of stimuli; thus, these cells have been termed on-off cells (Xie et al., 2007). An interesting feature of on-off cells is that they produce spiking responses to downward FM sweeps at all stimulus levels tested (10-60 dB), but only respond to tones and upward FM sweeps at low levels (< 20-25 dB; Xie et al., 2007).

Pollak and colleagues (2011) posit that the sources of onset and offset transient inhibitory post synaptic potentials are glycinergic neurons in the ventral nucleus of the lateral lemniscus and GABAergic neurons in the SPON, respectively (Kulesza Jr. and

Berrebi, 2000; Saldaña et al., 2009; Saldaña and Berrebi, 2000; Vater et al., 1997; Winer et al., 1995). The response properties of cells from both nuclei closely match those of IC on-off cells, including transient responses triggered by the stimulus onset and offset, respectively, as well as high thresholds and broad tuning at moderate to high sound levels (Covey and Casseday, 1991; Haplea et al., 1994; Kulesza Jr. et al., 2003). Because neurons in the ventral nucleus of the lateral lemniscus have directional selectivity for FM sweeps (Huffman et al., 1998), they are thought to determine FM selectivity in the IC. A mechanism has been proposed whereby spiking to preferred FM sweep directionality in the IC occurs at higher sound levels because such high level stimuli evoke either a weak response in the ventral nucleus of the lateral lemniscus or no response at all (Pollak et al., 2011). This lack of response would remove the source of onset inhibition for on-off cells, thereby allowing neurons to spike to the stimulus. The role of the SPON in shaping on-off responses is likely to suppress potential spiking near the offset of the stimulus at moderate to high stimulus levels. It is unlikely that the SPON is actively involved in creating selectivity for FM sweeps, as responses from these neurons do not show a preference for sweep directionality (Felix II and Berrebi, unpublished results). Thus, the SPON has a proposed role in encoding FM sound features, but the mechanism remains unclarified.

### *Growth of masking*

Temporal relationships between specific components of complex auditory scenes are important for the accurate perception of naturalistic, biologically relevant sounds. A well-studied example of temporal context dependence in the auditory system is forward masking, which can dramatically change the representation natural sounds, including speech (Fastl and Zwicker, 1997). Based on psychoacoustic studies, the ability to detect a short “probe” sound is degraded when a longer “masking” sound precedes the probe. (Oxenham and Plack, 2000; Plack and Oxenham, 1998). Detection thresholds for the probe systematically increase as the intensity level of the masker increases in a highly linear relationship that persists for maskers presented in excess of 80 dB SPL (physiological slope  $\sim 0.5$  dB probe detection threshold shift per dB masker intensity

level; Jesteadt et al., 1982; Plack and Oxenham, 1998). However, at the level of the auditory nerve, increasing the masker level causes increasing probe detection thresholds only up to 20 dB masker level, and regardless of how much the masker level is increased beyond this intensity, probe thresholds remain unchanged (i.e., the effect on the probe quickly saturates as the masker level increases; Relkin and Turner, 1988). Thus, the continuous “growth of masking” observed in behavioral studies (where the effects of the masker on probe detection occur beyond 80 dB SPL masker level) cannot be explained by auditory nerve responses (where the effects of the masker on probe detection occur only up to 20 dB SPL masker level); therefore the substrate for the growth of masking phenomenon must be created *de novo* somewhere in the central auditory system.

Recently, Nelson et al. (2009) have provided evidence for continuous growth of masking behavior by single neurons in the IC. Their data show that inhibition is likely key in creating forward masking properties, rather than peripheral neural adaptation. It was proposed that the SPON provides the input required for the growth of masking because it provides offset inhibition to IC neurons following the masker signal which is capable of suppressing the response to the probe. Moreover, SPON neurons possess high thresholds, narrow frequency tuning near threshold and broad tuning at higher sound levels, and have responses with large dynamic ranges (Kulesza Jr. et al., 2003; Kuwada and Batra, 1999). Hence, the role for the SPON in forward masking is expected to be most prominent at high sound levels, and may therefore be critical for the mechanism mediating growth of masking in the central auditory system.

### *Suggestions for future experiments*

A potential role for the SPON in representing frequency modulated sound features and forward making phenomena can be tested using a reversible inactivation procedure similar to experiments described in Chapter 5 of this dissertation. However, techniques for SPON inactivation can be improved to overcome some of the limitations inherent in the paradigm. For instance, to eliminate concerns of drugs spreading into neighboring auditory nuclei, genetic techniques can be employed, whereby non-native channels are expressed only on SPON cells and serve to reversibly silence neuronal responses

(Lechner et al., 2002; Tan et al., 2006). This approach was attempted by expressing the *drosophila* allatostatin receptor in the mouse SPON. The binding of the allatostatin ligand to its receptor potentiates voltage-gated potassium currents and acts to silence spiking activity. Although restricted expression of the allatostatin receptor was achieved in the mouse SPON in a pilot study, no additional experiments exploring the functionality of the receptor-ligand complex were conducted at the time this manuscript was written.

For the inactivation experiments presented in Chapter 5, all recorded pairs of SPON and IC units were included in the data set, regardless of whether silencing SPON cells resulted in observed changes in the IC. This likely led to an underestimation of the impact of SPON input on shaping IC responses. For a more accurate description of the contribution of SPON input to the IC, it may be helpful to formulate criteria to determine whether inactivated regions of the SPON are functionally connected to recorded neurons in the IC. Such metrics have been used to determine successful corticofugal modulation of auditory neuronal responses (Jen et al., 1998; Zhou and Jen, 2007). An additional approach to determine whether SPON neurons are functionally connected to their target cells in the IC is to iontophoretically stimulate the SPON with a combination of glutamate and aspartate and observe whether offset inhibition is evoked in the IC.

SPON neurons send substantial axonal projections to the inferior colliculus. Therefore, much of the focus on the function of the SPON has been in the context of the SPON-IC circuit. However, the SPON also projects to other auditory nuclei including the medial geniculate body in the thalamus and to the tectal-longitudinal column in the midbrain tectum (Jin and Berrebi, 2006; Saldaña et al., 2007). To date, virtually nothing is known of the impact of SPON-derived inhibition on neuronal response properties in these areas. Therefore, a major goal of future studies will be to investigate the functional impact of the SPON on multiple auditory processing circuits; building on the foundation of knowledge gained from previous anatomical and tract tracing studies.

## **Conclusions**

This dissertation provides a detailed characterization of SPON structure and function on several levels, from intrinsic cell properties and single cell morphology, to investigations

into how synaptic inputs shape response properties. Also, systems approach was taken to explore how the SPON shapes properties of its neuronal targets. A prominent role for the SPON in processing temporal features of acoustic signals has implications for the accurate encoding and perception of biologically relevant sounds, such as animal vocalizations and speech, which rely heavily on timing information.

## REFERENCES

- Aizenman CD, Linden DJ (1999) Regulation of the rebound depolarization and spontaneous firing patterns of deep nuclear neurons in slices of rat cerebellum. *J Neurophysiol* 82: 1697-1709.
- Allen PD, Burkard RF, Ison JR, Walton JP (2003) Impaired gap encoding in aged mouse inferior colliculus at moderate but not high stimulus levels. *Hear Res* 186: 17-29.
- Anis NA, Berry SC, Burton NR, Lodge D (1983) The dissociative anaesthetics, ketamine and phencyclidine, selectively reduce excitation of central mammalian neurones by N-methyl-aspartate. *Br J Pharmacol* 79:565-575.
- Aparicio MA, Viñuela A, Saldaña E (2010) Projections from the inferior colliculus to the tectal longitudinal column in the rat. *Neuroscience* 166: 653-664.
- Aschoff A, Ostwald J (1987) Different origins of cochlear efferents in some bat species, rats and guinea pigs. *J Comp Neurol* 264: 56-72.
- Aschoff A, Ostwald J (1988) Distribution of cochlear efferents and olivo-cochlear neurons in the brainstem of rat and guinea pig. A double labeling study with fluorescent tracers. *Exp Brain Res* 71: 241-251.
- Banks MI, Smith PH (1992) Intracellular recordings from neurobiotin-labeled cells in brain slices of the rat medial nucleus of the trapezoid body. *J Neurosci* 12:2819-2837.
- Barsz K, Ison JR, Snell KB, Walton JP (2002) Behavioral and neural measures of auditory temporal acuity in aging humans and mice. *Neurobiol Aging* 23: 565-578.
- Batschelet E (1981) *Circular statistics in biology*. London: Academic Press.
- Bauer EE, Klug A, Pollak GD (2000) Features of contralaterally evoked inhibition in the inferior colliculus. *Hear Res* 141: 80-96.
- Bazwinsky I, Hilbig H, Bidmon HJ, Rubsamen R (2003) Characterization of the human superior olivary complex by calcium binding proteins and neurofilament H (SMI-32). *J Comp Neurol* 456:292-303.
- Behrend O, Brand A, Kapfer C, Grothe B (2002) Auditory response properties in the superior paraolivary nucleus of the gerbil. *J Neurophysiol* 87:2915-2928.
- Benavides-Piccione R, Hamzei-Sichani F, Ballesteros-Yanez I, DeFelipe J, Yuste R (2005) Dendritic size of pyramidal neurons differs among mouse cortical regions. *Cereb Cortex* 16: 990-1001.

Beyerl BD (1978) Afferent projections to the central nucleus of the inferior colliculus in the rat. *Brain Res* 145: 209-223.

Bilak MM, Bilak SR, Morest DK (1996) Differential expression of N-methyl-D-aspartate receptor in the cochlear nucleus of the mouse. *Neuroscience* 75:1075-1097.

Bledsoe SC Jr, Snead CR, Helfert RH, Prasad V, Wenthold RJ, Altschuler RA (1990) Immunocytochemical and lesion studies support the hypothesis that the projections from the medial nucleus of the trapezoid body to the lateral superior olive is glycinergic. *Brain Res* 517:189-194.

Bryant JL, Roy S, Heck DH (2009) A technique for stereotaxic recordings of neuronal activity in awake head-restrained mice. *J Neurosci Meth* 178:75-79.

Burger RM, Pollak GD (1998) Analysis of the role of inhibition in shaping responses to sinusoidally amplitude-modulated signals in the inferior colliculus. *J Neurophysiol* 80:1686-1701.

Burger RM, Pollak GD (2001) Reversible inactivation of the dorsal nucleus of the lateral lemniscus reveals its role in the processing of multiple sound sources in the inferior colliculus of bats. *J Neurosci* 21: 4830-4843.

Campbell RE, Gaidamaka G, Han SK, Herison AE (2009) Dendro-dendritic bundling and shared synapses between gonadotropin-releasing hormone neurons. *Proc Natl Acad Sci USA* 106: 10835-10840.

Camps M, Kelly PH, Palacios JM (1990) Autoradiographic localization of dopamine D1 and D2 receptors in the brain of several mammalian species. *J Neural Transm Gen Sect* 80:105-127.

Cant NB, Casseday JH (1986) Projections from the anteroventral cochlear nucleus to the lateral and medial superior olivary nuclei. *J Comp Neurol* 247:457-476.

Caspary DM, Faingold CL (1989) Non-N-methyl-D-aspartate receptors may mediate ipsilateral excitation at lateral superior olivary synapses. *Brain Res* 503:83-90.

Caspary DM, Palombi PS, Hughes LF (2002) GABAergic inputs shape responses to amplitude modulated stimuli in the inferior colliculus. *Hear Res* 168: 163-173.

Church MW, Gritzke R (1987) Effects of ketamine anesthesia on the rat brain-stem auditory evoked potential as a function of dose and stimulus intensity. *Electroencephalogr Clin Neurophysiol* 67:570-583.

Cove J, Blinder P, Baranes D (2009) Contacts among non-sister dendritic branches at bifurcations shape neighboring dendrites and pattern their synaptic inputs. *Brain Res* 1251: 30-41.



Covey E, Casseday JH (1991) The monaural nuclei of the lateral lemniscus in an echolocating bat: parallel pathways for analyzing temporal features of sound. *J Neurosci* 11: 3456-3470.

Covey E, Vater M, Casseday JH (1991) Binaural properties of single units in the superior olivary complex of the mustached bat. *J Neurophysiol* 66:1080-1094.

Culling JF, Hodder KI, Toh CY (2003) Effects of reverberation on perceptual segregation of competing voices. *J Acoust Soc Am* 114: 2871-2876.

Darrow KN, Simons EJ, Dodds L, Liberman MC (2006) Dopaminergic innervation of the mouse inner ear: evidence for a separate cytochemical group of cochlear efferent fibers. *J Comp Neurol* 498:403-414.

Davis KA (2005) Spectral processing in the inferior colliculus. *Int Rev Neurobiol* 70: 169-205.

Dehmel S, Kopp-Scheinflug C, Dorrscheidt GJ, Rubsamen R (2002) Electrophysiological characterization of the superior paraolivary nucleus in the Mongolian gerbil. *Hear Res* 172:18-36.

Do MTH, Bean BP (2003) Subthreshold sodium currents and pacemaking of subthalamic neurons: modulation by slow inactivation. *Neuron* 39: 109-120.

Drullman R (1995) Temporal envelope and fine structure cues for speech intelligibility. *J Acoust Soc Am* 97: 585-592.

Ehret G (1976) Development of absolute auditory thresholds in the house mouse (*Mus musculus*). *J Am Audiol Soc* 1:179-184.

Egorova M, Ehret G, Vartanian I, Esser KH (2001) Frequency response areas of neurons in the mouse inferior colliculus. I. Threshold and tuning characteristics. *Exp Brain Res* 140: 145-161.

Eller P, Berjukov S, Wanner S, Huber I, Hering S, Knaus HG, Toth G, Kimball SD, Striessnig J (2000) High affinity interaction of mibefradil with voltage-gated calcium and sodium channels. *Br J Pharmacol.* 130: 669-677.

Faingold CL, Boersma Anderson CA, Caspary DM (1991) Involvement of GABA in acoustically-evoked inhibition in inferior colliculus neurons. *Hear Res* 52: 201-216.

Faingold CL, Hoffmann WE, Caspary DM (1989) Effects of excitant amino acids on acoustic responses of inferior colliculus neurons. *Hear Res* 40:127-136.

Fastl H, Zwicker E (1997) *Psychoacoustics: facts and models*. Berlin: Springer.

- Fay RR (1988) Comparative psychoacoustics. *Hear Res* 34: 295-305.
- Feinberg AP, Snyder SH (1975) Phenothiazine drugs: structure-activity relationships explained by a confirmation that mimics dopamine. *Proc Natl Acad Sci USA* 72:1899-1903.
- Feldman DE, Knudsen EI (1994) NMDA and non-NMDA glutamate receptors in auditory transmission in the barn owl inferior colliculus. *J Neurosci* 14:5939-5958.
- Felix II RA, Berrebi AS (2007) Characterization of the superior paraolivary nucleus in the unanesthetized mouse. *Assoc Res Otolaryngol Abs* 30:100.
- Felix II RA, Berrebi AS (2010) The superior paraolivary nucleus contributes to shaping the temporal response properties of neurons in the inferior colliculus. *Soc for Neurosci Abs* 40:671.
- Felix II RA, Fridberger A, Leijon S, Berrebi AS, Magnusson AK (2011) Sound rhythms are encoded by post-inhibitory rebound spiking in the superior paraolivary nucleus. *J Neurosci*, in press.
- Felix II RA, Portfors CV (2007) Excitatory, inhibitory and facilitatory frequency response areas in the inferior colliculus of hearing impaired mice. *Hear Res* 228:212-229.
- Ferragamo MJ, Golding NL, Oertel D (1998) Synaptic inputs to stellate cells in the ventral cochlear nucleus. *J Neurophysiol* 79:51-63.
- Forsythe ID, Barnes-Davies M (1993) The binaural auditory pathway: excitatory amino acid receptors mediate dual timecourse excitatory postsynaptic currents in the rat medial nucleus of the trapezoid body. *Proc Biol Sci* 251:151-157.
- Friauf E, Hammerschmidt B, Kirsch J (1997) Development of adult-type inhibitory glycine receptors in the central auditory system of rats. *J Comp Neurol* 385: 117-134.
- Friauf E, Ostwald J (1988) Divergent projections of physiologically characterized rat ventral cochlear nucleus neurons as shown by intra-axonal injection of horseradish peroxidase. *Exp Brain Res* 73:263-284.
- Frisina RD (2001) Subcortical neural coding mechanisms for auditory temporal processing. *Hear Res* 158:1-27.
- Fuzessery ZM, Hall JC (1996) Role of GABA in shaping frequency tuning and creating FM sweep selectivity in the inferior colliculus. *J Neurophysiol* 76: 1059-1073.
- Geissler DB, Ehret G (2002) Time-critical integration of formants for perception of communication calls in mice. *Proc Natl Acad Sci USA* 99:9021-9025.

Gentner TQ, Margoliash D (1994) The neuroethology of vocal communication: perception and cognition. New York: Springer.

Glasberg BR, Moore BC (1989) Psychoacoustic abilities of subjects with unilateral and bilateral hearing impairments and their relationship to the ability to understand speech. *Scand Audiol Suppl* 32: 1-25.

Goldberg JM, Brown PB (1969) Response of binaural neurons of dog superior olivary complex to dichotic tonal stimuli: some physiological mechanisms of sound localization. *J Neurophysiol* 32:613-636.

Golding NL, Ferragamo MJ, Oertel D (1999) Role of intrinsic conductances underlying responses to transients in octopus cells of the cochlear nucleus. *J Neurosci* 19:2897-2905.

Golding NL, Robertson D, Oertel D (1995) Recordings from slices indicate that octopus cells of the cochlear nucleus detect coincidence firing of auditory nerve fibers with temporal precision. *J Neurosci* 15:3138-3153.

Gonzalez-Hernandez T, Mantolan-Sarmiento B, Gonzalez-Gonzalez B, Perez-Gonzalez H (1996) Sources of GABAergic input to the inferior colliculus of the rat. *J Comp Neurol* 372: 309-326.

Green DM, Forrest TG (1989) Temporal gaps in noise and sinusoids. *J Acoust Soc Am* 86: 961-970.

Grothe B (1994) Interaction of excitation and inhibition in processing of pure tone and amplitude-modulated stimuli in the medial superior olive of the mustached bat. *J Neurophysiol* 71:706-721.

Grothe B, Pecka M, McAlpine D (2010) Mechanisms of sound localization in mammals. *Physiol Rev* 90:983-1012.

Grothe B, Schweitzer H, Pollak GD, Schuller G, Rosemann C (1994) Anatomy and projection patterns of the superior olivary complex in the Mexican free-tailed bat. *Tadarida brasiliensis Mexicana*. *J Comp Neurol* 343:630-646.

Grothe B, Vater M, Casseday JH, Covey E (1992) Monaural interaction of excitation and inhibition in the medial superior olive of the mustached bat: An adaptation for bisonar. *Proc Natl Acad Sci USA* 89: 5108-5112.

Guinan JJ, Guinan SS, Norris BE (1972) Single units in the superior olivary complex I: responses to sounds and classification based on physiological properties. *Int J Neurosci* 4:101-120.

Hamann M, Billups B, Forsythe ID (2003) Non-calyceal excitatory inputs mediate low fidelity synaptic transmission in rat auditory brainstem slices. *Eur J Neurosci* 18:2899-2902.

Haplea S, Covey E, Casseday JH (1994) Frequency tuning and response latencies at three levels in the brainstem of the echolocating bat, *Eptesicus fuscus*. *J Comp Physiol A* 174: 671-683.

Harding BN (1971) Dendro-dendritic synapses, including reciprocal synapses, in the ventral nucleus of the monkey thalamus. *Brain Res* 34: 181-185.

Harrison NL, Simmonds MA (1985) Quantitative studies on some antagonists of N-methyl D-aspartate in slices of rat cerebral cortex. *Br J Pharmacol* 84:381-391.

Havey DC, Caspary DM (1980) A simple technique for constructing "piggyback" multibarrel microelectrodes. *Electroencephalogr Clin Neurophysiol* 48:249-251.

Hawk TC, Leary SL, Morris TH (2005) *Formulary for laboratory animals*. Ames: Blackwell.

Heffner R, Heffner H, Masterton B (1971) Behavioral measurements of absolute and frequency-difference thresholds in guinea pig. *J Acoust Soc Am* 49: 1888-1895.

Helfert RH, Bonneau JM, Wenthold RJ, Altschuler RA (1989) GABA and glycine immunoreactivity in the guinea pig superior olivary complex. *Brain Res* 501:269-286.

Hevers W, Hadley SH, Luddens H, Amin J (2007) Modulation of GABAergic conductances in cerebellar granula cells by the anesthetic ketamine, *Proceedings of the 7<sup>th</sup> Gottingen Meeting of the German Neuroscience Society* T34-2C.

Holmstrom LA, Eeuwes LB, Roberts PD, Portfors CV (2010) Efficient encoding of vocalizations in the auditory midbrain. *J Neurosci* 30: 802-819.

Holmstrom L, Roberts PD, Portfors CV (2007) Responses to social vocalizations in the inferior colliculus of the mustached bat are influenced by secondary tuning curves. *J Neurophysiol* 98: 3461-3472.

Huffman RF, Argeles PC, Covey E (1998) Processing of sinusoidally frequency modulated signal in the nuclei of the lateral lemniscus of the big brown bat, *Eptesicus fuscus*. *Hear Res* 126: 161-180.

Irvine DRF (1992) *Physiology of the auditory brainstem*. In: *The mammalian auditory pathway: neurophysiology* (Popper AN, Fay RR, eds.) Berlin: Springer-Verlag.

Irwin RJ, McAuley SF (1987) Relations among temporal acuity, hearing loss, and the perception of speech distorted by noise and reverberation. *J Acoust Soc Am* 81: 1557-1565.

Isaacson JS, Walmsley B (1995) Receptors underlying excitatory synaptic transmission in slices of the rat anteroventral cochlear nucleus. *J Neurophysiol* 73:964-973.

Ison JR, Allen PD, Rivoli PJ, Moore JT (2005) The behavioral response of mice to gaps and noise depends on its spectral components and its bandwidth. *J Acoust Soc Am* 117: 3944-3951.

Jen PH, Chen QC, Sun XD (1998) Corticofugal regulation of auditory sensitivity in bat inferior colliculus. *J Comp Physiol [A]* 183: 683-697.

Jesteadt W, Bacon SP, Lehman JR (1982) Forward masking as a function of frequency, masker level, and signal delay. *J Acoust Soc Am* 71: 950-962.

Jin Y, Berrebi AS (2006) Direct projections from the superior olivary complex to the medial geniculate body in rats. *J Assoc Res Otolaryngol Abs* 29: 136.

Joris PX, Schreiner CE, Rees A (2004) Neural processing of amplitude-modulated sounds. *Physiol Rev* 84:541-577.

Kadner A, Berrebi AS (2008) Encoding of temporal features of auditory stimuli in the medial nucleus of the trapezoid body and superior paraolivary nucleus of the rat. *Neuroscience* 151:868-887.

Kadner A, Felix II RA, Berrebi AS (2007) Processing of amplitude modulated tones in the medial nucleus of the trapezoid body and the superior paraolivary nucleus of the rat. *J Assoc Res Otolaryngol Abs* 30:616.

Kadner A, Kulesza RJ Jr, Berrebi AS (2006) Neurons in the medial nucleus of the trapezoid body and superior paraolivary nucleus of the rat may play a role in sound duration coding. *J Neurophysiol* 95:1499-1508.

Kandler K, Katz LC (1995) Neuronal coupling and uncoupling in the developing nervous system. *Curr Opin Neurobiol* 5: 98-105.

Kandler K, Katz LC (1998) Relationship between dye coupling and spontaneous activity in developing ferret visual cortex. *Dev Neurosci* 20: 59-64.

Kelly JB, Liscum A, van Adel B, Ito M (1998) Projections from the superior olive and lateral lemniscus to tonotopic regions of the rat's inferior colliculus. *Hear Res* 116: 43-54.

Kelly JB, Masterton B (1977) Auditory sensitivity of the albino rat. *J Comp Physiol Psychol* 91:930-936.

Klug A, Bauer EE, Hanson JT, Hurley L, Meitzen J, Pollak GD (2002) Response selectivity for species-specific calls in the inferior colliculus of Mexican free-tailed bats is generated by inhibition. *J Neurophysiol* 88: 1941-1954.

Klug A, Bauer EE, Pollak GD (1999) Multiple components of ipsilaterally evoked inhibition in the inferior colliculus. *J Neurophysiol* 82: 593-610.

Koch U, Grothe B (1998) GABAergic and gltcinergic inhibition sharpens tuning for frequency modulations in the inferior colliculus of the big brown bat. *J Neurophysiol* 80:71-82.

Kopp-Scheinflug C, Robinson S, Forsythe I. (2010) Are chopper-like offset responses of SPN neurons mediated by a hyperpolarization-activated cyclic nucleotide-gated current (I<sub>h</sub>)? *Assoc Res Otolaryngol Abs* 33:263.

Kopp-Scheinflug C, Tolnai S, Malmierca MS, Rubsamen R (2008) The medial nucleus of the trapezoid body: comparative physiology. *Neuroscience* 154:160-170.

Krishna BS, Semple MN (2000) Auditory temporal processing: responses to sinusoidally amplitude-modulated tones in the inferior colliculus. *J Neurophysiol* 84:255-273.

Kulesza RJ Jr. (2008) Cytoarchitecture of the human superior olivary complex: nuclei of the trapezoid body and posterior tier. *Hear Res* 241:52-63.

Kulesza RJ Jr, Berrebi AS (2000) Superior paraolivary nucleus of the rat is a GABAergic nucleus. *J Assoc Res Otolaryngol* 1:255-269.

Kulesza RJ Jr., Holt GA, Spirou G, Berrebi AS (2000) Intracellular labeling of axonal collaterals of SPON neurons. *Assoc Res Otolaryngol Abs* 23: 37.

Kulesza RJ Jr, Kadner A, Berrebi AS (2007) Distinct roles for glycine and GABA in shaping response properties of neurons in the superior paraolivary nucleus of the rat. *J Neurophysiol* 97:1610-1620.

Kulesza RJ Jr., Lukose R, Stevens LV (2011) Malformation of the human superior olive in autistic spectrum disorders. *Brain Res* 1367:360-371.

Kulesza RJ Jr, Spirou GA, Berrebi AS (2003) Physiological response properties of neurons in the superior paraolivary nucleus of the rat. *J Neurophysiol* 89:2299-2312.

Kulesza Jr. RJ, Viñuela A, Saldaña E, Berrebi AS (2002) Unbiased stereological estimates of neuron number in subcortical auditory nuclei of the rat. *Hear Res* 168: 12-24.

Kurt S, Moeller CK, Jeschke, Schulze H (2008) Differential effects of iontophoretic application of the GABAA-antagonists bicuculline and gabazine on tone-evoked local

field potentials in primary auditory cortex: interaction with ketamine anesthesia. *Brain Res* 1220:58-69.

Kuwabara N, DiCaprio RA, Zook JM (1991) Afferents to the medial nucleus of the trapezoid body and their collateral projections. *J Comp Neurol* 314:684-706.

Kuwabara N, Zook JM (1991) Classification of principal cells of the medial nucleus of the trapezoid body. *J Comp Neurol* 314: 707-720.

Kuwabara N, Zook JM (1999) Local collateral projections from the medial superior olive to the superior paraolivary nucleus in the gerbil. *Brain Res* 846: 59-71.

Kuwada S, Batra R (1999) Coding of sound envelopes by inhibitory rebound in neurons of the superior olivary complex in the unanesthetized rabbit. *J Neurosci* 19:2273-2287.

Lester RA, Clements JD, Westbrook GL, Jahr CE (1990) Channel kinetics determine the time course of NMDA receptor-mediated synaptic currents. *Nature* 346:565-567.

Langner G (1992) Periodicity coding in the auditory system. *Hear Res* 60:115-142.

Langner G (1997) Neural processing and representation of periodicity pitch. *Acta Otolaryngol Suppl* 532:68-76.

Langner G (2005) Neuronal mechanisms underlying the perception of pitch and harmony. *Am N.Y. Acad Sci* 1060:50-52.

Lechner HA, Lein ES, Callaway EM (2002) A genetic method for selective and quickly reversible silencing of mammalian neurons. *J Neurosci* 22: 5287-5290.

LeDoux JE, Farb C, Ruggiero DA (1990) Topographic organization of neurons in the acoustic thalamus that project to the amygdale. *J Neurosci* 10: 1043-1054.

LeDoux JE, Sakaguchi A, Reis DJ (1984) Subcortical efferent projections of the medial geniculate nucleus mediate emotional responses to conditioned acoustic stimuli. *J Neurosci* 4: 683-698.

Leitner DS, Carmody DP, Girtten EM (1997) A signal detection theory analysis of gap detection in the rat. *Percept Psychophys* 59: 774-782.

Leitner DS, Hammond GR, Springer CP, Ingham KM, Mekilo AM, Bodison PR, Aranda MT, Shawaryn MA (1993) Parameters affecting gap detection in the rat. *Percept Psychophys* 54: 395-405.

Liu RC, Linden JF, Schreiner CE (2006) Improved cortical entrainment to infant communication calls in mothers compared with virgin mice. *Eur J Neurosci* 23:3087-3097.

Logvinov AK, Kirichenko EY, Povilaitte PE (2009) Laminar distribution of gap-junctions in rat somatic cortical columns. *J Integr Neurosci* 8: 425-431.

Macdonald JF, Miljkovic Z, Pennefather PS (1987) Use-dependent block of excitatory amino acid currents in cultured neurons by ketamine. *J Neurophysiol* 58:251-266.

Magnusson AK, Fridburger A, Leigon S (2010) Rebound spiking in the mouse superior olivary nucleus. *Assoc Res Otolaryngol Abs* 33:263.

Malmierca MS, Blackstad TW, Osen KK, Karagulle T, Molowny RL (1993) The central nucleus of the inferior colliculus in rat: a golgi and computer reconstruction study of neuronal and laminar structure. *J Comp Neurol* 333: 1-27.

Malmierca MS, Hackett TA (2010) Structural organization of the ascending auditory system. In: *The oxford handbook of auditory science: the auditory brain* (Moore DR, Fuchs PA, Rees A, Palmer AR, eds.). New York: Oxford Press.

Marshall AF, Pearson JM, Falk SE, Skaggs JD, Crocker WD, Saldaña E, Fitzpatrick DC (2008) Auditory response properties of neurons in the tectal longitudinal column of the rat. *Hear Res* 244: 35-44.

Martin MR (1985) Evidence for an excitatory amino acid as the transmitter of the auditory nerve in the in vitro mouse cochlear nucleus. *Hear Res* 20:215-220.

Mazelova J, Popelar J, Syka J (2003) Auditory function in presbycusis: peripheral vs. central changes. *Exp Gerontol* 38: 87-94.

McGarry LM, Packer AM, Fino E, Nikolenko V, Sippy T, Yuste R (2010) Quantitative classification of somatostatin-positive neocortical interneurons identifies three interneuron subtypes. *Front Neural Circuits* 4: 12.

Meller K, Krah K, Theiss C (2005) Dye coupling in Purkinje cells of organotypic slice cultures. *Brain Res Dev Brain Res* 160: 101-105.

Moore DR (2006) Auditory processing disorder (APD) – potential contribution of mouse research. *Brain Res* 1091: 200-206.

Moore MJ, Caspary DM (1983) Strychnine blocks inhibition in lateral superior olivary neurons. *J Neurosci* 3: 237-242.

Morest DK (1968) The collateral system of the medial nucleus of the trapezoid body of the cat, its neuronal architecture and relation to the olivo-cochlear bundle. *Brain Res* 9:288-311.

Morrison D (1967) *Multivariate statistical methods*. New York: McGraw-Hill.



Mugnaini E, Oertel WH (1985) An atlas of the distribution of GABAergic neurons and terminals in the cat CNS as revealed by GAD immunohistochemistry. In: Handbook of chemical neuroanatomy. Vol. 4: GABA and neuropeptides in the CNS (Björklund A, Hökfelt T, eds.). Amsterdam: Elsevier.

Nagarajan SS, Cheung SW, Bedenbaugh P, Beitel RE, Schreiner CE, Merzenich MM (2002) Representation of spectral and temporal envelope of twitter vocalizations in common marmoset primary auditory cortex. *J Neurophysiol* 87: 1723-1737.

Nakagawa H, Sato K, Shiraishi Y, Kuriyama H, Altschuler RA (2000) NMDAR1 isoforms in the rat superior olivary complex and changes after unilateral cochlear ablation. *Brain Res Mol Brain Res* 77:246-257.

Nelson PC, Smith ZM, Young ED (2009) Wide-dynamic-range forward suppression in marmoset inferior colliculus neurons is generated centrally and accounts for perceptual masking. *J Neurosci* 29:2553-2562.

Nordeen KW, Killackey HP, Kitzes LM (1983) Ascending auditory projections to the inferior colliculus in the adult gerbil, *Meriones unguiculatus*. *J Comp Neurol* 214: 131-143.

Nyby J, Whitney G (1983) Sound communication among adults. In: The auditory psychobiology of the mouse (Willott JF, ed.). Springfield: Charles C Thomas.

Oertel D (1999) The role of timing in the brain stem auditory nuclei of vertebrates. *Ann Rev Physiol* 61:497-519.

Ohl FW, Wetzel W, Wagner T, Rech A, Scheich H (1999) Bilateral ablation of auditory cortex in Mongolian gerbil affects discrimination of frequency modulated tones but not pure tones. *Learn Mem* 6: 347-362.

Ollo C, Schwartz IR (1979) The superior olivary complex in C57BL/6 mice. *Am J Anat* 155:349-373.

Orser BA, Pennefather PS, MacDonald JF (1997) Multiple mechanisms of ketamine blockade of N-methyl-D-aspartate receptors. *Anesthesiology* 86:903-917.

Oxenham AJ, Plack CJ (2000) Effects of masker frequency and duration in forward masking: further evidence for the influence of peripheral nonlinearity. *Hear Res* 150: 258-266.

Ozawa S, Kamiya H, Tsuzuki K (1998) Glutamate receptors in the mammalian central nervous system. *Prog Neurobiol* 54:581-618.

Palombi PS, Caspary DM (1996) GABA inputs control discharge rate primarily within frequency receptive fields of inferior colliculus neurons. *J Neurophysiol* 75: 2211-2219.

Park TJ, Monsivais P, Pollak GD (1997) Processing of interaural intensity differences I the LSO: the role interaural threshold differences. *J Neurophysiol* 77: 2863-2878.

Paxinos G, Franklin K (2001) *The mouse brain in stereotaxic coordinates*. San Diego: Academic Press.

Paxinos G, Watson C (1986) *The rat brain in stereotaxic coordinates*. San Diego: Academic Press.

Peruzzi D, Sivaramakrishnan S, Oliver DL (2000) Identification of cell types in brain slices of the inferior colliculus. *Neuroscience* 101: 403-416.

Petralia RS, Rubio ME, Wang YX, Wenthold RJ (2000) Differential distribution of glutamate receptors in the cochlear nuclei. *Hear Res* 147:59-69.

Petralia RS, Wang YX, Wenthold RJ (1994a) The NMDA receptor subunits NR2A and NR2B show histological and ultrastructural localization patterns similar to those of NR1. *J Neurosci* 14:6102-6120.

Petralia RS, Yokotani N, Wenthold RJ (1994b) Light and electron microscope distribution of the NMDA receptor subunit NMDAR1 in the rat nervous system using a selective anti-peptide antibody. *J Neurosci* 14:667-696.

Phillips DP (1999) Auditory gap detection, perceptual channels, and temporal resolution in speech perception. *J Am Acad Audiol* 10: 343-354.

Peinado A, Yuste R, Katz LC (1993) Extensive dye coupling between rat neonatal neurons during the period of circuit formation. *Neuron* 10: 103-114.

Plack CJ, Oxenham AJ (1998) Basilar-membrane nonlinearity and the growth of forward masking. *J Acoust Soc Am* 103: 1598-1608.

Plomp R (1976) Binaural and monaural speech intelligibility of connected discourse in reverberation as a function of a single competing sound source (speech or noise). *Acoustica* 34: 200-211.

Pollak GD, Burger RM, Kulg A (2003) Dissecting the circuitry of the auditory system. *Trends Neurosci* 26: 33-39.

Pollak GD, Burger RM, Park TJ, Klug A, Bauer EE (2002) Roles of inhibition for transforming binaural properties in the brainstem auditory system. *Hear Res* 168: 60-78.

Pollak GD, Gittelman JX, Li N, Xie R (2010) Inhibitory projections from the ventral nucleus of the lateral lemniscus and superior paraolivary nucleus create directional

selectivity of frequency modulations in the inferior colliculus: A comparison of bats with other mammals. *Hear Res* 273: 134-144..

Pollak GD, Xie R, Gittelman JX, Andoni S, Li N (2011) The dominance of inhibition in the inferior colliculus. *Hear Res* 274: 27-39.

Portfors CV (2007) Types and functions of ultrasonic vocalizations in laboratory rats and mice. *J Am Assoc Lab Anim Sci* 46:28-34.

Portfors CV, Felix II RA (2005) Spectral integration in the inferior colliculus of the CBA/CaJ mouse. *Neuroscience* 136:1159-1170.

Recanzone GH, Sutter ML (2008) The biological basis of audition. *Annu Rev Psychol* 59: 119-142.

Relkin EM, Turner CW (1988) A reexamination of forward masking in the auditory nerve. *J Acoust Soc Am* 84: 584-591.

Rhode WS, Greenberg S (1994) Encoding of amplitude modulation in the cochlear nucleus of the cat. *J Neurophysiol* 71:1797-1825.

Rhode WS, Oertel D, Smith PH (1983) Physiological response properties of cells labeled intracellularly with horseradish peroxidase in cat ventral cochlear nucleus. *J Comp Neurol* 213:448-463.

Robinson RB, Siegelbaum SA (2003) Hyperpolarization-activated cation currents: from molecules to physiological function. *Annu Rev Physiol* 65: 453-480.

Rosen S (1992) Temporal information in speech: acoustic, auditory and linguistic aspects. *Philos Trans R Soc Lond B Biol Sci* 336:367-373.

Rosowski JJ, Ravicz ME, Teoh SW, Flandermeyer D (1999) Measurements of middle-ear function in the Mongolian gerbil, a specialized mammalian ear. *Audiol Neurootol* 4:129-136.

Rybalko N, Syka J (2005) Effect of noise exposure on gap detection in rats. *Hear Res* 200: 63-72.

Saint Marie RL, Baker RA (1990) Neurotransmitter-specific uptake and retrograde transport of [<sup>3</sup>H]glycine from the inferior colliculus by ipsilateral projections of the superior olivary complex and nuclei of the lateral lemniscus. *Brain res* 524: 244-253.

Saldaña E, Aparicio MA, Fuentes-Santamaria V, Berrebi AS (2009) Connections of the superior paraolivary nucleus of the rat: projections to the inferior colliculus. *Neuroscience* 163:372-387.

- Saldaña E, Berrebi AS (2000) Anisotropic organization of the rat superior paraolivary nucleus. *Anat Embryol (Berl)* 202:265-279.
- Saldaña E, Viñuela A, Marshall AF, Fitzpatrick DC, Aparicio MA (2007) The TLC: a novel auditory nucleus in the mammalian brain. *J Neurosci* 27: 13108-13116.
- Sanchez JT, Gans D, Wenstrup JJ (2007) Contribution of AMPA and NMDA receptors to temporal patterning of auditory responses in the inferior colliculus. *J Neurosci* 27:1954-1963.
- Sanchez-Alonso JL, Halliwell JV, Colino A (2008) ZD7288 inhibits T-type calcium current in rat hippocampal pyramidal cells. *Neurosci Lett* 439: 275-280.
- Sato K, Kuriyama H, Altschuler RA (1998) Differential distribution of NMDA receptor subunit mRNA in the rat cochlear nucleus. *Microsc Res Tech* 41:217-223.
- Sato K, Nakagawa H, Kuriyama H, Altschuler RA (1999) Differential distribution of N-methyl-D-aspartate receptor-2 subunit messenger RNA in the rat superior olivary complex. *Neuroscience* 89:839-853.
- Sato K, Shiraishi S, Nakagawa H, Kuriyama H, Altschuler RA (2000) Diversity and plasticity in amino acid subunits in the rat auditory brain stem. *Hear Res* 147:137-144.
- Schmidt E, Wolski TP Jr., Kulesza RJ Jr. (2010) Distribution of perineuronal nets in the human superior olivary complex. *Hear Res* 265:15-24.
- Schofield BR (1991) Superior paraolivary nucleus in the pigmented guinea pig: separate classes of neurons that project to the inferior colliculus and the cochlear nucleus. *J Comp Neurol* 312: 68-76.
- Schofield BR (1994) Projections to the cochlear nuclei from principal cells in the medial nucleus of the trapezoid body in guinea pigs. *J Comp Neurol* 344: 83-100.
- Schofield BR (1995) Projections from the cochlear nucleus to the superior paraolivary nucleus in guinea pigs. *J Comp Neurol* 360: 135-149.
- Schofield BR (2005) Superior olivary and lateral lemniscus connections of the auditory midbrain. In: *The inferior colliculus* (Winer JA, Schreiner C, eds.). New York: Springer.
- Seeman P, Lee T (1975) Antipsychotic drugs: direct correlation between clinical potency and presynaptic action on dopamine neurons. *Science* 188:1217-1219.
- Shannon RV, Zeng FG, Kathman V, Wygonski J, Ekelid M (1995) Speech recognition with primarily temporal cues. *Science* 270: 303-304.

Sivaramkrishnan S, Oliver DL (2001) Distinct K currents result in physiologically distinct cell types in the inferior colliculus of the rat. *J Neurosci* 21: 2861-2877.

Sloper JJ, Powell TP (1978) Gap junctions between dendrites of neurons in the primate sensori-motor cortex. *Proc R Soc Lond B Biol Sci* 203: 39-47.

Smith AJ, Owens S, Forsythe ID (2000) Characterisation of inhibitory and excitatory postsynaptic currents of the rat medial superior olive. *J Physiol* 529:681-698.

Smith DI, Mills JH (1989) Anesthesia effects: auditory brain-stem response. *Electroencephalogr Clin Neurophysiol* 72:422-428.

Smith DI, Mills JH (1991) Low-frequency component of the gerbil brainstem response: response characteristics and anesthesia effects. *Hear Res* 54:1-10.

Smith PH, Joris PX, Yin TCT (1991) Projections of physiologically characterized spherical bushy cell axons from the cochlear nucleus of the cat: evidence for delay lines to the medial superior olive. *J Comp Neurol* 331: 245-260.

Smith PH, Joris PX, Yin TCT (1998) Anatomy and physiology of principal cells of the medial nucleus of the trapezoid body (MNTB) of the cat. *J Neurophysiol* 79:3127-3142.

Snell KB, Frisina DR (2000) Relationships among age-related differences in gap detection and word recognition. *J Acous Soc Am* 107: 1615-1626.

Snell KB, Ison JR, Frisina DR (1994) The effects of signal frequency and absolute bandwidth on gap detection in noise. *J Acoust Soc Am* 96: 1458-1464.

Sommer I, Lingenhohl K, Friauf E (1993) Principal cells of the rat medial nucleus of the trapezoid body: an intracellular in vivo study of their physiology and morphology. *Exp Brain Res* 95:223-239.

Sonntag M, Englitz B, Kopp-Scheinflug C, RübSamen R. (2009) Early postnatal development of spontaneous and acoustically evoked discharge activity of principal cells of the medial nucleus of the trapezoid body: an in vivo study in mice. *J Neurosci* 29:9510-9520.

Spangler KM, Warr WB, Henkel CK (1985) The projections of principal cells of the medial nucleus of the trapezoid body in the cat. *J Comp Neurol* 238: 249-262.

Stiebler I, Ehret G (1985) Inferior colliculus of the house mouse. I. A quantitative study of tonotopic organization, frequency representation, and tone-threshold distribution. *J Comp Neurol* 238: 65-76.

Sun H, Wu SH (2008) Modification of membrane excitability of neurons in the rat's dorsal cortex of the inferior colliculus by preceding hyperpolarization. *Neuroscience* 154: 257-272.

Syka J, Rybalko N, Mazelova J, Druga R (2002) Gap detection threshold in the rat before and after auditory cortex ablation. *Hear Res* 172: 151-159.

Tan EM, Yamaguchi Y, Horowitz GD, Gosgnach S, Lein ES, Goulding M, Albright TD, Callaway EM (2006) Selective and quickly reversible inactivation of mammalian neurons in vivo using the *Drosophila* allatostatin receptor. *Neuron* 51: 157-170.

Theunissen FE, Doupe AJ (1998) Temporal and spectral sensitivity of complex auditory neurons in the nucleus HVC of male zebra finches. *J Neurosci* 18: 3786-3802.

Thompson AM, Thompson GC (1991) Projections from the posteroventral cochlear nucleus to the superior olivary complex in guinea pig: light and EM observations with the PHA-L method. *J Comp Neurol* 311:495-508.

Tollin DJ (2003) The lateral superior olive: a functional role in sound source localization. *Neuroscientist* 9:127-143.

Trussell LO (1999) Synaptic mechanisms for coding timing in auditory neurons. *Ann Rev Physiol* 61:477-496.

Trussell LO (2002) Modulation of transmitter release at giant synapses of the auditory system. *Curr Opin Neurobiol* 12: 400-404.

Tyler RS, Summerfield Q, Wood EJ, Fernandes MA (1982) Psychoacoustic and phonetic temporal processing in normal and hearing-impaired listeners. *J Acous Soc Am* 72: 740-752.

van Looij MA, Liem SS, van der Burg H, van der Wees J, De Zeeuw CI, van Zanten BG (2004) Impact of conventional anesthesia on auditory brainstem responses in mice. *Hear Res* 193:75-82.

Vater M, Covey E, Casseday JH (1997) The columnar region of the ventral nucleus of the lateral lemniscus in the big brown bat (*Eptesicus fuscus*): synaptic arrangements and functional correlates of feedforward inhibitory function. *Cell Tissue Res* 289: 223-233.

Vetter DE, Adams JC, Mugnaini E (1991) Chemically distinct rat olivocochlear neurons. *Synapse* 7: 21-43.

Vetter DE, Mugnaini E (1992) Distribution and dendritic features of three groups of rat olivocochlear neurons. A study with two retrograde cholera toxin tracers. *Anat Embryol (Berl)* 185: 1-16.

Vetter DE, Saldaña E, Mugnaini E (1993) Input from the inferior colliculus to medial olivocochlear neurons in the rat: a double label study with PHA-L and cholera toxin. *Hear Res* 70: 173-186.

Viñuela A, Aparicio MA, Berrebi AS, Saldaña E (2011) Connections of the superior paraolivary nucleus of the rat. II. reciprocal connections with the tectal longitudinal column. *Front Neuroanat* 22: 1-5.

Walton JP (2010) Timing is everything: temporal processing deficits in the aged auditory brainstem. *Hear Res* 264: 63-69.

Walton JP, Frisina RD, Ison JR, O'Neill WE (1997) Neural correlates of behavioral gap detection in the inferior colliculus of the young CBA mouse. *J Comp Physiol [A]* 181: 161-176.

Ward JH (1963) Hierarchical grouping to optimize an objective function. *J Am Stat Assoc.* 58: 236-244.

Warr WB (1972) Fiber degeneration following lesions in the multipolar and globular bushy cell areas in the ventral cochlear nucleus of the cat. *Brain Res* 40: 247-270.

Watanabe M, Mishina M, Inoue Y (1994) Distinct distributions of five NMDA receptor channel subunit mRNAs in the brainstem. *J Comp Neurol* 343:520-531.

Willott JF (1983) *The auditory psychobiology of the mouse*. Springfield: Charles C Thomas.

Wilson WW, Walton JP (2002) Background noise improves gap detection in tonically inhibited inferior colliculus neurons. *J Neurophysiol* 87: 240-249.

Winer JA, Larue DT, Pollak GD (1995) GABA and glycine in the central auditory system of the mustache bat: structural substrates for inhibitory neuronal organization. *J Comp Neurol* 355: 317-353.

Winer JA, Schreiner CE (2005) *The inferior colliculus*. New York: Springer.

Winter IM, Robertson D, Cole KS (1989) Descending projections from auditory brainstem nuclei to the cochlea and cochlear nucleus of the guinea pig. *J Comp Neurol* 280: 143-157.

Wu SH, Kelly JB (1992) Synaptic pharmacology of the superior olivary complex studied in mouse brain slice. *J Neurosci* 12:3084-3097.

Wu SH, Ma CL, Sivaramakrishnan S, Oliver DL (2002) Synaptic modification of neurons of the central nucleus of the inferior colliculus. *Hear Res* 168:43-54.

Xie R, Gittelman JX, Li N, Pollak GD (2008) Whole cell recordings of intrinsic properties and sound-evoked responses from the inferior colliculus. *Neuroscience* 154: 245-256.

Xie R, Gittelman JX, Pollak GD (2007) Rethinking tuning: in vivo whole-cell recordings of the inferior colliculus in awake bats. *J Neurosci* 27: 9469-9481.

Yang L, Pollak GD (1997) Differential response properties of amplitude modulated signals in the dorsal nucleus of the lateral lemniscus of the mustache bat and the roles of GABAergic inhibition. *J Neurophysiol* 77: 324-340.

Zhang H, Kelly JB (2001) AMPA and NMDA receptors regulate glutamate responses of neurons in the rat's inferior colliculus. *J Neurophysiol* 86:871-880.

Zhang H, Kelly JB (2003) Glutamatergic and GABAergic regulation of neural responses in inferior colliculus to amplitude-modulated sounds. *J Neurophysiol* 90:477-490.

Zhang H, Kelly JB (2006) Responses of neurons in the rat's ventral nucleus of the lateral lemniscus to amplitude-modulated tones. *J Neurophysiol* 96:2905-2914.

Zhou X, Jen PH (2007) Corticofugal modulation of multi-parametric auditory selectivity in the midbrain of the big brown bat. *J Neurophysiol* 98: 2509-2516.

Zwicker H, Fastl H (1990) *Psychoacoustics. Facts and Models*. Berlin: Springer-Verlag.



## **Richard A. Felix II**

*felix3435@gmail.com*  
1413 Eastern Avenue  
Morgantown, WV 26505  
*updated 07/18/11*

### **Personal**

DOB – 1979  
Place of birth – Vallejo, California

### **Education**

Washington State University, Vancouver, WA (2000-2002) B.S. in Biology  
Washington State University, Vancouver, WA (2003-2005) M.S. in Zoology  
West Virginia University, Morgantown, WV (2005-2011) Ph.D. in Neuroscience

### **Research Experience**

Complex Response Properties in the Inferior Colliculus of Normal Hearing  
CBA/CaJ and Hearing Impaired C57BL/6 Mice.  
Advisor: Dr. Christine Portfors, Washington State University (2003-2005).

Encoding of Temporal Sound Features in the Rodent Superior Paraolivary  
Nucleus.  
Advisor: Dr. Albert Berrebi, West Virginia University (2005-2011).

### **Teaching Experience**

Behavioral Neuroscience – Spatial Memory (Fall 2004) WSU  
Fundamentals of Integrated Systems – Synaptic Plasticity (Fall 2009) WVU

### **Manuscripts**

Portfors CV, **Felix II RA** (2005) Spectral integration in the inferior colliculus of the CBA/CaJ mouse. *Neuroscience* 136: 1159-70.

Roberts PD, Portfors CV, Sawtell N, **Felix II RA** (2006) Model of auditory prediction in the dorsal cochlear nucleus via spiketiming dependent plasticity. *Neurocomputing* 69: 1191-94.

**Felix II RA**, Portfors CV (2007) Excitatory, inhibitory and facilitatory frequency response areas in the inferior colliculus of hearing impaired mice. *Hearing Research* 228: 212-229.

**Felix II RA**, Fridberger A, Leijon S, Berrebi AS, Magnusson AK (2011) Sound rhythms are encoded by post-inhibitory rebound spiking in the superior paraolivary nucleus. *Journal of Neuroscience*, *in press*.

**Felix II RA**, Kadner A, Berrebi AS (2011) Effects of ketamine on response properties of neurons in the superior paraolivary nucleus of the mouse. *Neuroscience*, *submitted*.

## **Presentations**

Portfors CV, **Felix II RA** (2003) Multiply tuned neurons in the inferior colliculus of the mouse as revealed by single unit recordings and inducible gene expression. *Society for Neuroscience Abstracts* 33: 487.

**Felix RA II**, Portfors CV (2004) High frequency hearing loss may unmask non-tonotopic inputs to neurons in the inferior colliculus. *Association for Research in Otolaryngology Abstracts* 27:94.

Sawtell N, **Felix II RA**, Tzounopoulos T, Portfors CV (2005) Response properties of neurons in the dorsal cochlear nucleus of the unanesthetized mouse. *Association for Research in Otolaryngology Abstracts* 28:123.

Kadner A, **Felix II RA**, Berrebi AS (2007) Processing of amplitude modulated tones in the medial nucleus of the trapezoid body and the superior paraolivary nucleus of the rat. *Association for Research in Otolaryngology Abstracts* 30:616.

**Felix II RA**, Kadner A, Berrebi AS (2009) Characterization of the superior paraolivary nucleus in awake and anesthetized mice. *Society for Neuroscience Abstracts* 39: 259.

**Felix II RA**, Berrebi AS (2010) The superior paraolivary nucleus contributes to shaping temporal response properties of neurons in the inferior colliculus. *Society for Neuroscience Abstracts* 40: 671.

Leijon S, **Felix II RA**, Fridberger A, Berrebi AS, Magnusson AK (2011) Transient A-type K currents contribute to the electrical properties of superior paraolivary nucleus neurons. *Association for Research in Otolaryngology Abstracts* 34: 888.